

# Technical Program for Long-Term Management of Canada's Used Nuclear Fuel – Annual Report 2018

NWMO-TR-2019-01

December 2019

**J. Chen, M. Behazin, J. Binns, K. Birch, A. Blyth, S. Briggs, J. Freire-Canosa, G. Cheema, R. Crowe, D. Doyle, F. Garisto, J. Giallonardo, M. Gobien, R. Guo, S. Hirschorn, M. Hobbs, M. Ion, J. Jacyk, H. Kasani, P. Keech, E. Kremer, C. Lawrence, H. Leung, K. Liberda, T. Liyanage, J. McKelvie, C. Medri, M. Mielcarek, L. Kennell-Morrison, A. Murchison, A. Parmenter, M. Sanchez-Rico Castejon, U. Stahmer, Y. Sui, E. Sykes, M. Sykes, T. Yang, X. Zhang, B. Zhao**

Nuclear Waste Management Organization

**nwmo**

NUCLEAR WASTE  
MANAGEMENT  
ORGANIZATION

SOCIÉTÉ DE GESTION  
DES DÉCHETS  
NUCLÉAIRES



**Nuclear Waste Management Organization**  
22 St. Clair Avenue East, 6<sup>th</sup> Floor  
Toronto, Ontario  
M4T 2S3  
Canada

Tel: 416-934-9814  
Web: [www.nwmo.ca](http://www.nwmo.ca)

# **Technical Program for Long-Term Management of Canada's Used Nuclear Fuel – Annual Report 2018**

**NWMO-TR-2019-01**

December 2019

**J. Chen, M. Behazin, J. Binns, K. Birch, A. Blyth, S. Briggs, J. Freire-Canosa, G. Cheema, R. Crowe, D. Doyle, F. Garisto, J. Giallonardo, M. Gobien, R. Guo, S. Hirschorn, M. Hobbs, M. Ion, J. Jacyk, H. Kasani, P. Keech, E. Kremer, C. Lawrence, H. Leung, K. Liberda, T. Liyanage, J. McKelvie, C. Medri, M. Mielcarek, L. Kennell-Morrison, A. Murchison, A. Parmenter, M. Sanchez-Rico Castejon, U. Stahmer, Y. Sui, E. Sykes, M. Sykes, T. Yang, X. Zhang, B. Zhao**

Nuclear Waste Management Organization



### Document History

Title:	Technical Program for Long-Term Management of Canada's Used Nuclear Fuel – Annual Report 2018		
Report Number:	NWMO-TR-2019-01		
Revision:	R000	Date:	December 2019
Nuclear Waste Management Organization			
Authored by:	J. Chen, M. Behazin, J. Binns, K. Birch, A. Blyth, S. Briggs, J. Freire-Canosa, G. Cheema, R. Crowe, D. Doyle, F. Garisto, J. Giallonardo, M. Gobien, R. Guo, S. Hirschorn, M. Hobbs, M. Ion, J. Jacyk, H. Kasani, P. Keech, E. Kremer, C. Lawrence, H. Leung, K. Liberda, T. Liyanage, J. McKelvie, C. Medri, M. Mielcarek, L. Kennell-Morrison, A. Murchison, A. Parmenter, M. Sanchez-Rico Castejon, U. Stahmer, Y. Sui, E. Sykes, M. Sykes, T. Yang, X. Zhang, B. Zhao		
Reviewed by:	P. Gierszewski and C. Boyle		
Approved by:	D. Wilson		



**ABSTRACT**

**Title:** Technical Program for the Long-Term Management of Canada's Used Nuclear Fuel – Annual Report 2018  
**Report No.:** NWMO-TR-2019-01  
**Author(s):** J. Chen, M. Behazin, J. Binns, K. Birch, A. Blyth, S. Briggs, J. Freire-Canosa, G. Cheema, R. Crowe, D. Doyle, F. Garisto, J. Giallonardo, M. Gobien, R. Guo, S. Hirschorn, M. Hobbs, M. Ion, J. Jacyk, H. Kasani, P. Keech, E. Kremer, C. Lawrence, H. Leung, K. Liberda, T. Liyanage, J. McKelvie, C. Medri, M. Mielcarek, L. Kennell-Morrison, A. Murchison, A. Parmenter, M. Sanchez-Rico Castejon, U. Stahmer, Y. Sui, E. Sykes, M. Sykes, T. Yang, X. Zhang, B. Zhao  
**Company:** Nuclear Waste Management Organization  
**Date:** December 2019

**Abstract**

This report is a summary of activities and progress in 2018 for the Nuclear Waste Management Organization's Technical Program. The primary purpose of the Technical Program is to support the implementation of Adaptive Phased Management (APM), Canada's approach for the long-term management of used nuclear fuel.

The work continued to develop the repository design; to understand the engineered barrier, geological and other processes important to the safety case; and to assess the candidate siting areas.

NWMO continued to participate in international research activities, including projects associated with the SKB Äspö Hard Rock Laboratory, the Mont Terri Underground Rock Laboratory, the Greenland ICE Project, the OECD (Organisation for Economic Co-operation and Development) Nuclear Energy Agency and BioProta.

NWMO's technical program issued 15 NWMO technical reports, published 24 journal articles, and provided over 40 presentations at national and international conferences.



**TABLE OF CONTENTS**

	<b><u>Page</u></b>
<b>ABSTRACT</b> .....	<b>v</b>
<b>1. INTRODUCTION</b> .....	<b>1</b>
<b>2. OVERVIEW OF NWMO TECHNICAL PROGRAMS</b> .....	<b>3</b>
<b>3. REPOSITORY ENGINEERING</b> .....	<b>5</b>
<b>3.1 USED FUEL TRANSPORTATION</b> .....	<b>5</b>
3.1.1 Used Fuel Transportation System Development .....	5
3.1.2 Transportation Package Material Testing .....	6
<b>3.2 USED FUEL CONTAINER (UFC)</b> .....	<b>8</b>
3.2.1 Used Fuel Container Design .....	8
3.2.2 Used Fuel Container Manufacturing & Inspection .....	10
3.2.2.1 UFC Serial Production .....	10
3.2.2.2 HLAW Closure Weld Development .....	10
3.2.2.3 Non-Destructive Examination Development .....	13
3.2.2.4 Copper Coating Development .....	13
<b>3.3 BUFFER AND SEALING SYSTEMS</b> .....	<b>20</b>
3.3.1 Emplacement Equipment .....	20
3.3.2 Highly Compacted Bentonite Storage Room .....	21
3.3.3 Shaping Cell Operation .....	22
<b>3.4 MATERIAL STUDIES</b> .....	<b>23</b>
3.4.1 Used Fuel Container Corrosion Studies .....	23
3.4.1.1 Anoxic Corrosion of Copper .....	23
3.4.1.2 Corrosion of Copper Coatings .....	25
3.4.1.3 Corrosion of Copper in Radiolytic Environments .....	26
3.4.1.4 Oxidic Corrosion of Copper .....	26
3.4.2 Internal Corrosion of UFC .....	27
3.4.3 Microbial Studies .....	27
3.4.4 Bentonite .....	28
<b>4. GEOSCIENCE</b> .....	<b>30</b>
<b>4.1 HYDROGEOCHEMISTRY</b> .....	<b>30</b>
4.1.1 Porewater Chemistry and Isotopes .....	30
4.1.2 Mont Terri: Geochemical Data (GD) .....	36
<b>4.2 REDOX PROCESSES</b> .....	<b>37</b>
<b>4.3 SUBSURFACE MASS TRANSPORT</b> .....	<b>37</b>
4.3.1 Diffusion .....	37
4.3.2 Geochronology and Fluid Inclusions .....	38
4.3.3 Sorption .....	39
<b>4.4 REACTIVE TRANSPORT MODELLING</b> .....	<b>41</b>
<b>4.5 NORTHERN ONTARIO SEISMIC MONITORING</b> .....	<b>41</b>
<b>4.6 PALEOSEISMICITY</b> .....	<b>42</b>
4.6.1 Sediment Coring and Mapping in Lakes Duparquet and Dufresnoy, Quebec .....	42
4.6.2 Mapping and Dating a Fault Feature in Round Lake, Ontario .....	42
4.6.3 Estimating Magnitude and Epicentre of a Paleoearthquake Occurring ~9100 BP .....	43
4.6.3.1 Core for Lakes Chasignole and Malartic, Quebec .....	43

4.6.3.2	The vvr 1483 MTD Signature in Northeastern Ontario.....	43
<b>4.7</b>	<b>DOLOMITE PALEOGENESIS .....</b>	<b>45</b>
<b>4.8</b>	<b>NATURAL RESOURCE ASSESSMENT – SOUTHERN ONTARIO .....</b>	<b>47</b>
<b>4.9</b>	<b>FRACTURE NETWORK MODELLING.....</b>	<b>48</b>
<b>4.10</b>	<b>GLACIAL SYSTEMS MODELLING.....</b>	<b>49</b>
<b>4.11</b>	<b>GROUNDWATER SYSTEM EVOLUTION.....</b>	<b>49</b>
<b>4.12</b>	<b>GEOMECHANICAL RESEARCH .....</b>	<b>50</b>
4.12.1	Effects of Saturation on Mechanical Parameters.....	50
4.12.2	Exploration of Boundary Condition Effects on Direct Shear Testing.....	52
4.12.3	Assessment of Natural Variability of Mechanical Parameters Using Continuous Logging .....	52
4.12.4	Parametric Variability and Reliability of EDZ Predictions.....	54
<b>4.13</b>	<b>THERMO-HYDRO-MECHANICAL PROPERTIES OF LOW-POROSITY ROCKS .....</b>	<b>56</b>
4.13.1	Permeability of Cobourg Limestone .....	56
4.13.2	Thermal Conductivity of Cobourg Limestone.....	57
4.13.3	Physical and Mineralogical Characteristics of Stanstead and Lac du Bonnet Granites .....	58
4.13.4	Permeability of Stanstead and Lac du Bonnet Granites .....	59
<b>4.14</b>	<b>NUMERICAL DEVELOPMENT OF ROCK MASS EFFECTIVE PROPERTIES.....</b>	<b>60</b>
<b>4.15</b>	<b>FRACTURE PARAMETRIZATION AND UPSCALING - POST PROJECT .....</b>	<b>61</b>
<b>4.16</b>	<b>FIELD EXPERIMENTS IN MONT TERRI, SWITZERLAND .....</b>	<b>63</b>
4.16.1	Long-Term Monitoring of the Full Scale Emplacement Experiment (FE-M) .....	63
4.16.2	Gases in an Unsaturated SF/HLW Emplacement Drift Experiment (FE-G).....	64
4.16.3	Characterization of EDZ Development - Sandy Facies Experiment (GC-A).....	64
<b>4.17</b>	<b>LONG-TERM STABILITY ANALYSIS OF DGR .....</b>	<b>64</b>
<b>5.</b>	<b>REPOSITORY SAFETY .....</b>	<b>65</b>
<b>5.1</b>	<b>MODEL AND DATA DEVELOPMENT .....</b>	<b>65</b>
5.1.1	Used Fuel Characterization.....	65
5.1.1.1	Used Fuel Inventory Update .....	65
5.1.1.2	Unirradiated Fuel Bundle Trace Element Composition .....	66
5.1.1.3	Irradiated End Plate Analysis .....	66
5.1.2	Wasteform Modelling .....	67
5.1.2.1	Validation of Mechanistic Model of UO <sub>2</sub> Fuel Corrosion .....	67
5.1.2.2	Kinetics of Anodic and Cathodic Reactions .....	68
5.1.3	Near-Field Modelling.....	69
5.1.3.1	Thermodynamic Database Review.....	69
5.1.3.2	Gas-Permeable Seal Test (GAST).....	70
5.1.3.3	Shaft Seal Properties .....	71
5.1.3.4	Thermal Response of a Conceptual DGR in Sedimentary Rock.....	72
5.1.3.5	Reactive Transport Modelling of Concrete-Bentonite Interactions .....	73
5.1.4	Biosphere Modelling .....	74
5.1.4.1	Chemical Toxicity.....	74
5.1.4.2	Participation in BIOPROTA .....	74
5.1.5	System Modelling.....	75
5.1.5.1	Updates to T2GGM.....	76
<b>5.2</b>	<b>SAFETY STUDIES .....</b>	<b>76</b>
5.2.1	Preclosure Studies.....	76
5.2.1.1	Preliminary Accident Dose Analysis.....	76
5.2.1.2	Climate Change Impacts Study.....	77

5.2.1.3	Knowledge Management .....	77
5.2.2	Postclosure Studies .....	77
5.2.2.1	Features, Events, and Processes .....	77
5.2.2.2	Sedimentary Rock Case Study .....	78
<b>6.</b>	<b>SITE ASSESSMENT .....</b>	<b>79</b>
<b>6.1</b>	<b>IGNACE WABIGOON.....</b>	<b>79</b>
6.1.1	Geological Investigation .....	79
6.1.2	Environmental Assessment.....	80
<b>6.2</b>	<b>NORTH OF SUPERIOR.....</b>	<b>83</b>
6.2.1	Geological Investigation .....	83
6.2.2	Environmental Assessment.....	83
6.2.2.1	Hornepayne .....	83
6.2.2.2	Manitouwadge .....	85
<b>6.3</b>	<b>SOUTHERN ONTARIO .....</b>	<b>85</b>
	<b>REFERENCES .....</b>	<b>87</b>
	<b>APPENDIX A: NWMO TECHNICAL REPORTS, REFEREED JOURNAL ARTICLES AND TECHNICAL CONFERENCE PRESENTATIONS .....</b>	<b>101</b>
<b>A.1</b>	<b>NWMO TECHNICAL REPORTS .....</b>	<b>102</b>
<b>A.2</b>	<b>REFEREED JOURNAL ARTICLES.....</b>	<b>104</b>
<b>A.3</b>	<b>TECHNICAL CONFERENCE PRESENTATIONS (INCLUDING PROCEEDINGS, ORAL AND POSTER PRESENTATIONS) .....</b>	<b>107</b>

**LIST OF TABLES**

	<b><u>Page</u></b>
Table 3-1: Summary of Electrodeposited Copper Material Performance Test Results for Hemi-Spherical Head.....	14
Table 4-1: Preliminary Thermal conductivity of the Cobourg limestone from McGill University compared to published literature [W/mK].....	58
Table 4-2: Mineralogical Compositions of the Stanstead Granite .....	59
Table 5-1: Typical Physical Attributes Relevant to Long-term Safety.....	65
Table 5-2: Main Safety Assessment Codes.....	76

**LIST OF FIGURES**

	<b><u>Page</u></b>
Figure 1-1: Illustration of a Deep Geological Repository Reference Design .....	2
Figure 1-2: Communities Expressing Interest in the APM Siting Process and Status as of 31 December 2018.....	2
Figure 3-1: Interim Storage Facility Locations .....	5
Figure 3-2: Tensile Test Equipment to Obtain the True Stress-Strain Relationship from Initial Load to Fracture at Cambridge Materials Testing Ltd. ....	7
Figure 3-3: Averaged True Stress-Strain Curve of ASME SA-965 F304L Forging Obtained from the Tensile Test.....	7
Figure 3-4: Illustration of Used Fuel Container with Design Features Identified.....	8
Figure 3-5: Prototype of 2018 UFC Insert Design.....	9
Figure 3-6: Fabricated Hemi-Spherical Heads and Cylindrical Shells for the UFC Serial Production .....	10
Figure 3-7: Cross Section of UFC Partial Penetration HLAW Closure Weld Area Showing Cylindrical Shell, Hemi-Spherical Head and Integral Backing Ring .....	11
Figure 3-8: Computer Simulated Stress Fields around UFC Weld Joint .....	12
Figure 3-9: Weld Area Stress Field Variation vs. GMAW Arc Power .....	12
Figure 3-10: Copper Coated Hemi-Spherical Head from Optimization Trials.....	14
Figure 3-11: Bend Test Sample Showing No Delamination of Electrodeposited Copper from the Steel after Several Cycles .....	15
Figure 3-12: Electrodeposited Copper Test Sample after Controlled Distortion around Mandrel Representing > 20 % Elongation .....	15
Figure 3-13: Electrodeposited Copper Microstructure Showing Equiaxed / Uniform (Fine) Grain Structure .....	16
Figure 3-14 Illustration of the Nanovate™ Tank System .....	17
Figure 3-15: New Version of the Rotational Equipment: (a) Loading of UFC and (b) Placement Trials of Cold Spray Gun and Nozzle in Closure Weld Zone Area .....	18
Figure 3-16: Cold Sprayed Copper Ductility Relationships: (a) % Elongation as A Function of Heat Treatment Temperature and Atmosphere and (b) % Elongation as A Function of Microhardness.....	19
Figure 3-17: Cold Spray Gun and Nozzle with Laser Attachment.....	20
Figure 3-18: Buffer Box Emplacement Attachment.....	21
Figure 3-19: Highly Compacted Bentonite Storage Room .....	22
Figure 3-20: Robotic Shaping Cell for Bentonite Blocks (Left – Enclosure, Right – Shaping Robot and Block Table).....	23

Figure 3-21: (a) Schematic of Test Cell for Anoxic Copper Corrosion Investigations at CanmetMATERIALS; (b) Hydrogen Collection Versus Time for 6 Test Cells as a Function of Chloride Concentration, Sulphide Addition and pH Changes. ....	25
Figure 3-22: SEM Micrographs of Cu Coupons after Immersion in Deaerated (a and b), and Aerated (c and d) HNO <sub>3</sub> for Seven Days. ....	26
Figure 3-23: a) Components of Pressure Vessels for Laboratory Bentonite/Microbiology Experiments at Western University. b) Set of Eighteen Pressure Vessels Used to Investigate a Variety of Physical and Chemical Parameters on Bentonite/Microbiology Properties.....	28
Figure 4-1: Isotope Diagram of Porewaters Extracted from Crystalline Rock Showing a Depletion Trend Attributed to the Resaturation Process .....	32
Figure 4-2: Correlation between BET Surface Area and CEC (expressed by probe consumption).....	35
Figure 4-3: 2 SPNE SC/CE Model Simulation of Sorption of Np(IV) (Left) and Se(-II) (Right) on MX-80 .....	40
Figure 4-4: Annual Seismic Activity on the Canadian Shield for 2018 (Red) with Historic Seismicity (Pink).....	42
Figure 4-5: Example of an Overwater Seismic Line Acquired from Round Lake .....	43
Figure 4-6: Map Showing the Study Sites (Marked by Stars) in Northeastern Ontario-Northwestern Quebec .....	44
Figure 4-7: Photograph of Varves Exposed along the Abitibi River, near Twin Falls Dam, Ontario .....	45
Figure 4-8: Plot of Salinity vs Homogenization Temperatures for Samples in the Huron Domain.....	46
Figure 4-9: Isopachs of the Upper Ordovician Shale Units (Collingwood and Rouge River Members) Showing Geographic Variation in Thickness of the Shale Units in Relation to the Study Area (Red Polygon).....	47
Figure 4-10: Average TDS Concentration vs Average Depth for Modelled Domains .....	50
Figure 4-11: Effects of Saturation on BTS for the Cobourg Limestone (Left) and Point du Bois Granite (Right).....	51
Figure 4-12: Effects of Saturation on Damage Threshold and Strength Envelopes in the Cobourg Limestone (Left) and Point Du Bois Granite (Right) .....	52
Figure 4-13: Example Data from Continuous Acoustic Logging of Drill Core .....	53
Figure 4-14: Workflow for Comprehensive Study of EDZ Reliability from Continuum and Discontinuum Models .....	55
Figure 4-15: Influence of Sparse, Non-persistent Jointing on EDZ Development .....	55
Figure 4-16: Details of 1D Thermal Conductivity Experiment of the Cobourg Limestone .....	58
Figure 4-17: A Schematic View of GDS Cell Used in Permeability Testing of the Granitic Samples .....	60
Figure 4-18: Surface Scan and Contact Pressure Measurements of a Natural Fracture and its Three Replicas .....	62
Figure 4-19: Shear Stress vs. Shear Displacement Plots of a Natural Sample under CNL Conditions (N1-CNL) and Replicas under Different CNS Conditions .....	62
Figure 4-20: Visualization of Final Arrangement of FE-M Experiment at Mont Terri Rock Laboratory (Muller et al. 2017).....	63
Figure 5-1: Endplate Sample Pieces Prior to Analysis.....	66
Figure 5-2: Comparison of Experimental Corrosion Rates from Poinssot et al. (2005) with Simulation Results (Stars Connected by a Dashed Line): (A) Full Experimental Data Set; (B) Only Data Measured under Similar Experimental Conditions (i.e., for $\alpha$ -doped UO <sub>2</sub> , in Deaerated Solutions Containing Carbonate) .....	67

Figure 5-3: Temperatures in the Rock along the Vertical Surfaces near the Tunnel at 47 Years after Placement .....73

Figure 6-1: 1001 Metres of Core from Borehole IG\_BH01 .....79

Figure 6-2: Ignace Wabigoon - Location of Borehole Sites 1 to 6 and Area of Interest 1 and 2 .81

Figure 6-3: Hornepayne - Location of Borehole 1, 2, and 3 – For Discussion with People in the Area .....84

Figure 6-4: Manitouwadge - Location of Borehole 1, 2, and 3 – For Discussion with People in the Area .....84

## 1. INTRODUCTION

The Nuclear Waste Management Organization (NWMO) is implementing Adaptive Phased Management (APM) for the long-term management of used nuclear fuel. This is the approach recommended in *“Choosing a Way Forward: The Future Management of Canada’s Used Nuclear Fuel”* (NWMO 2005) and selected by the Government of Canada in June 2007.

The technical objective of the APM approach is a Deep Geological Repository (DGR) that provides long-term isolation and containment, to ensure safety of people and the environment while the radioactivity in the used fuel decays.

The deep geological repository is a multiple-barrier system designed to safely contain and isolate used nuclear fuel over the long term. It will be constructed at a depth of approximately 500 metres, depending upon the geology of the site, and consist of a series of tunnels leading to a network of placement rooms where the used nuclear fuel will be contained using a multiple-barrier system. A conceptual design for a DGR is illustrated in Figure 1-1 for a generic rock setting (the design will be varied for actual crystalline or sedimentary rock conditions).

The NWMO is presently in the Site Selection phase. No site has been selected to host the DGR. The process for selecting a host community is described in *“Moving Forward Together: Process for Selecting a Site for Canada’s Deep Geological Repository for Used Nuclear Fuel”* (NWMO 2010). The steps for evaluating the geological suitability of willing and informed host communities consists of: a) initial screenings to evaluate the suitability of candidate sites against a list of preliminary screening criteria, using readily available information; b) preliminary assessments to further determine if candidate sites may be suitable for developing a safe used fuel repository; and c) detailed field investigations to confirm suitability of one site.

Initially, 22 communities had expressed interest in the program. By 2018 the number of communities engaged in the site selection process had been narrowed to five, based on preliminary desktop assessments of potential geological suitability and potential for the project to contribute to community well-being. The status of each community as of December 2018 is shown in Figure 1-2. All reports completed are published on the NWMO’s site selection website ([http://www.nwmo.ca/sitingprocess\\_feasibilitystudies](http://www.nwmo.ca/sitingprocess_feasibilitystudies)).

The NWMO continues to conduct technical work to support design, site assessment and safety case for a DGR, in parallel with work to engage with and establish a partnership with communities. This report summarizes technical work conducted in 2018. In the near term, this information will support selection of a preferred site by 2023. In the longer term, this will support an impact assessment and licence application at the selected site. NWMO’s overall implementation plan is described in *Implementing Adaptive Phased Management 2019-2023* (NWMO 2019).

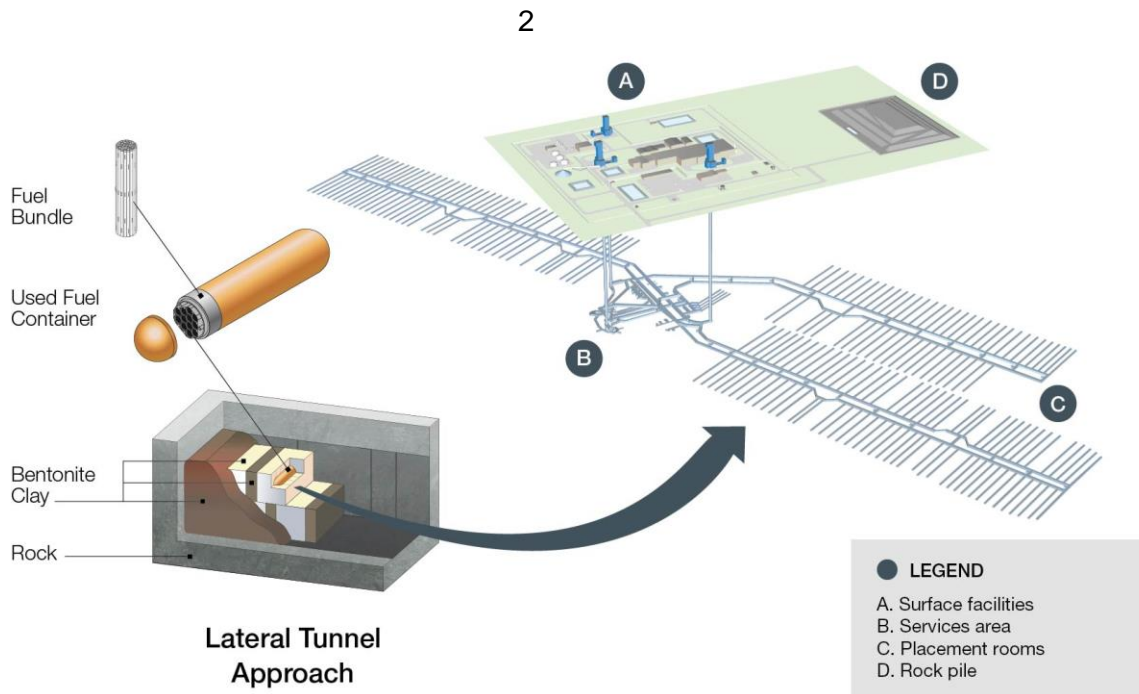


**Figure 1-1: Illustration of a Deep Geological Repository Reference Design**



**Figure 1-2: Communities Expressing Interest in the APM Siting Process and Status as of 31 December 2018**

## 2. OVERVIEW OF NWMO TECHNICAL PROGRAMS

The APM Technical Program includes site investigations, preliminary design and proof testing, and developing the safety case for a used fuel DGR. Work conducted and progress made during 2018 is summarized in this report.

The work is summarized in the following sections divided into Engineering, Geoscience, Repository Safety and Site Assessment.

This work involved 15 universities, as well as a variety of industrial and governmental research partners. A list of the 2018 technical reports produced by NWMO is provided in Appendix A.1. Appendix A.2 and A.3 provide a list of journal articles and conference presentations made by NWMO staff and contractors.

An important aspect of the NWMO's technical program is collaboration with radioactive waste management organizations in other countries. In 2018, the NWMO has formal agreements with ANDRA (France), KORAD (South Korea), NAGRA (Switzerland), NDA (United Kingdom), NUMO (Japan), ONDRAF (Belgium), POSIVA (Finland) and SKB (Sweden) to exchange information arising from their respective national programs to develop a deep geologic repository for nuclear waste.

One important aspect of this collaboration is work undertaken at underground research facilities. In 2018, NWMO supported projects at the SKB Äspö Hard Rock Laboratory in Sweden, the ONKALO facility in Finland, the Mont Terri Underground Rock Laboratory in Switzerland, and the Grimsel Test Site (GTS) in Switzerland. These provide information in both crystalline (Aspo, ONKALO, GTS) and sedimentary (Mont Terri) geological environments.

NWMO was involved with the following projects in 2018:

- POST Project (Fracture Parameterization for Repository Design & Post-closure Analysis) at Äspö and ONKALO;
- FISST demonstration project at ONKALO;
- Deep Borehole Experiment (DB, DB-A) at Mont Terri;
- Long-term Diffusion (DR-B) at Mont Terri;
- Full Scale Emplacement Experiment (FE-G, FE-M) at Mont Terri;
- Hydrogen Transfer (HT) test at Mont Terri;
- Iron Corrosion – Bentonite (IC-A) test at Mont Terri;
- Long-term Pressure Monitoring (LP-A) at Mont Terri;
- Microbial Activity (MA) at Mont Terri;
- Materials Corrosion Test (MaCoTe) at GTS; and
- Gas-Permeable Seal Test (GAST) at GTS.

The NWMO also collaborated with NAGRA, SKB and POSIVA on an ice drilling project (ICE) to establish constraints on the impact of ice sheets on groundwater boundary conditions at the ice-bed contact. The work uses field studies of the Greenland ice sheet, collected as part of the Greenland Analogue Project (2009-2012; final reports published in 2016) and as part of a larger

National Science Foundation project focused on ice dynamics. This project focused on three aspects of boundary conditions that ice sheets place on groundwater systems: 1) transient high water-pressure pulses; 2) glacial-bed water-pressure gradients; and, 3) constraining the flooding and transmissivity of water across the bed. The ICE project ran through the end of 2017, with a final report planned for publication at project completion in 2018-2019.

The NWMO continued to participate in the international radioactive waste management program of the Organisation for Economic Co-operation and Development (OECD) Nuclear Energy Agency (NEA). Members of this group include all the major nuclear energy countries, including waste owners and regulators. NWMO participated in the following NEA activities:

- Working Group on the Characterization, the Understanding and the Performance of Argillaceous Rocks as Repository Host Formations (i.e., Clay Club);
- Crystalline Club (CRC);
- Integration Group for the Safety Case (IGSC);
- IGSC Safety Case Symposium;
- Thermodynamic/Sorption Database Development Project;
- IGSC FEP Database Project;
- Radioactive Waste Management Committee (RWMC);
- RWMC Reversibility & Retrievability Project; and
- Preservation of Records, Knowledge and Memory Project.

The NWMO also continued its participation in the DECOVALEX and BIOPROTA working groups. DECOVALEX is an international working group on Thermal-Hydraulic-Mechanical (THM) modelling. NWMO participated in the Task E on modelling a heater experiment in the clay rock at the Andra Bure underground facility. BIOPROTA is an international working group on biosphere modelling. The main projects in 2018 were the C-14 Project and the BIOMASS 2020 Update.

### 3. REPOSITORY ENGINEERING

The main activities in the Repository Engineering program during 2018 were: used fuel transportation; the proof testing program, engineered barrier science, and design. Summaries of the research and development activities are provided in the following sections.

#### 3.1 USED FUEL TRANSPORTATION

##### 3.1.1 Used Fuel Transportation System Development

Canada's used nuclear fuel is currently safely managed in facilities licensed for interim storage. These facilities are located at nuclear reactor sites in Ontario, Quebec, and New Brunswick, and at Atomic Energy of Canada Limited's sites at Whiteshell Laboratories in Manitoba and Chalk River Laboratories in Ontario as illustrated in Figure 3-1.



**Figure 3-1: Interim Storage Facility Locations**

As part of its responsibility for long-term management of this used fuel, the NWMO will be responsible for the transport of this fuel to its selected repository site. Based on current projections and announced life plans for the reactor fleet, approximately 5.5 million bundles will need to be transported to the repository site from these interim storage facilities.

Key components of the used fuel transportation system include:

- transportation modes;

- conveyances and fleets;
- routing;
- transportation infrastructure;
- interfacing facility infrastructure at interim storage facilities and at the DGR;
- transportation packages;
- nuclear security / escort requirements;
- emergency response and recovery requirements;
- logistics, i.e. cycle times including transit times and non-transit times for on- and off-loading of transport packages; and
- operations, i.e. operations at facilities, operations during transport for modes of transport, escort operations, communication, tracking and monitoring.

Technical, operational and cost evaluations of options for the used fuel transportation systems and key components (listed above) are ongoing, and are a focus of detailed study for 2018. The objective is to compare various options for transportation systems including modes (i.e. road, rail, and combination), package designs, and operational considerations considering region specific attributes and infrastructure. The purpose is to confirm and update the reference transportation system design for the 2021 Life Cycle Cost Estimate. This work is expected to conclude in 2019.

### **3.1.2 Transportation Package Material Testing**

The used fuel transportation packages are designed to withstand severe accident conditions. The certification basis for these packages includes both field testing and numerical modelling. Basic material properties for the materials used in these packages can be obtained from the ASME (American Society of Mechanical Engineers) or the ASTM (American Society for Testing and Materials) code. However, additional material properties beyond yield strength are required for some advanced stress or strain analyses of extreme conditions. These properties must be obtained through physical testing. NWMO has conducted a series of mechanical tests on sample material coupons to establish a database of material properties beyond what is currently available.

Materials being tested include stainless steel forgings, plates, and round bars. To capture the variation of the material properties due to various materials fabrication processes and environments, material coupons from multiple material heats were collected from different manufacturers. Additionally, the coupons were taken from various locations within a given heat to capture the variation across the heat as well as across the volume of materials received. The coupons collected were then subjected to a series of tensile tests to obtain mechanical properties of the material, such as Young's modulus, yield strength, ultimate strength, and elongation at various temperatures (i.e., room temperature, 100°C and 600°C). Specialized equipment, as shown in Figure 3-2, was used to obtain the true stress-strain curve from initiation of the test to rupture of the specimen. An example of such a curve is shown in Figure 3-3. The material properties obtained will be used in the finite element modelling of the used fuel transportation packages for enhanced mechanical integrity evaluations.

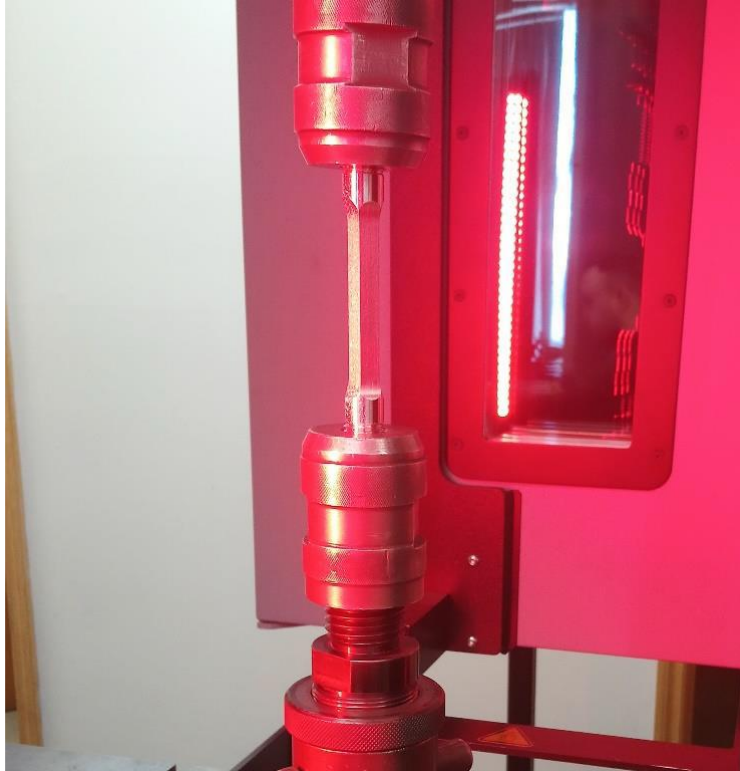


**Figure 3-2: Tensile Test Equipment to Obtain the True Stress-Strain Relationship from Initial Load to Fracture at Cambridge Materials Testing Ltd.**

ASME SA-965 F304L Forging, Heat #: S3401 and S4291, 1/4t,  
Transverse, 20°C, Sample #: 763473 and 763474  
Average True Stress vs True Strain

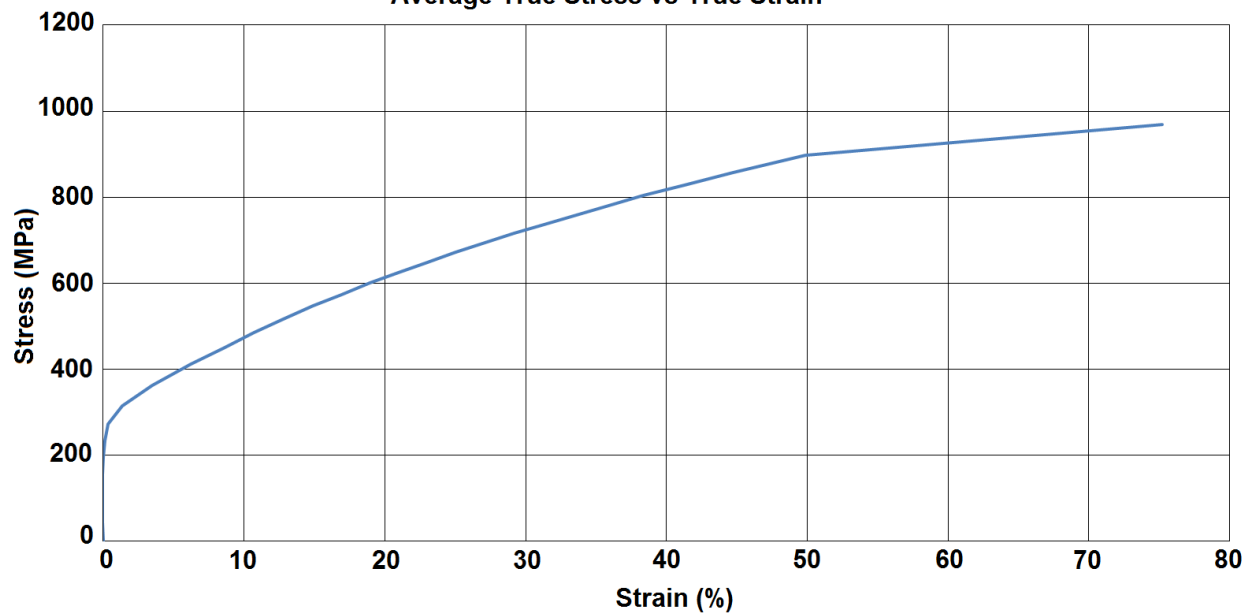


**Figure 3-3: Averaged True Stress-Strain Curve of ASME SA-965 F304L Forging Obtained from the Tensile Test**

### 3.2 USED FUEL CONTAINER (UFC)

In 2018, the NWMO focused on UFC serial production and optimization of the UFC manufacturing processes. This is part of the Proof Test Program to validate the design of the reference Used Fuel Container (Figure 3-4). Advancement in design qualification, manufacturing and inspection technology are documented in the following sections.

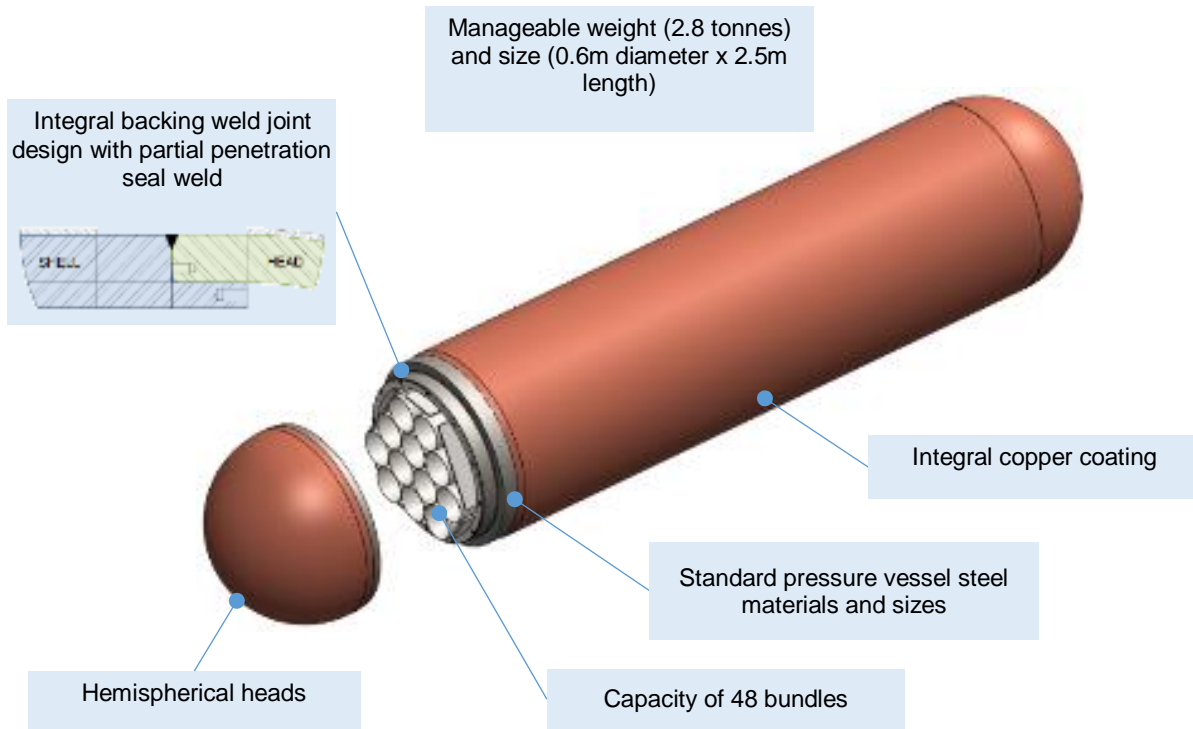


**Figure 3-4: Illustration of Used Fuel Container with Design Features Identified**

#### 3.2.1 Used Fuel Container Design

The UFC Design Specification is a comprehensive document that summarizes the design of the UFC. It was completed in 2017 and submitted to the CNSC (Canadian Nuclear Safety Commission) for a pre-licensing technical review in 2018. The purpose of this review is to identify gaps between the UFC design at the current stage and existing regulatory requirements and expectations. This review is not for licensing purposes (i.e. certification), but helps the NWMO improve the design and documentation to achieve a licensable UFC product.

One of the challenges of the UFC design is the lack of a technical standard for disposal containers. Significant efforts have been spent by NWMO assessing the applicability of existing industrial codes and standards, such as the ASME Boiler and Pressure Vessel Code (BPVC), and developing suitable rules for the design of a used fuel container for a Deep Geological Repository (DGR). These efforts led to the development of design methods and criteria for the UFC Design Specification.

Based on the UFC Design Specification, the mechanical design qualification activities were launched at the end of 2017 and continued into 2018. The purpose of the design qualification is to demonstrate that the UFC design fulfills the intended containment function in the DGR

environment, meets the regulatory requirements, and follows best engineering practices. The qualification activities are divided into three parts with each part containing a number of analyses or calculation activities. The first part contains the compilation of input data and calculation of specific loads to be used in the analyses. The second part focuses on the evaluation of the mechanical integrity of the steel structural vessel. The third part focuses on the evaluation of the copper coating.

The first part and the majority of the analyses activities in the second part were completed in 2018, except for the evaluation of impact loads (e.g., the dynamic impact loads resulting from a container drop, mechanical impact during operation and rock impact during a placement room cave-in event). The analyses showed that the UFC structural vessel is able to maintain its mechanical integrity under evaluated operational and repository loads, including the extreme loads from the hypothetical event associated with a future glaciation and fire accidents. The evaluation of the UFC resistance to impact is in progress and will be completed in 2019.

UFC design improvement activities were continued in the past year. A dimensional tolerance stack-up analysis was performed to confirm manufacturability of the UFC. Options on improving manufacturability based on the current fabrication processes were also explored, such as alternative weld joint design and the possibility of fabricating the UFC lower assembly (i.e., shell welded to lower hemi-spherical head) as a one piece component.

The conceptual design of the UFC internal structure which houses 48 used fuel bundles, known as the Insert (Figure 3-5), was completed in late 2017. The Insert design was modified to implement better safety and manufacturability features. Prototypes of the Insert were fabricated in 2018. Physical testing, design optimization, and determination of a cost-estimate for high-volume production are activities for 2019 and beyond.



**Figure 3-5: Prototype of 2018 UFC Insert Design**

### 3.2.2 Used Fuel Container Manufacturing & Inspection

#### 3.2.2.1 UFC Serial Production

In 2018, the NWMO began execution of the UFC serial production initiative of the Proof Test Program. The objective of this work is to fabricate up to 20 UFCs using reference materials, fabrication and inspection technologies and to verify the product against the reference design requirements and quality acceptance standards. During the execution of this work, further design refinement and manufacturing optimizations will be applied as necessary based on feedback from testing, inspection, and validation programs.

In 2018, UFC component steel materials, transportation crates, and industrial racking were procured. A Request for Proposal for machine shop services was issued. Machining of the UFC components, welding, Non-Destructive Examination (NDE), and copper coating services will be arranged and executed starting in 2019, to be completed by 2021.

Figure 3-6 shows the hot-formed hemi-spherical heads and the extruded cylindrical shell fabricated for the UFC serial production. During manufacturing, the UFC structural vessel is referred to as two components; the upper hemi-spherical head and the lower assembly (lower hemi-spherical head welded to cylindrical shell).



**Figure 3-6: Fabricated Hemi-Spherical Heads and Cylindrical Shells for the UFC Serial Production**

#### 3.2.2.2 HLAW Closure Weld Development

NMWO's welding vendor Novika Solutions (La Pocatière, Quebec, Canada) performed a comprehensive Hybrid Laser Arc Weld (HLAW) process optimization study in 2015 to determine weld parameter tolerances within which sound closure welds can be consistently made under a specified range of weld joint fit-up conditions. HLAW is a welding process that combines laser welding with Gas Metal Arc Welding (GMAW). GMAW is more commonly referred to as MIG welding (Metal Inert Gas). Following this study, Novika prepared a reference Welding Procedure

Specification (WPS) and Procedure Qualification Record (PQR) in accordance with ASME BPVC Sections IX and III (Division 3 Subsection WC) for use on prototype UFC lower assembly and closure welds.

In 2018, the NWMO contracted the Fraunhofer Institute (Berlin, Germany) to conduct thermomechanical modeling of NWMO's HLAW process as part of ongoing investigations into weld quality. This modeling was performed to determine the stress state of the partial penetration weld (Figure 3-7) and surrounding areas of the weld joint. Fraunhofer investigated the stresses resulting from the HLAW process on NWMO's weld joint design as well as possible weld parameter or joint design modifications to optimize the weld. Results of the modeling of the reference weld design/process are shown in Figure 3-8. As expected, modeling confirmed a higher level of stress at the root area resulting from the partial penetration nature of the weld.

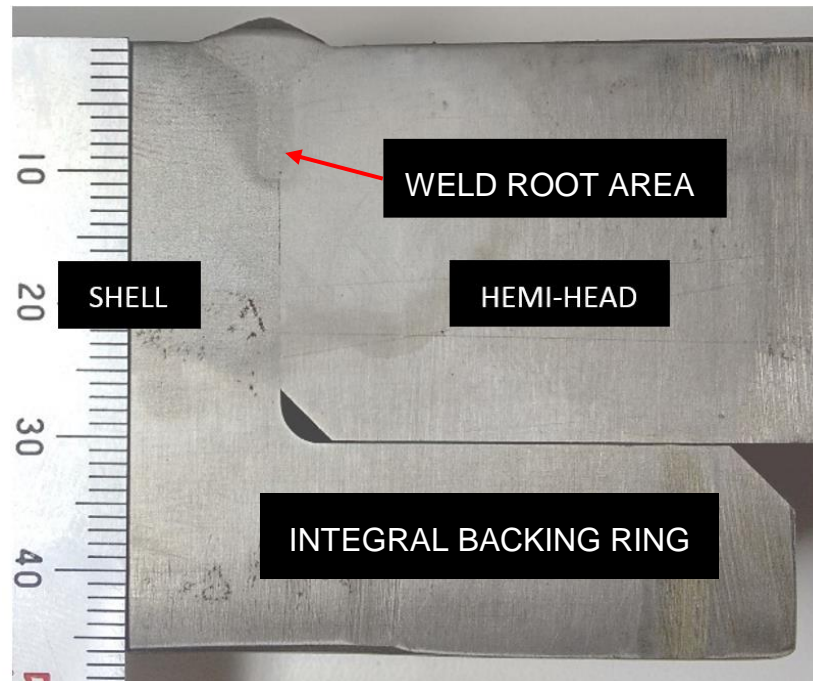
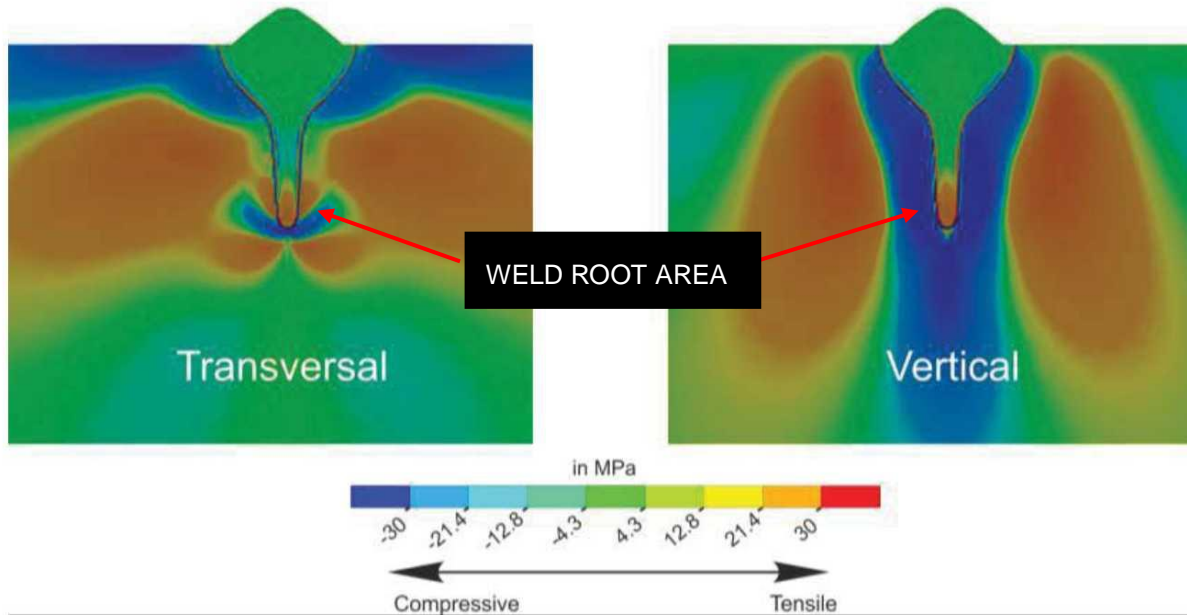


**Figure 3-7: Cross Section of UFC Partial Penetration HLAW Closure Weld Area Showing Cylindrical Shell, Hemi-Spherical Head and Integral Backing Ring**

Additional modelling was performed to check the resulting stress fields generated when varying process parameters (laser/GMAW separation, GMAW arc power, and weld speed) in order to reduce the stresses at the weld root area. Results and recommendations from the modeling work (Figure 3-9) have been incorporated into the HLAW development program with test welds being prepared and assessed by Novika Solutions.



Note: Transversal stress oriented "into" the image.

**Figure 3-8: Computer Simulated Stress Fields around UFC Weld Joint**

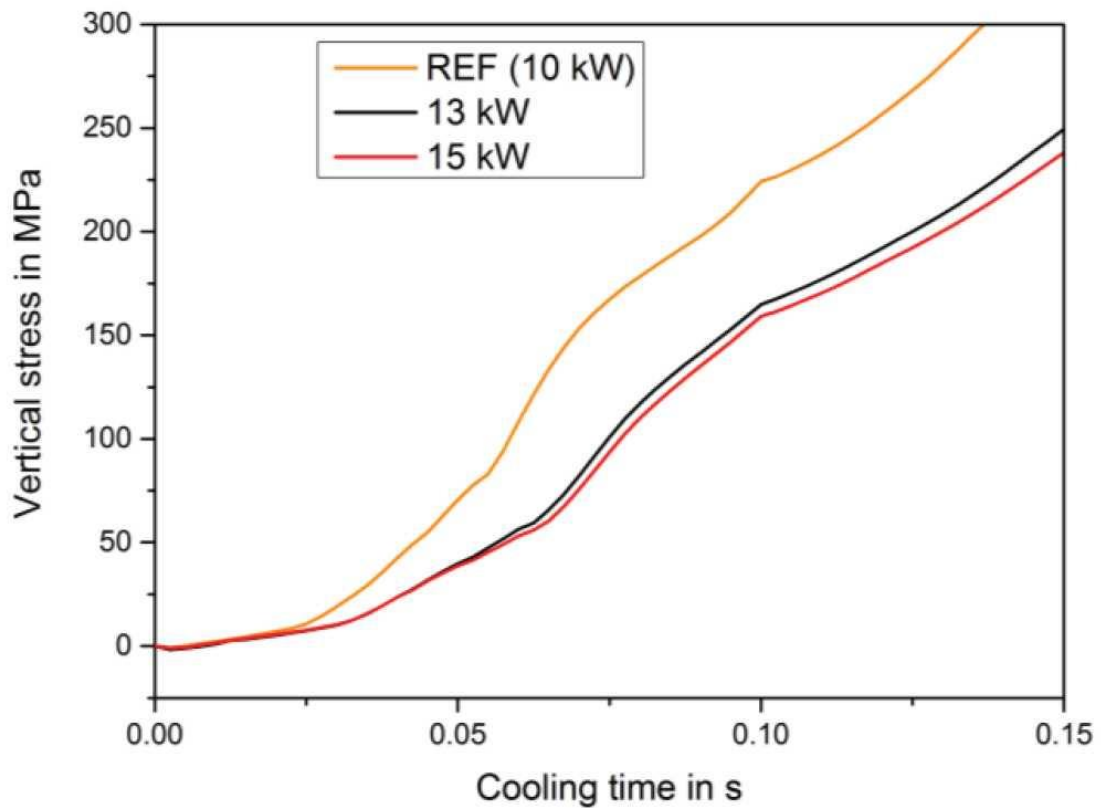


**Figure 3-9: Weld Area Stress Field Variation vs. GMAW Arc Power**

### 3.2.2.3 Non-Destructive Examination Development

In 2015, Nucleom Inc. (Quebec City, Quebec Canada) commenced work on the Non-Destructive Examination (NDE) development program for the inspection of the UFC closure welds and external copper coating. The main objectives of the NDE development program were to select, develop, and qualify establish ultrasonic and eddy current NDE methods appropriate for the volumetric and surface examination of the UFC partial penetration welds and external copper coating. The results of the program were finalized NDE methods, recommended inspection equipment (probes, calibration blocks, etc.), and the expected inspection sensitivity (target flaw size).

In 2018, these results were used to develop preliminary procedures for the inspection of full-scale UFC components in the serial production demonstration campaign. These inspection procedures detailed the techniques, equipment, and acceptance criteria used in non-destructive inspections. The preliminary inspection procedures are to be trialed on full-scale UFC components, and revised (if required) prior to use in the serial production campaign in 2019.

### 3.2.2.4 Copper Coating Development

After the successful application of both electrodeposition and cold spray processes for the prototype UFCs in previous programs, a manufacturing optimization effort at the pilot scale was initiated. The main objective is to refine the two technologies with respect to manufacturing methods using technologies and equipment that are amenable for serial production.

#### Electrodeposition Process Development

Since 2012, NWMO has conducted a multi-phased program with the vendor Integran Technologies Inc. (Mississauga, Ontario, Canada) for the development of a copper electrodeposition technology via the use of a pyrophosphate (solution chemistry) system. This program has resulted in the acquisition of baseline data, process optimization and technology transfer for the application to prototype UFCs.

In previous years, the NWMO and Integran have demonstrated the method's suitability for producing a range of copper coated samples, from small (i.e., coupon size) scale through full-sized hemispherical heads and lower assemblies. Following this, a program was put in place in 2016 to optimize and improve manufacturing methods for eventual use in the pilot line and serial production campaign. Since then, three primary streams of work were carried out: (1) process tolerancing on a coupon scale, (2) pilot line construction and commissioning, and (3) process optimization, demonstration and validation for the production of hemi-spherical heads. During the 2018 timeframe, the latter was performed and completed rendering the process for hemi-spherical heads ready for serial production to be initiated during 2019.

Process optimization for the hemi-spherical head consisted of performing 13 plating trials while implementing improvements focused on providing the best finish possible for the copper coating, namely a significant reduction of defects such as pits, nodules, and machining induced asperities. Major improvements were achieved by minimizing the occurrence of nodules in the coating process and refining the steel substrate surface roughness specification.

Following the optimization trials, all processing parameters were locked-down and used for demonstration and validation. During this phase of work, three hemi-spherical heads were produced and subjected to thickness and visual inspection (see Figure 3-10). One of the three

was destructively tested to verify all critical material performance requirements, including chemistry (or purity), copper-to-steel adhesion, copper strength (hardness), and microstructure. Table 3-1 provides a summary of the material performance test results. Figure 3-11 through Figure 3-13 show samples of these test results. Future work (in 2019) for electrodeposition of copper includes pursuing a similar process optimization effort for the lower assembly. This will be carried out in a newly designed system that will be discussed in the next section.

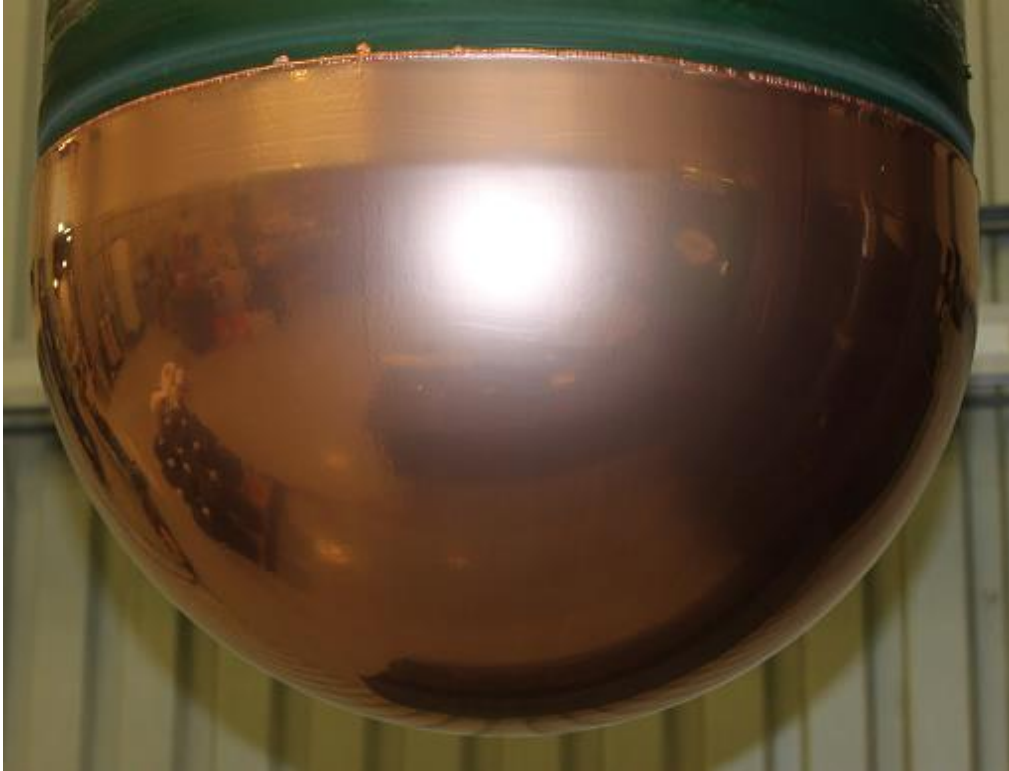


**Figure 3-10: Copper Coated Hemi-Spherical Head from Optimization Trials**

**Table 3-1: Summary of Electrodeposited Copper Material Performance Test Results for Hemi-Spherical Head**

<b>Criteria</b>	<b>Method</b>	<b>Requirement (Method)</b>	<b>Result</b>
Copper Purity	ASTM E53: Gravimetry	> 99.9 %	99.9+ %
Adhesion	ASTM B571: Modified bend test	No delamination along coating substrate interface	PASS
Strength	ASTM E384: Microhardness	90 – 200 HV	95 – 106 HV
Ductility	ASTM B489: Controlled distortion around mandrel	> 20 % elongation	PASS
Microstructure	ASTM E3: Microscopic inspection (etched cross-sections)	Equiaxed / uniform (fine) grain structure	PASS



**Figure 3-11: Bend Test Sample Showing No Delamination of Electrodeposited Copper from the Steel after Several Cycles**

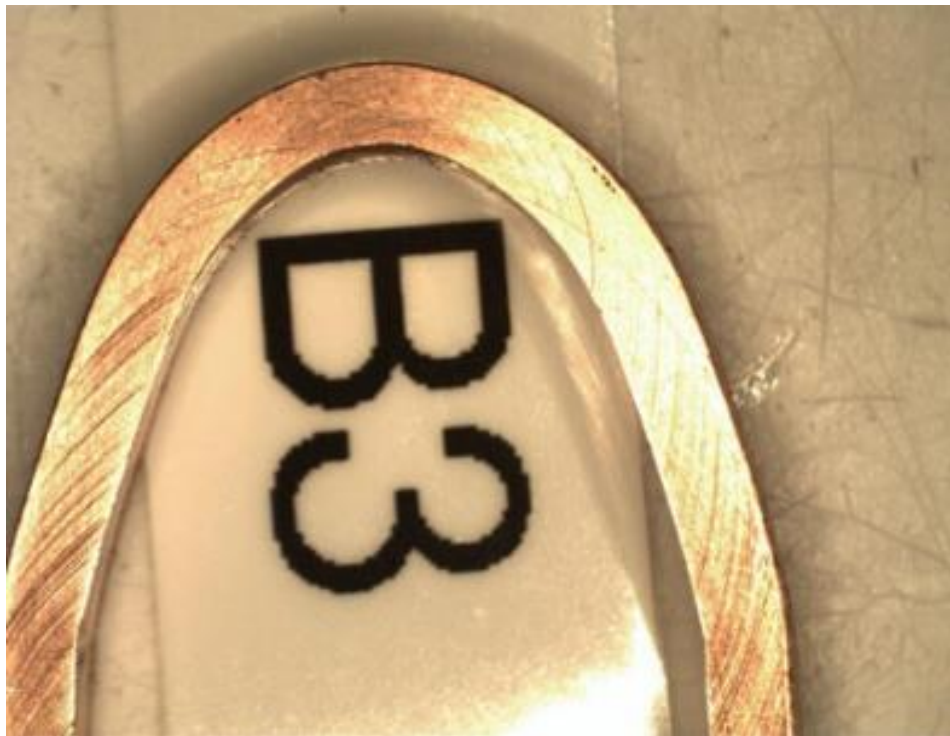


**Figure 3-12: Electrodeposited Copper Test Sample after Controlled Distortion around Mandrel Representing > 20 % Elongation**

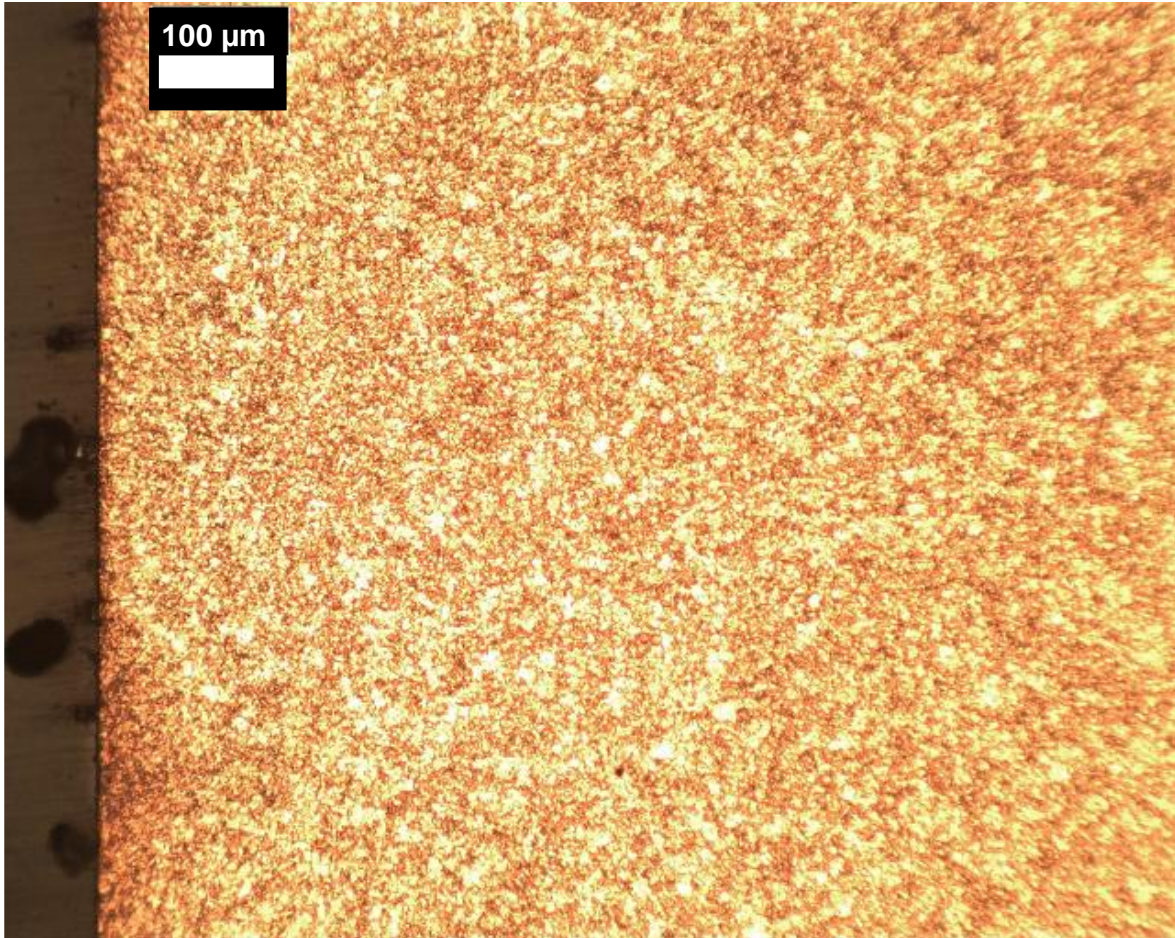


**Figure 3-13: Electrodeposited Copper Microstructure Showing Equiaxed / Uniform (Fine) Grain Structure**

#### Serial Production Equipment Design & Fabrication for Electrodeposition

In 2018, the design of an improved electrodeposition tank was completed. This design took into consideration the experience from 2017 concerning the main root cause for “nodule” formation. This design is customized for processing lower assemblies and is based on the same tank configuration currently employed at Integran Technologies, Inc. for processing hemi-spherical heads. Figure 3-14 presents the design of the “Nanovate™ Tank System” (NTS) for processing lower assemblies.

Upon completion of the design, fabrication was initiated in two phases and is expected to be delivered, installed, and commissioned at Integran in mid-2019.

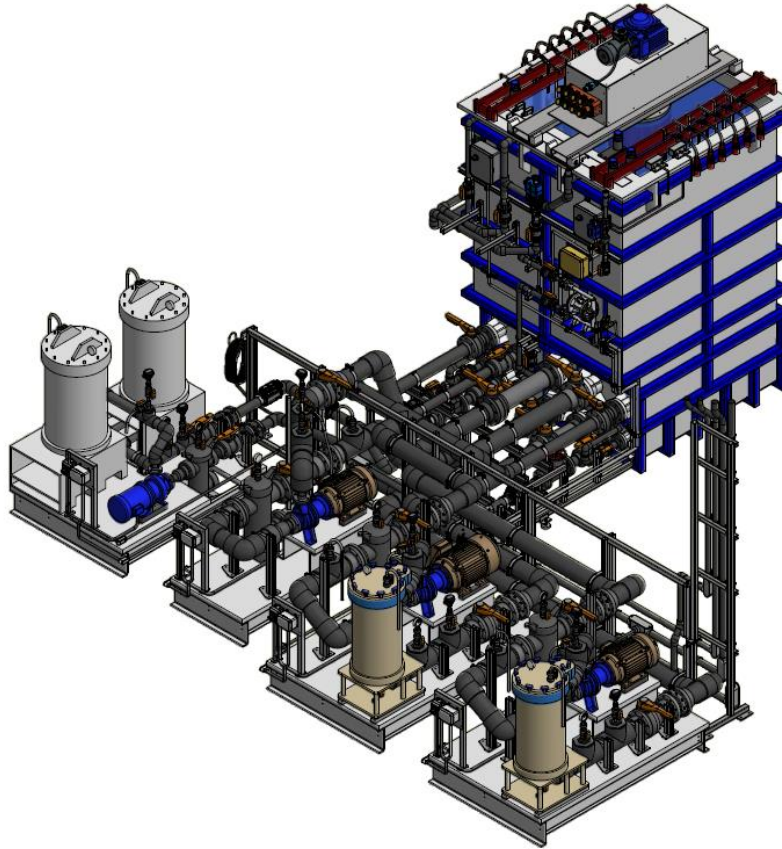


**Figure 3-14 Illustration of the Nanovate™ Tank System**

### Cold Spray

Following the successful development of a copper cold spray method to completely coat UFC components (hemi-spherical heads and lower assembly) by the National Research Council (NRC) (Boucherville, Quebec, Canada) in 2012 and 2013, the NWMO had focused on adapting this technique to the UFC closure weld zone. The closure weld zone remains uncoated prior to the loading of used fuel, and is to be coated after the attachment of the upper hemi-spherical head, closure welding and weld inspection.

Significant optimization was carried out over 2014 to 2017 towards developing a reference process including a heat treatment method, surface preparation (e.g., mechanical abrasion) and laser preheating of the substrate. Where possible, automation was implemented in anticipation of future use in a radioactive environment. The work in 2017 concluded with a demonstration of the techniques on a representative scale.

In 2018, two additional streams of work performed. First, rotational equipment that had been used for HLAW technology development was installed. The goal was to obtain an improved UFC support and rotation device, especially in accommodating a fully loaded UFC (simulated with a concrete plug inside). The rotation equipment was modified to accommodate the cold spray process by creating an access point for the spray gun nozzle allowing it to traverse the width of the closure weld zone (see Figure 3-15). The new version of the rotational equipment was delivered and commissioned at the NRC.



(a)



(b)

**Figure 3-15: New Version of the Rotational Equipment: (a) Loading of UFC and (b) Placement Trials of Cold Spray Gun and Nozzle in Closure Weld Zone Area**

Secondly, an investigation was carried out to better understand the ductility behaviour (percentage elongation) of the cold sprayed copper with focus on heat treatment conditions, namely temperature and atmosphere (i.e., air and argon gas), while keeping the spray configuration constant. The results of this study yielded a relatively linear relationship with elongation (through tensile testing) and temperature (see Figure 3-16a). In addition to this, it was also concluded that elongation is linearly correlated to hardness (see Figure 3-16b), and therefore, hardness can be used as a convenient means to assess ductility on the cold sprayed closure weld zone using a portable hardness tester for each spray configuration. Furthermore, no notable effect of atmosphere was observed, thereby adding to the robustness of this important process step. These results were transferred to the current heat band method for applying the treatment to the closure weld zone of the UFC and found to be effective at meeting and exceeding the minimum requirement.

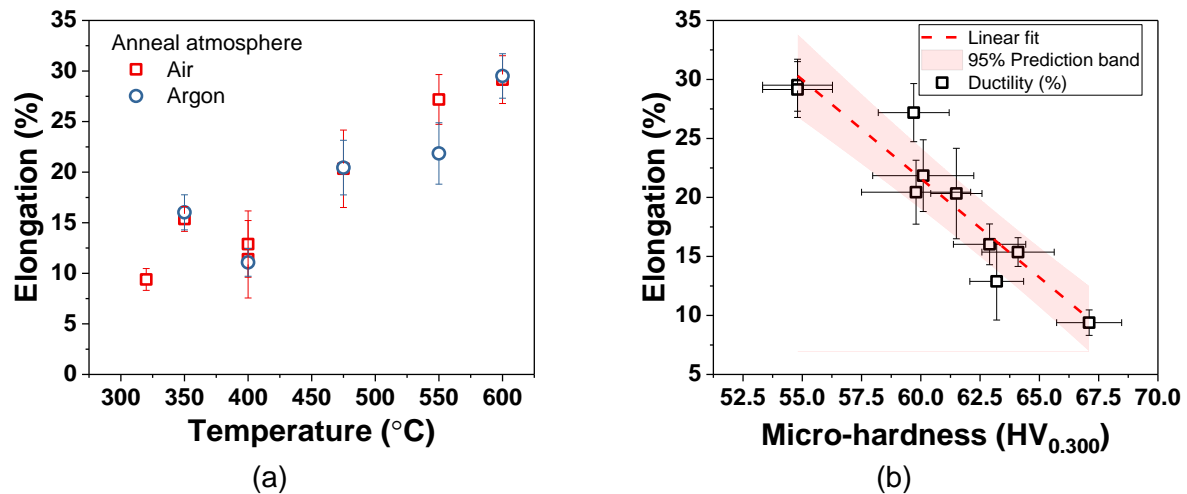


**Figure 3-16: Cold Sprayed Copper Ductility Relationships: (a) % Elongation as A Function of Heat Treatment Temperature and Atmosphere and (b) % Elongation as A Function of Microhardness**

In the later part of 2018, a new program was initiated to further advance aspects of the reference process with two main objectives: (1) to eliminate the use of helium in the cold spray process; and (2) to develop non-contact techniques for surface preparation and heat treatment for operations in the Used Fuel Packaging Facility (UFPP).

In regards to helium elimination, the goal is to remove helium from the initial “bond layer” step in order to reduce costs for future mass production. In the reference process, helium is employed for the first several passes in the cold spray process due its ability to accelerate particles at a velocity high enough to adhere to the steel surface. Once this steel-to-copper “bond layer” is complete, the particle velocity can be lowered and still form quality bond between the subsequent copper layers. This allows for nitrogen to be used as the carrier gas to build-up the remainder of the required thickness. It is proposed to use laser to heat or soften the steel prior to the trailing cold spray spot so that the copper particles can adhere to the steel surface with nitrogen as the carrier gas. Figure 3-17 shows the cold spray gun with a laser attachment.

Laser assistance is also proposed for use in the second objective to develop non-contact techniques for surface preparation and heat treatment. The reference process currently employs a mechanical abrasion technique to remove scale or oxide from the steel surface prior to cold spray. In this new program, laser ablation, which is known to work well for this purpose on steel, will be investigated as a candidate technique. Furthermore, a laser assisted technique would also be used to replace the current post-spray heat treatment of the cold sprayed copper. Preliminary evidence suggests that obtaining a recrystallized microstructure with laser is feasible. Additional investigations will be performed to prove this concept and eventually optimize it for implementation into the current reference process. Work on all fronts using laser assistance will be pursued in 2019.

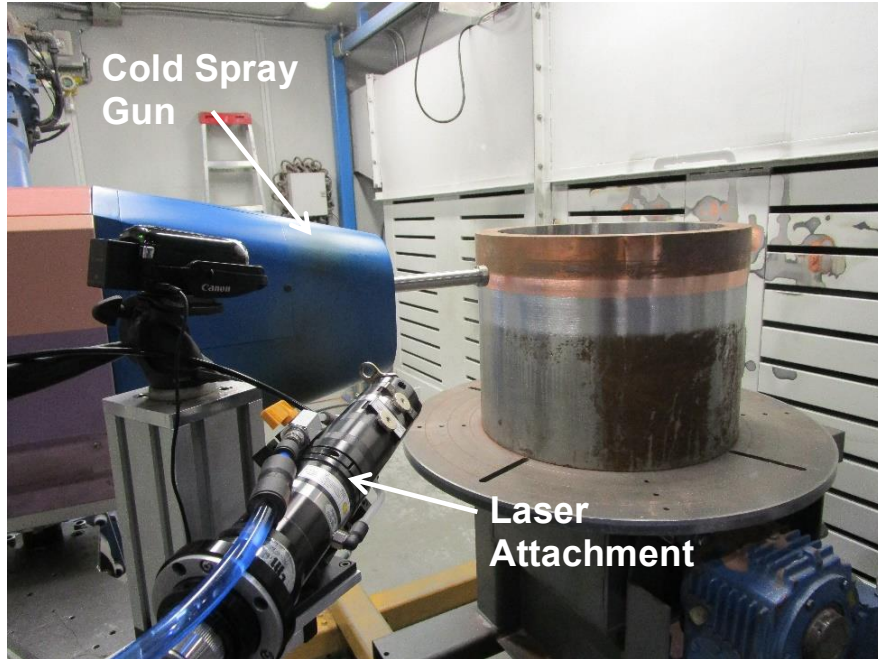


**Figure 3-17: Cold Spray Gun and Nozzle with Laser Attachment**

### **3.3 BUFFER AND SEALING SYSTEMS**

The NWMO continued to support the development of the buffer and sealing systems including optimized manufacturing, storage, and emplacement technology for the Highly Compacted Bentonite (HCB) blocks that are placed directly around the UFCs.

#### **3.3.1 Emplacement Equipment**

An enhanced emplacement technology development program was completed in 2018. The two concepts were advanced independently, one with an external design organization for design and build, and the second performed by the NWMO for design only.

The finalized prototype emplacement equipment was designed and built by Medatech Engineering Services (Collingwood, Ontario, Canada) to NWMO requirements, see Figure 3-18.



**Figure 3-18: Buffer Box Emplacement Attachment**

The equipment is a purpose built attachment that replaces the fork lift attachment of a standard heavy forklift. The attachment provides a rigid surface to lift and emplace the Buffer Box assembly into location. The ends of the attachment have paddles containing inflatable air bags to apply compressive forces to the Buffer Box Assembly during lift and emplacement activities. The equipment is designed to keep the Buffer Box assembly in compression.

### **3.3.2 Highly Compacted Bentonite Storage Room**

Literature reviews and practical experience from international programs identify the need to keep the HCB at a uniformly high humidity to minimize water loss. The HCB blocks are consolidated with a moisture content of 20%. NWMO's confirmatory experiments observed that blocks will crack if the relative humidity in the storage area drops below ~75%. A storage room was designed and assembled to house the blocks that have been fabricated. The HCB blocks will be stored in this room long-term until the full scale emplacement trial is completed with no loss in quality. See Figure 3-19 for a photograph of the Storage Room.



**Figure 3-19: Highly Compacted Bentonite Storage Room**

### **3.3.3 Shaping Cell Operation**

In order to provide the precisely controlled dimensions necessary for implementation of the technology, a robotic shaping cell was designed and built. The cell was tested and commissioned at Novika Solutions in 2017, and installed at the NWMO Oakville engineering test facility in 2018. The shaping cell consists of an environmental enclosure to control the humidity, a feed table to bring the block into and out of the cell, a robot outfitted with a spindle for machining, and a rotation frame to permit block lifting and rotation to change block orientation. The shaping cell will be used as a development platform to investigate buffer box configurations and prepare blocks for the emplacement trial. The shaping cell will be used extensively in 2019-2020 to support the planned emplacement trials in 2021-2022. See Figure 3-20 for the shaping cell.



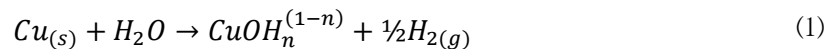
**Figure 3-20: Robotic Shaping Cell for Bentonite Blocks (Left – Enclosure, Right – Shaping Robot and Block Table)**

### 3.4 MATERIAL STUDIES

#### 3.4.1 Used Fuel Container Corrosion Studies

##### 3.4.1.1 Anoxic Corrosion of Copper

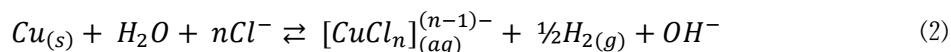
Although oxygen will be present in the DGR for a brief period following closure and decommissioning, anoxic conditions will persist for the majority of the repository's lifetime. Using thermodynamics, it is possible to predict very long lifetimes of copper in these conditions, an assertion supported by natural analogues such as "native" copper, which can be excavated as a metallic species that is millions or even billions of years old. Despite this, in some experiments where copper is placed in oxygen-free water, trace amounts of hydrogen have been detected, and some researchers have claimed the hydrogen is a corrosion product of Equation (1).



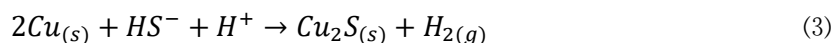
Despite being forbidden by classical thermodynamics and the inability of independent researchers to reproduce experimental results or unequivocally identify the copper corrosion product, " $\text{CuOH}_n^{(1-n)}$ ", the existence of such a mechanism must be validated or invalidated by the NWMO.

Equation (1) is related to a second, anoxic corrosion of copper that occurs in acidic, highly saline solutions according to Equation (2). As per the above example, some observations of hydrogen have been made during immersion of copper in brine; however in this case trace hydrogen is expected as the system comes to equilibrium. In a DGR, the forward (corrosion) reaction will be suppressed owing to the neutral (i.e. not acidic) pH, the low diffusivity of the copper-chloride reaction products through bentonite clay, and the dissolved hydrogen in the

groundwater that is present in the anoxic condition. At extremely high brine concentrations (i.e. 5 to 10 X seawater), there is some question regarding the precise equilibrium conditions, which require characterization and quantification.



The third process of interest, anoxic copper corrosion in the presence of sulphide, Equation (3), is afforded the largest UFC copper corrosion allowance. Although Canadian groundwater contains virtually no sulphide, it is possible that microorganisms existing far away from the UFC could produce sulphide from their metabolic processes, which would enter the groundwater. Due to the presence of the bentonite buffer, diffusion of sulphide inward to the UFC will be slow. However, once the sulphide reaches the container corrosion proceeds quickly; thus more information is required with respect to the mechanism of this process, as well as the affect other groundwater species may have on the process or the products of the process.



Work being conducted by NWMO at CanmetMATERIALS (Hamilton, Ontario, Canada) in collaboration with the University of Toronto investigates the individual and combined effects of Equations 1-3 along with pH effects. This work utilizes a specialized corrosion cell, depicted in Figure 3-21(a), which maintains an anoxic environment at 75 °C while allowing for the introduction of chemical species (gas or liquid) into the cell. Hydrogen is measured by purging the headspace of the cell and the amount is correlated to a rate of corrosion by assuming the reactions shown in Equation 1-3 take place. Notably, the release of trapped hydrogen from within the copper, or the production of hydrogen from other corrosion reactions within the cell (i.e. through the interaction of steels and water) will be assumed to be copper corrosion using this calculation method, and this will overestimate copper corrosion. Similarly, hydrogen produced via corrosion that is absorbed by the metal will be missed in a corrosion calculation; although this process is not expected. Nonetheless, a representative graph of the results is shown in Figure 3-21(b) which plots the cumulative hydrogen collected versus time as a function of the various chemical environments discussed above. Using the reaction stoichiometries above, (maximum) copper corrosion rates can be calculated and used to assess a corrosion allowance.

The corrosion experiments are ongoing but preliminary conclusions can be drawn following the approximately two year duration of the program. In pure water, hydrogen was evolved, and initial corrosion rates were calculated to be a maximum of 0.22 nm/year before falling below the detection limit of the experiment after 50 days. Similar results were seen for dilute chloride solution, as indicated by the grey lines in Figure 3-21(b). However, at this point, neither the initial nor final copper samples have been analyzed for hydrogen content, so it is unclear what impact (if any) hydrogen release or absorption may have on these measurements.

When the hydrogen evolution halted in pure water, introducing neutral, highly saline solutions did not produce a significant effect on corrosion rates. For these cells, a maximum individual value of 0.03 nm/year of copper corrosion (blue lines) was calculated. As expected, the introduction of sulphide to either saline or pure water environments did result in hydrogen evolution, producing low corrosion rates of 0.1 and 0.2 nm/year, respectively. The largest of these miniscule rates would produce less than 0.25 mm of damage in 1 000 000 a, and are consistent with the NWMO total corrosion allowance of 1.27 mm over that period of time.

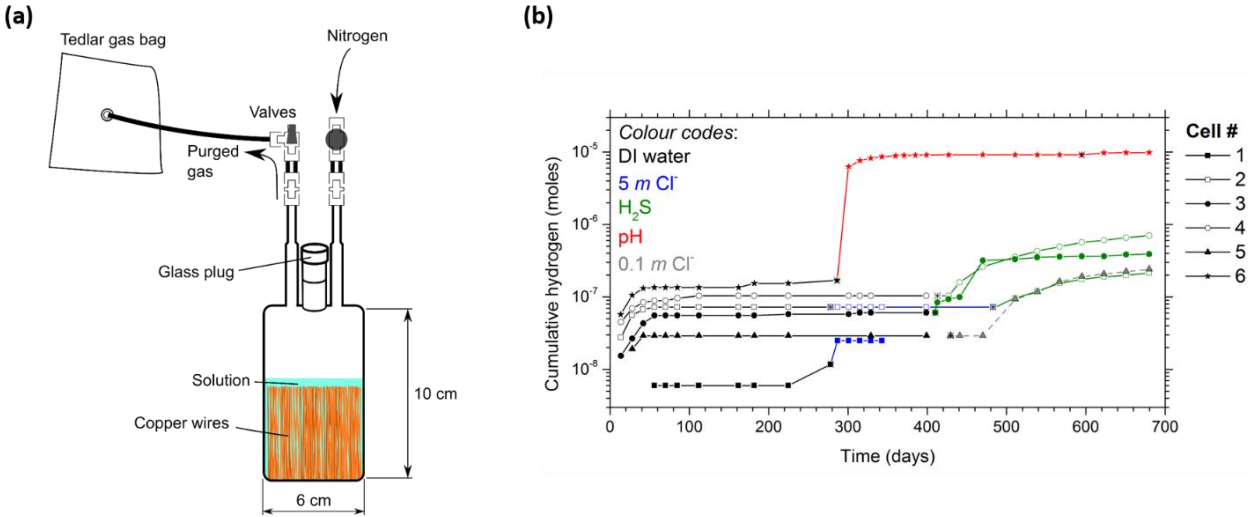


**Figure 3-21: (a) Schematic of Test Cell for Anoxic Copper Corrosion Investigations at CanmetMATERIALS; (b) Hydrogen Collection Versus Time for 6 Test Cells as a Function of Chloride Concentration, Sulphide Addition and pH Changes.**

### 3.4.1.2 Corrosion of Copper Coatings

With the development of copper coatings, it has become necessary to investigate different copper forms to ensure that corrosion does not occur preferentially via mechanisms that do not occur for wrought coppers. Because thermodynamic arguments are used (as opposed to kinetic arguments) to describe the ability of copper to have a very long life in the repository, there is little risk of this occurring in a general sense, but there is a possibility that localized effects may differ among copper species. NWMO has done extensive work in this area with its research partner, Western University, including:

- Long-term exposures of copper samples;
- Electrochemical polarizations to simulate corrosion;
- Comprehensive surface analysis to assess samples before and after the exposures noted above.

Despite more than five years of effort, little difference can be found among the samples, regardless of test method. Only very slight differences can be seen only where extensive cycles of electrical currents to initiate copper oxidation (i.e., corrosion) are used. In these experiments, there is some weak evidence that the copper coatings made by electrodeposition or cold spray undergo a very minor preferential grain etching, such that corrosion depth may be very slightly greater near grain boundaries. Studies are ongoing to quantify this depth, which at present appears to be a few micrometres (and thus, insignificant to the safety of copper coatings on the order of 3 mm thick). An upcoming Technical Report will provide a comprehensive description of the current understanding of copper coating corrosion.

### 3.4.1.3 Corrosion of Copper in Radiolytic Environments

The exposure conditions experienced by copper coated used fuel containers in a deep geologic repository will evolve with time. One important input is the radiation from the used fuel, and penetrates the UFC wall to the outside. This leads to one early exposure period involving the gamma irradiation of aerated humid vapour. In principle, the combination of radiation, oxygen, water and nitrogen could produce extremely small quantities of nitric acid, which could, in theory, condense in tiny volumes on the container surface. Work conducted at Western University investigated the evolution of the corrosion processes under conditions designed to simulate this effect. Damage was topical, with virtually no depth of penetration; although some minor grain etching was observed (Figure 3-22). The project led to an academic publication that extensively discusses the reaction mechanism and the relative impact of the species present (i.e. oxygen, nitrogen, etc.) (Turnbull et al. 2018), and it continues to demonstrate the extremely small impact radiation/radiolysis will have on the corrosion barrier.

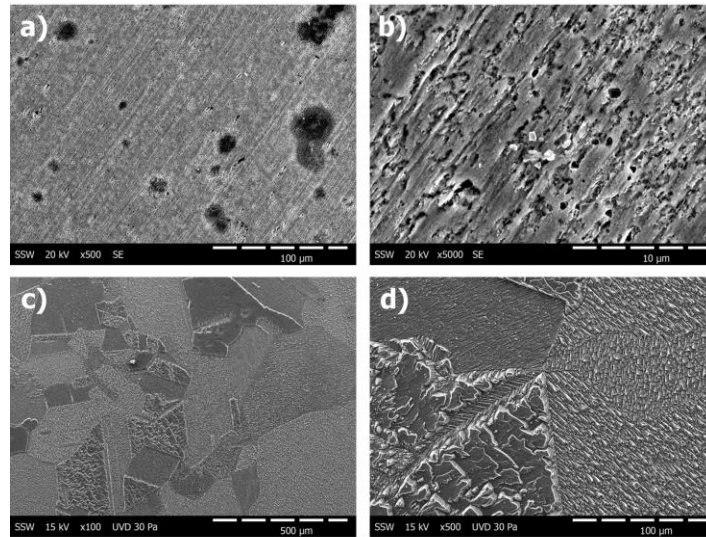


**Figure 3-22: SEM Micrographs of Cu Coupons after Immersion in Deaerated (a and b), and Aerated (c and d)  $\text{HNO}_3$  for Seven Days.**

### 3.4.1.4 Oxidic Corrosion of Copper

An important consideration is the maximum possible depth of corrosion, by various processes, into the copper-coating on the UFCs. It is by now established that following closure of a DGR, the conditions will evolve from an initial warm oxidic period to a long-term cool, anoxic period (Guo 2016). The maximum depth of copper corrosion during the early oxidic stage was evaluated from the quantity of  $\text{O}_2$  trapped when the DGR is sealed closed. The post-closure  $\text{O}_2$  inventory of a Canadian-design DGR placement room has been calculated previously and utilized to predict an oxidic corrosion allowance of a UFC (King 2005a,b).

With the substantial changes to the NWMO DGR and container designs, it was necessary to reassess the quantity of  $\text{O}_2$  trapped within a sealed placement room and to update the allowance for the oxidic corrosion of copper. To accommodate future activities, this work also determined the effects of several possible changes to the placement room dimensions, depths, etc.

The inventory of trapped oxygen in the current design, was determined to be 13 mol per UFC (Hall et al. 2018). Assuming uniform corrosion to copper (I), this corresponds to a maximum corrosion depth) of 81  $\mu\text{m}$ , which is significantly less than the previous oxidic corrosion allowance of 170  $\mu\text{m}$  used in the total corrosion allowance (Kwong 2011). The revised value will be used in future efforts to calculate the total corrosion allowance, and demonstrates an improvement in design and understanding of the corrosion processes expected in the DGR.

### 3.4.2 Internal Corrosion of UFC

When the used fuel container is welded closed, it is possible that there will be some air and moisture in the internal atmosphere. Its proximity to the used nuclear fuel has the potential to produce a very small amount of corrosive species. Although these trace species do not present a safety concern, the NWMO is investigating these constituents through ongoing research.

In 2018, progress was made in modelling the reactive environment, using more than 700 equations describing chemical and radiolytic reactions. From this work, it was demonstrated that nitric acid will be the most abundant species formed from moist air at doses relevant to the inside of a used fuel container. This species has the tendency to interact with steel via general corrosion, not forming pits or other localized corrosion features. In addition, it is much less harmful than many other oxidants formed via radiolysis, such as hydrogen peroxide. Ongoing experiments are being conducted to both validate the models with respect to formation of nitric acid, as well as to demonstrate the corrosion mechanism inside the container.

### 3.4.3 Microbial Studies

The design of the repository emplacement room utilizes highly compacted bentonite to suppress microbiological activity near the used fuel container. However, as microbiological activity may occur within bentonite that is improperly placed, as well as elsewhere underground, considerable efforts are being made to study it. Much of this work is conducted in concert with corrosion and bentonite programs, as well as within work that is performed at the underground research laboratories (Mont Terri and Grimsel) in Switzerland. To supplement the *in situ* work being performed in underground labs, a set of 18 pressure vessels (Figure 3-23) have also been designed and fabricated to perform a large number of *ex situ* experiments at Western University.

In 2018, NWMO and partners at Waterloo invested considerable effort in developing equipment and protocols to combine corrosion and microbiology experiments that utilize a range of bentonite densities. Results from these experiments, which range in duration of 6 to 24 months will begin to be available in upcoming reports, as well as academic articles. The highly unique sampling and characterization protocols that were developed for the underground experiments, were published as two technical reports by authors at the Universities of Waterloo, McMaster, and Toronto (Engel et al 2018, Slater et al 2018, respectively).



**Figure 3-23: a) Components of Pressure Vessels for Laboratory Bentonite/Microbiology Experiments at Western University. b) Set of Eighteen Pressure Vessels Used to Investigate a Variety of Physical and Chemical Parameters on Bentonite/Microbiology Properties.**

Researchers at Ryerson and Saskatchewan Universities submitted a final report regarding a multi-year effort to investigate commercially available bentonite materials at a range of high densities. The general conclusions indicate that there is very little potential for microbial activity in DGR conditions, and highlighted that the processes that produce the potentially corrosive sulphide species are very readily suppressed. In addition, they confirmed sulphide production is suppressed at lower densities of bentonite, if groundwater salinity exceeds 50 g/L. A portion of this work was published in a peer-reviewed article (Grigoryan et al. 2018).

#### **3.4.4 Bentonite**

Based on the success of previous work analyzing trace amounts of carbon in bentonite (Michaela et al. 2014a,b), new work was initiated to further the understanding of what percentage of natural organic carbon is available as “food” for microbial processes. The goals of this program are to compare various bentonite clays from additional sources such as that from Japanese and Swedish formations with current NWMO’s reference material MX-80, as well as to assess if there is any change to bioavailability of carbon when bentonite undergoes exposure to radiation and/or high temperature and salinity, as will occur in the DGR. Through this research project, the natural organic carbon in the bentonite samples employed in the pressure cells experiment will be also evaluated to assess its molecular structure and potential for use as a microbial substrate. Demonstrating that the natural organic carbon composition at the molecular-level does not change over time, is an additional line of evidence to support that microbial growth and activity does not occur in highly compacted bentonite clay.

In 2018, the NWMO initiated a series of experiments to place bentonite and container materials into modules that will be deployed in the deep Pacific Ocean. Test modules were designed and fabricated based on modules initially developed by Nagra for the underground research described above. In 2018, methodologies for filling modules with bentonite, container materials

and simulated sea water were developed for these new test modules. The trial modules will then be deployed by Ocean Network Canada in 2019, who provided scientist and ship time. In future years, these modules will be deployed to greater depths and for longer durations to understand the long-term impact of high pressure on the corrosion of copper inside bentonite.

Based on their previous success in developing three dimensional models to describe movement of groundwater species within repository rooms after water has saturated the bentonite (Briggs and Krol 2018), researchers at York University initiated modelling of species movement in unsaturated bentonite. To date, the models are only suitable for very simple geometrical segments of an emplacement room, such as bentonite near an arc segment of a hemispherical head. Additional complicating features of the design, such as the transition between the hemispherical and cylindrical portions of the used fuel container have not yet been incorporated, and the models require significant development.

## 4. GEOSCIENCE

The NWMO's multi-disciplinary, applied geoscience research program supports the site selection and characterization processes and the development of the safety case, in an iterative and integrated manner. Advancing scientific understanding of the safety attributes of crystalline and sedimentary rocks currently being considered as potential host rocks is achieved through research designed to:

- Develop methods for characterizing the properties or attributes of a site; and
- Reduce uncertainty with respect to the long-term evolution and stability of the geosphere environments (sedimentary or crystalline) potentially hosting a repository.

In the following sections, a brief description and highlights from the applied geoscience research conducted during 2018 is presented by discipline.

### 4.1 HYDROGEOCHEMISTRY

Chemical and isotopic compositions of groundwater, matrix porewater and rock provide information on the evolution of the geosphere and can be used to determine fluid and solute transport over geologic time frames. In 2018, the NWMO continued to support work programs with researchers in Canada and abroad, focused on the development and testing of methods to enhance porewater extraction and characterization from low-permeability sedimentary and crystalline rock formations.

#### 4.1.1 Porewater Chemistry and Isotopes

Measurement of porewater hydrogen ( $\delta^2\text{H}$ ) and oxygen ( $\delta^{18}\text{O}$ ) isotope compositions is a key component of any geochemical characterization program for a potential deep geologic repository. Isotopic information is used to assess mixing relationships, groundwater/porewater origin and evolution, as well as water-rock interaction processes. Research undertaken in 2018 focused on enhancing abilities to measure porewater chemistry and stable water isotope composition, as well as to characterize rock-mass transport properties; highlights from these programs are summarized below. This work was carried out at University of Ottawa, University of Bern, and Western University.

##### pH of Saline Fluids

Hydrogeochemical research commonly requires knowledge of the master variable, pH. pH measurements are commonly done potentiometrically, with electrodes, which is very challenging in high ionic strength (I) systems, such as the brines that make up the porewater and deep groundwaters in the Michigan Basin (up to  $I = 8 \text{ M}$ ). Spectroscopic methods offer an alternative approach for pH measurement in brines. This approach involves calibration of the spectroscopic properties of colorimetric indicators using specially-prepared buffer solutions, with the pH of the buffers determined by geochemical modelling. Work to-date on such measurements involves only a single indicator (phenol red), which is limited to  $\text{pH} \approx 7\text{-}9$ . Work to extend the spectroscopic technique over a wider range of pH ( $\sim 3$  to 9) was initiated in 2017 and continued in 2018. A multi-indicator solution was prepared and test measurements have been conducted to confirm that the solution responds over a significant pH range. A titration approach was adopted in 2018 that involves calibration of the spectroscopic measurements

against potentiometric and model-generated pH data. The spectroscopic response of the multi-indicator solution is now being calibrated over a range of pH from 4 to 9 and up to  $I = 8 \text{ M}$ .

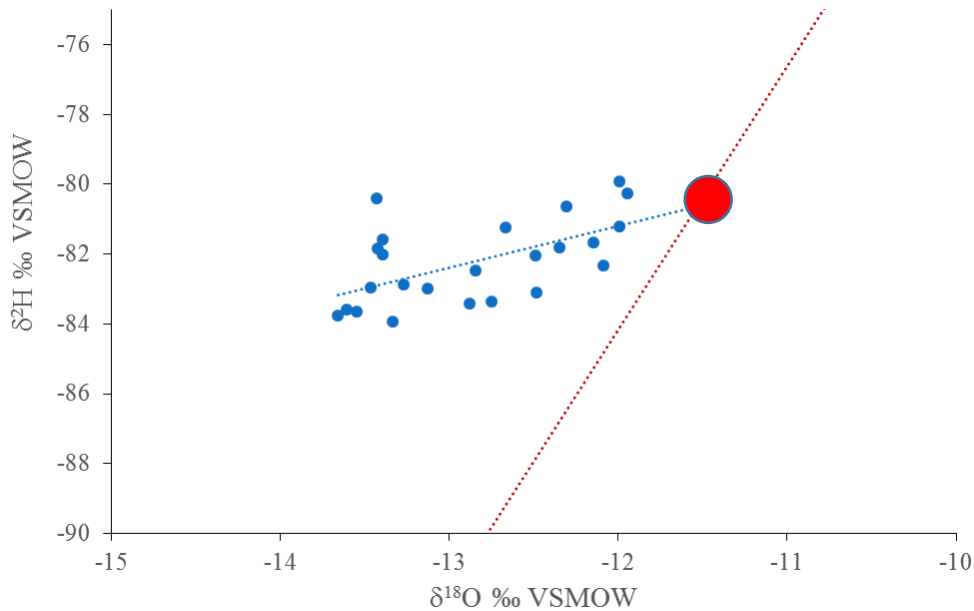
#### Porewater Extraction in Crystalline Rock: Vacuum Distillation and Leaching

Vacuum distillation methods are used to extract porewater from low permeability and/or low water content sedimentary rocks. During vacuum distillation, water is evaporated from a substrate under low pressure and cryogenically trapped (liquid nitrogen) in a sample vessel, before analysis for stable water isotopes ( $\delta^{18}\text{O}$ ,  $\delta^2\text{H}$ ). Vacuum distillation can be coupled with aqueous leaching of solutes from post-dehydrated samples to provide insight into the geochemistry of the porewaters within sedimentary rock (e.g. Clark et al. 2013; Al et al. 2015).

The objectives of this work are to develop and optimize a novel method to fully extract porewater from whole core samples of crystalline rock, and to test whether or not porewater geochemistry can be elucidated from the core following porewater extraction. The initial testing undertaken has utilized archived, unpreserved crystalline core, which was resaturated with a fluid of known chemical and isotopic composition. This resaturated core was then used to test the vacuum distillation method. Research findings to date include:

- Many iterations of the extraction protocol revealed the importance of time and temperature as dominant parameters in ensuring complete extraction.
- A depletion in  $^{18}\text{O}$  and  $^2\text{H}$  of 1 to 3‰ depletion was observed. This appears to be an artefact of the core re-saturation protocol, in which vapour and liquid diffusion into the core interior favours the lighter isotopes – with a characteristic diffusion slope on a  $\delta^{18}\text{O}$  -  $\delta\text{D}$  plot (Figure 4-1). Thus, the extraction process is considered to reliably extract the core porewater, which for test samples has a diffusion-depleted signature. Current experiments are testing new resaturation methods to preclude diffusion effects.
- To determine the chemical composition of the porewater, the intact cores were leached and the concentrations of ions in the leachates were normalized to the amount of porewater extracted using vacuum distillation. The higher concentrations of Na, Cl and Br measured in the leachates are likely due to leaching of minerals originally present within the pore space of the archived cores.
- Results from resaturated core suggest that full extraction of porewater at relatively low temperature, from intact crystalline core samples, is possible using vacuum extraction. This approach precludes the need to crush the cores, which could otherwise release fluid inclusions and alter the composition of the test waters, and consequently estimates of porewater chemical composition.

Future work includes: 1) testing different core re-saturation methods, 2) using varying compositions of synthetic salt solutions for saturation, and 3) applying the described methods to naturally-saturated cores.



Note: red disc is the value of the resaturation solution.

**Figure 4-1: Isotope Diagram of Porewaters Extracted from Crystalline Rock Showing a Depletion Trend Attributed to the Resaturation Process**

### Li, Mg and Ca Isotopes

Site characterization activities at the Bruce nuclear site (as part of a proposed Deep Geologic Repository (DGR) for Low and Intermediate Level Radioactive Waste) in low permeability Ordovician sediments of the Michigan Basin show that they contain Na-Ca-Mg-Cl brines (>5M) considered to originate as evaporated, post-dolomitic Silurian seawater, with residence times exceeding 400 Ma.

To further constrain solute migration at this site, this study has generated  $\delta^7\text{Li}$  and  $\delta^{26}\text{Mg}$  profiles of porewaters in these strata. During 2018, porewater leachates were prepared for isotope analysis, based on extensive pretreatment using ion-specific column chromatography to remove interfering geochemical matrices.

To interpret the isotope profiles for  $\delta^{26}\text{Mg}$ , shifts related to porewater-matrix exchanges are examined, including dolomitization ( $\uparrow\delta^{26}\text{Mg}_{\text{pw}}$ ), possible secondary silicate formation ( $\downarrow\delta^{26}\text{Mg}_{\text{pw}}$ ) and possible shield-derived fluid mixing in the deep Ordovician formations. In the case of lithium, the composition may be altered through sorption onto clays and organics ( $\uparrow\delta^7\text{Li}_{\text{pw}}$ ) and mixing with a shield-derived fluid in the deep Ordovician section.

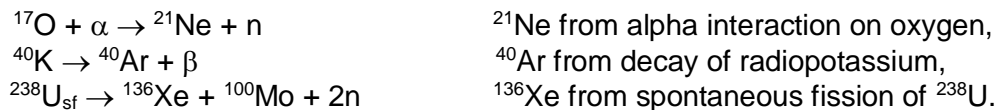
Going forward, research is focused on completing additional sample preparation and ICP-MS analysis, to further refine the  $\delta^{26}\text{Mg}$  profiles and completion of the calcium isotopic measurements ( $\delta^{44}\text{Ca}$ ). In addition to expanding the  $\delta^{26}\text{Mg}_{\text{pw}}$  porewater dataset, measuring  $\delta^{44}\text{Ca}$  in porewater will help to constrain the nature of fluid-rock interactions and potential mixing with a shield brine source in the Ordovician limestones. The methods and understanding from this work will help interpret the evolution of fluids within the Ordovician limestones in the potential APM siting areas in southern Ontario.

### Porewater Extraction: Cellulosic Paper Technique

A novel method that aims to absorb porewater from rock cores into cellulosic papers has been under development for several years (e.g. Celejewski et al. 2014; Celejewski et al. 2018). As Applications of this technique, using shales from the Michigan Basin and Opalinus Clay samples from Switzerland (Mazurek et al. 2017), suggest that the cellulosic paper is selective for the mobile fraction of porewater only (exclusive of bound water and water occupying interlayer positions in clays). The paper absorption technique is now being tested for use in extracting porewater for stable isotope measurements. The main challenges are avoidance of artifacts from evaporative fractionation and minimizing the blank signal from atmospheric water that adsorbs on the highly-hygroscopic cellulosic paper. Two analytical approaches are being tested to extract water from the paper and measure stable isotope ratios: cavity-ring-down spectrometry coupled to an induction-heating module, and high-temperature conversion followed by isotope-ratio mass spectrometry.

### Porewater Dating: Noble Gases and Strontium

Isotopic analysis of heavy noble gases in porewaters within preserved cores was initiated to complement helium isotope studies that were performed as part of geosphere model development for the Bruce nuclear site (Clark et al. 2013). In this new work, the Helix multi-collector noble gas mass spectrometer is being interfaced with a noble gas purification and separation line to allow the simultaneous analysis of  $^{36}\text{Ar}/^{40}\text{Ar}$  and  $^{136}\text{Xe}/^{128}\text{Xe}$ . The noble gas laboratory at the Advanced Research Centre is the only one in Canada with instrumentation for analysis of the isotopes of helium and the higher-mass noble gases, and the ingrowth of geogenic noble gases, including  $^4\text{He}$ ,  $^{21}\text{Ne}$ ,  $^{40}\text{Ar}$  and  $^{136}\text{Xe}$ , can be used as measures of groundwater and porewater age. Ingrowth arises from the following nuclear reactions in the subsurface:



Designs for sample extraction include heating the core sample under vacuum with cryo-trapping and reactive gas gettering, as noble gas concentrations are typically low in hypersaline brines. The gas prep and inlet system required for this work was completed in 2018 with a heating system for baking rock samples to release the noble gases.

Sample material for analysis of noble gases in the aquiclude formations from the Bruce site are restricted to archived material. Observations of archive core sample bags from the Bruce nuclear site have suggested that many of the samples have degassed into the vacuum-sealed aluminum foil packaging over time. Work in 2019 will focus on further analysis of the gases which have diffused out of these archived samples and which are trapped within the packaging materials used to preserve the samples. Gases will then also be extracted from the rock material using the newly developed heating system on the inlet, and analysed.

It is anticipated that determination of the ingrowth of the higher-mass noble gas isotopes above their atmospheric ratios will provide robust chronologies of the porewaters in this system, which will be complementary to the He, CH<sub>4</sub>, and  $^{87}\text{Sr}$  chronometers that have already been developed during characterization activities (Bouchard et al. 2018).

### Surface Area

In 2018, the University of Bern undertook research to characterize external surface area (BET) and cation exchange capacity (CEC) in sedimentary rock cores from the Bruce nuclear site. Samples from the Queenston, Georgian Bay, Blue Mountain and Collingwood Member formations were evaluated, and the rock types ranged from claystone to marl to limestone. The main questions to be addressed included:

- 1) Does the separation of grain-size fractions by sieving induce a mineralogical fractionation (i.e., can a specific fraction for geochemical experiments be used and the results considered representative of the whole rock)?
- 2) Does crushing create new mineral surfaces, and how does CEC depend on the grain size used for the experiments (i.e., is it permissible to extrapolate geochemical data obtained on disintegrated or crushed material to the intact rock)?

The main findings are as follows:

- The chemical and mineralogical compositions do not vary systematically between grain-size fractions, indicating that size reduction and sieving do not lead to a resolvable fractionation (exception: limestone sample).
- The BET surface area increases with decreasing grain-size fraction by 50 – 100% (claystone and marl) and 300% (limestone). This means that crushing to smaller particle sizes provides access to surfaces that are inaccessible or not present in the intact rock.
- CEC of claystone and marl samples increase by 7–31% between fractions 1–4 mm and <0.063 mm. This is less than the increase of the BET surface area. While crushing to smaller grain size creates new surfaces, these are predominantly related to minerals with a small or negligible CEC, such as carbonates or quartz. It is concluded that the effect of grain size plays a relatively limited role for CEC.
- CEC of the limestone sample between fractions 1–4 mm and <0.063 mm increases by 110%. While this is less than the increase of the BET surface, the effect is more substantial. Care needs to be taken when extrapolating data produced on crushed limestone samples to the intact rock.
- Good linear correlations can be found between clay content, BET surface area and CEC (Figure 4-2). BET surface measurement, thus, can be used as a proxy of the cation-exchange capacity of the sample – a feature known for other sedimentary rocks.

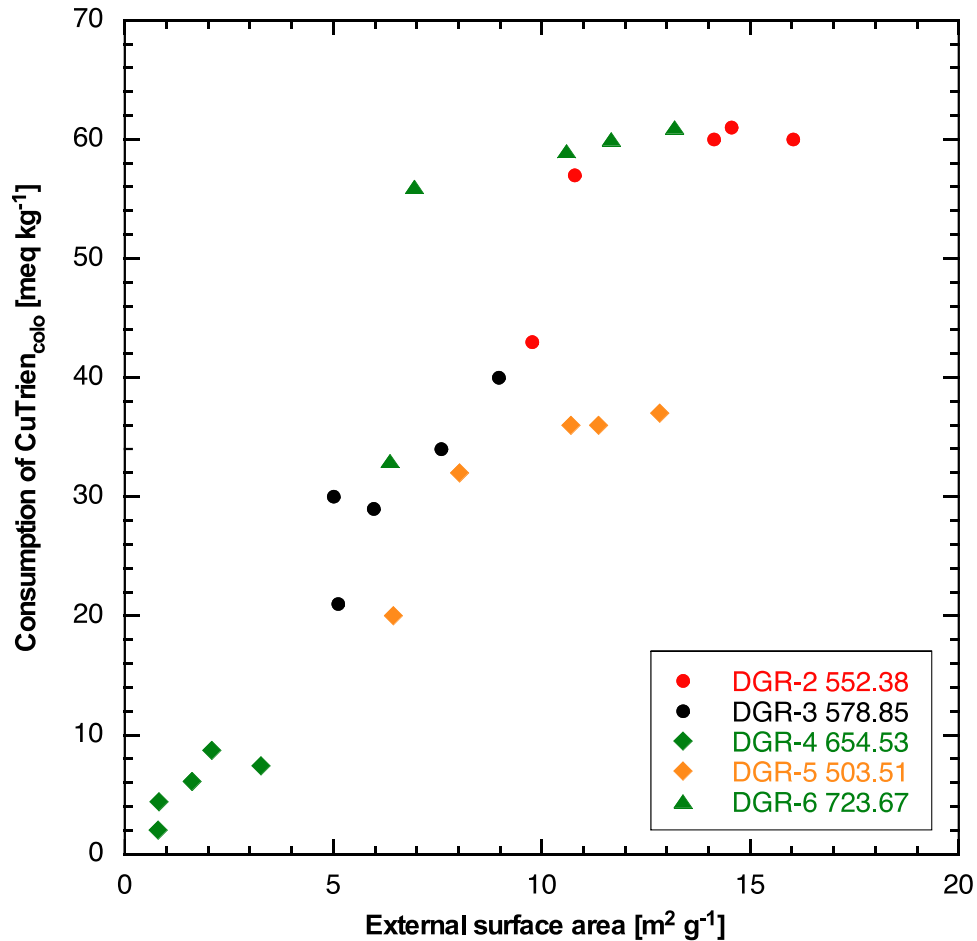


**Figure 4-2: Correlation between BET Surface Area and CEC (expressed by probe consumption)**

#### Porewater Extraction: Squeezing and Isotope Diffusion Exchange

The final NWMO technical report documenting benchmarking activities using the squeezing and isotope diffusive exchange methods was published in 2018 (Rufer and Mazurek 2018). Key findings from the work include: i) stable water isotope measurements between squeezing and diffusive exchange are generally identical, within error; ii) confinement to prevent swelling, as well as equilibration with a fluid of known isotopic composition, is possible for the tight and low-porosity Ordovician shales and carbonates encountered at the Bruce nuclear site; and iii) evaporation, as a factor influencing the results, is generally considered to be negligible with respect to the specially-designed confining cells.

#### Porewater Extraction: Vacuum Distillation

The reliable measurement of water stable isotope compositions in the porewaters of the Paleozoic formations of the Michigan Basin in southern Ontario presents a challenge due to the very low water content and, potentially, because of the presence of clay minerals. In collaboration with the University of Ottawa, the potential for bias of the vacuum-distillation method due to isotopic fractionation between connected-porosity water and clay hydration water is being examined.

Characterization of the clays in Ordovician shales from the Bruce nuclear site and elsewhere in southwestern Ontario is prerequisite to this work, along with parallel examination of standard clays from the Clay Minerals Society (CMS) Source Clay repository. This effort has included detailed determination of: (i) clay mineralogy (<2µm) by X-ray diffraction, (ii) clay dehydration and dehydroxylation behaviour by thermal gravimetric analysis (TGA), and (iii) the hydrogen (H) and oxygen (O) isotope compositions of the <2µm clays. Experiments to test for H-isotope exchange between clays typical of the Bruce nuclear site and porewater accompanied this work, and will be published in a thesis and in a final Technical Report. Initial results suggest that hydroxyl group hydrogen within non-swelling clays (illite> kaolinite>chlorite) can undergo limited isotopic exchange with water at 68°C in ~10 weeks. Such temperatures are near the lower limit of the maximum experienced by the shales at the Bruce nuclear site during burial. Such exchange may result in changes in the porewater H-isotope compositions over geological time.

Challenges have been encountered in isolating sufficient quantities of water bound to clay mineral surfaces from the mobile porewater. Success at that step is essential to determining whether or not there is H- or O-isotope fractionation between these two water reservoirs. This difficulty arises from 1) the nature of the clay minerals in samples currently being examined and 2) the instrumentation used. Non-swelling clays comprise the Ordovician shale assemblages in southwestern Ontario. The clay surface areas to which porewater can be bound is expected to be much lower than those in swelling clays. Hence, the amount of bound water that can be collected is much lower and, typically, below the minimum amount required for isotopic measurement.

Solutions to this difficulty are being sought in three directions. First, new methods are being developed to measure the H- and O-isotope compositions of clay mineral using much smaller amounts of sample. Second, low water content swelling clay minerals, for which the proportions of bound versus mobile porewater should be much higher, will be examined. The H- and O-isotope exchange properties of swelling clay minerals, and for bound water–mobile water isotopic fractionation, will be tested using CMS swelling clay standards of varying chemistry and layer charge. New instrumentation packages for effective separation of bound and mobile water, in quantities sufficient for isotopic analysis for both swelling and non-swelling clays, could potentially also be developed.

In addition, the following activities will be the focus of research during 2019: (i) conduct further experiments on the non-swelling clays and clay assemblages, testing both for H- and O-isotope exchange with water over longer time periods and to higher temperatures (150°C); and, (ii) investigate the diagenesis of clay minerals in the Ordovician shales of southern Ontario, and its implications for porewater isotopic compositions.

#### **4.1.2 Mont Terri: Geochemical Data (GD)**

The NWMO joined the Geochemical Data (GD) Experiment at Mont Terri in 2018. The GD Experiment serves as a platform to advance and share knowledge about the geochemistry of the Opalinus Clay, with emphasis on porewater chemistry and its evolution. Geochemical data from various experiments are evaluated and used to assess how new data agrees with the existing porewater conceptual model. Different approaches are taken to try to address gaps in understanding (e.g., lab investigations, in-situ measurements, modelling). Research undertaken in GD focuses on a number of processes relevant to the APM siting program, including anion-accessible porosity, solubility controls for sulphate, representative determination of external surface area & cation-exchange capacity, as well as carbonate mineral solubility and buffering capacity.

## 4.2 REDOX PROCESSES

The increase in organic matter down through the Ordovician shales to the Cobourg Formation are of considerable interest in the context of the redox conditions that would persist in the far field for a DGR. Previous studies of the concentrations and isotopic properties of CH<sub>4</sub> and CO<sub>2</sub> in sedimentary cores from the Bruce nuclear site indicate that biological and thermochemical processes are responsible for the formation of gases present at various depths in the Upper Ordovician and are discussed in detail in Clark et al. (2013, 2015) and Jautzy et al. (2018).

Further work in 2018 used clumped isotopes of methane as an indicator for the occurrence and rate of biological activity in the system. As biogenic CH<sub>4</sub> can form in apparent isotopic equilibrium with respect to coexisting water at very low rates, methanogenic metabolism in such environments can operate through slow and fully-reversible enzymatic reactions. The vertical profile of clumped isotopic indices for methane is used to conclude that syntrophic formation of methane has taken place at ultra-slow rates. These results identify the production of methane at thermodynamic equilibrium from the syntrophic degradation of sedimentary n-alkanes.

The sulphur system is the focus of a related redox project at the University of Ottawa using <sup>34</sup>S and <sup>18</sup>O in sulphate, together with <sup>34</sup>S in reduced sulphur phases including organics, framboidal pyrite and other iron-bearing phases. The aim of the work was to link the reduction of seawater sulphate to biogenic activity in the Ordovician sediments which would have sequestered sulphate in the Silurian evaporite formations prior to Silurian salinization/dolomitization. This research, which was completed in 2018, focused on the source and timing of the emplacement of sulphate in the Ordovician aquiclude formations, and the relationship of this residual sulphate to co-existing framboidal pyrite in the shales. The  $\delta^{34}\text{S}$  and the morphology of framboidal pyrite in the Ordovician layers was examined, and provided a strong evidence for diagenetic sulfate reduction. However, no enrichment of  $\delta^{34}\text{S}$  and  $\delta^{18}\text{O}$  in porewater sulfate associated microbial activity was observed in this study, indicating that the existing sulphate reservoir in these formations was not involved in the formation of the framboidal pyrite, and that sulphide formation was likely para-diagenetic during the Ordovician under normal salinity conditions. The stable isotopes of the existing porewater sulphate in these formations is consistent with Silurian seawater, and it is concluded that this is the residual sulphate carried by the infiltrating Silurian brines following evaporite formation higher in the section. A minor portion of the porewater sulphates analyzed have lower  $\delta^{34}\text{S}$  values and  $\delta^{18}\text{O}$  values consistent with pyrite oxidation, which likely took place in-situ, perhaps using ferric iron minerals as electron acceptors (Jautzy et al. 2018).

## 4.3 SUBSURFACE MASS TRANSPORT

Near-field performance, safety assessment and groundwater transport/evolution models require knowledge of groundwater and porewater geochemical compositions, as well as petrophysical and solute transport properties, in order to provide representative estimations of long-term system behaviour. The following research programs contribute to the NWMO's technical capabilities in the context of assessing long-term solute mobility and retention.

### 4.3.1 Diffusion

The X-ray Computed Tomography (CT) method is being applied to measure effective diffusion coefficients in low-porosity rock samples. The University of Ottawa acquired an X-ray CT system in 2016; this has since been optimized and applied to partially saturated argillaceous

rocks from the Michigan Basin in Ontario and crystalline rocks from the Lac Du Bonnet batholith in Manitoba.

In order to investigate potential effects of the presence of a gas phase in sedimentary rocks on measured diffusion coefficients, a novel method was developed between 2015 and 2017 (Nunn et al. 2018). The method involves inducing differing degrees of partial N<sub>2</sub> saturation into these rocks, which containing high-salinity porewater, before measuring effective diffusion coefficients.

Experiments on low-porosity samples (less than 1%) have demonstrated that X-ray CT is capable of detecting tracer signals with acceptable signal-to-noise ratios; however, similar experiments with archived granitic Lac Du Bonnet samples (porosity ~ 0.1%) have not succeeded. The failure seems to be due to the coarse-grained nature of the granite, which causes artifacts during the image-analysis step in the data processing. A new, dynamic-imaging technique is being developed to overcome this limitation.

Experiments on the low-porosity limestone have also demonstrated that the iodide tracer experiments are affected by the presence of organic-rich zones in the argillaceous limestone from the Trenton-Black River groups in the Michigan Basin. Iodide is known to adsorb on organics and these experiments have demonstrated that the adsorption capacity of organics in these rocks (kerogen and associated petroleum) is sufficiently high to invalidate the common assumption that iodide would behave as a conservative tracer.

The NWMO also is a partner in the Long-term Diffusion Experiment (DR-B) at the Mont Terri URL. The experimental setup consists of a central borehole and 3 surrounding observation boreholes. Sodium iodide (NaI) solution was injected in the central borehole in April 2017, and is expected to diffuse over time toward the observation boreholes.

In addition to DR-B, the NWMO is a partner in the Concrete Interface (CI) characterization Experiment. The objective of this long-term experiment (now in its 11<sup>th</sup> year) is to enhance understanding of the influence of cement on both the Opalinus Clay (OPA) host rock and bentonite. In 2019, the NWMO will join the diffusion component of this experiment, CI-D. A tracer cocktail is being circulated through an existing interval in the CI Experiment for 2-3 years, after which time the interfaces will be overcored and analysed to evaluate solute movement.

#### **4.3.2 Geochronology and Fluid Inclusions**

Fluid inclusions trapped within the infilling minerals of rock cores (veins and vugs) during their growth and later deformation can provide representative samples of the chemical composition, density and temperature of ancient fluids (i.e., paleofluids). In collaboration with the University of Toronto, fluid inclusion studies at the University of Bern were performed. These studies involved petrographic examination of the vein and vug infilling mineral phase(s) from selected intervals (Devonian and Ordovician in 2015, Silurian in 2016-2017) within cores from the Bruce nuclear site. The Devonian and Ordovician results were published in 2016 (Diamond et al. 2016) and in a final report documenting results from the Silurian-aged samples was published in 2018 (Diamond and Richter 2018). This collaborative research between the University of Toronto and the University of Bern focused on evaluating the data for any meaningful interpretations about the timing of fluid movement in the sedimentary rocks at the Bruce nuclear site, as well as the nature (i.e., temperature and salinity) of the fluids.

### 4.3.3 Sorption

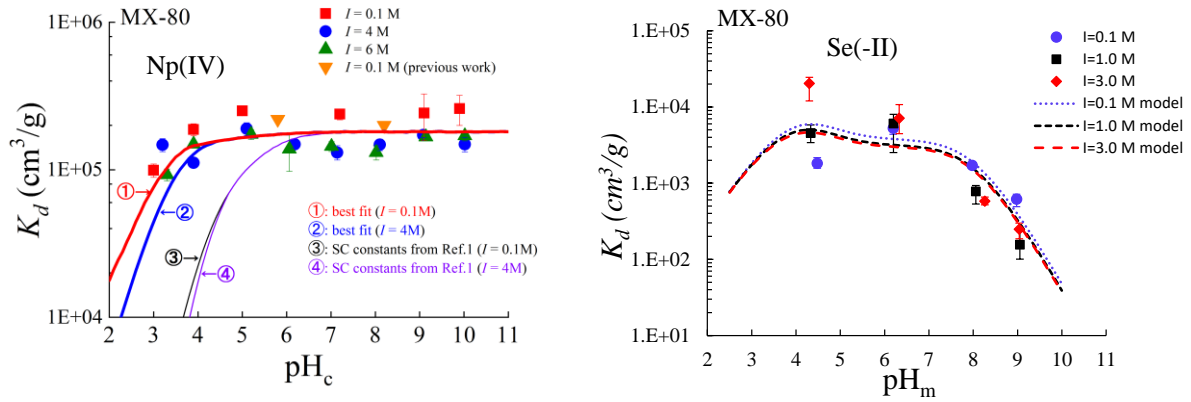
Sorption is a mechanism for retarding sub-surface radionuclide transport from a DGR to the environment. The NWMO has initiated the development of a sorption distribution coefficient ( $K_d$ ) database for elements of importance to the safety assessment of a DGR (Vilks 2011). This initial database was further developed as described in (Vilks et al. 2011; Vilks and Miller 2014, 2018; Bertetti 2016; Nagasaki 2018; Nagasaki et al. 2017, 2016).

Sorption coefficients for Ni(II), Cu(II), Zr(IV), Pd(II), Sn(IV), Cs(I), Eu(III), Pb(II), Th(IV) and U(VI) onto Canadian sedimentary rocks and bentonite in saline solutions (with ionic strength  $I = 0.23$ - $7.2$  M) were measured by Canadian Nuclear Laboratories (CNL). The experiments were completed with a reference porewater brine solution (SR-270-PW, Na-Ca-Cl type,  $I = 6.0$  M) using both batch sorption tests (up to 195 days) and long-term (up to 1 year) through-diffusion tests. Sorption measurements were also conducted in Na-Ca-Cl dilute solutions with an ionic strength of  $0.01$  M to investigate the effect of ionic strength on sorption (Vilks et al. 2011; Vilks and Miller 2014, 2018).

Sorption studies under reducing conditions were carried out by the Southwest Research Institute and by McMaster University. The Southwest Research Institute pioneered sorption measurements for six key redox-sensitive elements: Se(-II), As(III), Pu(III), U(IV), Tc(IV) and Np(IV) (Bertetti 2016). McMaster University continued to systematically study the sorption properties of Np onto bentonite, shale and illite in highly saline solutions, under both oxidizing and reducing conditions (Nagasaki et al. 2017, 2016). It was found that  $K_d$  values of Np(IV) under reducing conditions were about three orders of magnitude larger than  $K_d$  values of Np(V) under oxidizing conditions in the SR-207-PW reference brine solution. Under reducing conditions, the  $K_d$  values for Np(IV) on illite, shale and bentonite slightly decreased with increasing ionic strength from  $0.1$  to  $0.5$  M but were independent of the ionic strength at greater than  $0.5$  M). The 2-site protolysis non-electrostatic surface complexation and cation exchange model (2 SPNE SC/CE model, Bradbury and Baeyens 2005) was applied to simulate the pH dependence of  $K_d$  values of Np(IV) on MX-80 and illite at  $I = 0.1$  M and  $4$  M (Nagasaki 2018; Nagasaki et al. 2017, 2016).

The measured sorption  $K_d$  values have been used to update the NWMO sorption database for Canadian sedimentary rocks and bentonite (Vilks and Yang 2018).

A three-year research program was initiated in 2017 with McMaster University to further study the sorption properties of Se and Tc onto shale, limestone and bentonite in SR-270-PW brine solution, as well as onto crystalline rocks in a reference groundwater (CR-10, Ca-Na-Cl type,  $I = 0.24$  M) under reducing conditions. The effects of ionic strength and pH on sorption of Se and Tc on shale, limestone, bentonite and crystalline rocks are being investigated (e.g. Walker et al. 2018). The 2 SPNE SC/CE model was applied to simulate the pH dependence of  $K_d$  values of Se(-II) on MX-80 and illite at  $I = 0.1$ ,  $1.0$  and  $3$  M. It was found that the sorption model well predicted the pH dependence of  $K_d$  (Figure 4-3).



Note: "SC constant" represents surface complexation constant (Ref. Bradbury and Baeyens 2005. Previous Work: Nagasaki 1994)

**Figure 4-3: 2 SPNE SC/CE Model Simulation of Sorption of Np(IV) (Left) and Se(-II) (Right) on MX-80**

#### 4.4 REACTIVE TRANSPORT MODELLING

Reactive transport modelling is a useful approach for assessing long-term geochemical stability in geological formations. Reactive transport modelling is used to assess: 1) the degree to which dissolved oxygen in recharging waters may be attenuated within the proposed host rock; 2) how geochemical reactions (e.g., dissolution-precipitation, oxidation-reduction, and ion exchange reactions) may affect groundwater salinity (density) along flow paths; and 3) how diffusive transport of reactive solutes may evolve in the porewaters of low-permeability geological formations.

MIN3P is a multi-component reactive transport code that has been previously used to evaluate redox stability in crystalline rocks of the Canadian Shield (Spiessl et al. 2009, Xie et al. 2015, Bea et al. 2011a, 2011b, 2015, 2018). A parallel version of MIN3P-THCm (ParMIN3P-THCm) was developed (Su et al. 2015, 2017).

Research continued in 2018 to complete the implementation of unstructured grid capabilities in MIN3P-THCm for 3-dimensional systems, including the parallelization of the unstructured grid functions, and to perform benchmarking simulations contributing to the international SSBench code inter-comparison. A technical report documenting the implementation of unstructured grids in MIN3P-THCm is expected in 2019.

MIN3P-THCm has been applied to investigate the formation mechanisms for sulfur water observed in the Michigan Basin. The salinity-dependent sulfate reduction model provides a possible explanation for the observations by Carter (2012) that sulfur water exists at intermediate depths, but not in the deep subsurface. The reactive transport simulations of sulfur water formation mechanisms in the Michigan Basin were recently published by Xie et al. (2018).

A two-year research program will be initiated in 2019, in collaboration with the University of British Columbia and the University of New Brunswick to further develop and evaluate MIN3P-THCm capabilities. In particular, application to large scale 3D flow and reactive transport problems, as well as extension of reactive transport simulations on the formation of sulphidic waters in sedimentary basins subjected to a glaciation/deglaciation cycle will be the key areas of research (Xie et al. 2018). A generalized formulation for heat transport and the temperature-dependence of chemical reactions based on empirical experimental data will be implemented.

#### 4.5 NORTHERN ONTARIO SEISMIC MONITORING

The Canadian Hazards Information Service (a division of NRCan) maintains a cross-Canada seismic monitoring network. With NWMO support, this network in Northern Ontario was augmented to provide a greater number of monitoring stations. The geographic distribution of Northern Ontario seismic activity for 2018 followed that of previous years, with earthquakes being detected mainly in the Severn Highlands, James Bay and Kipawa-Cochrane. In all, 51 known earthquakes were catalogued. The largest earthquake in the study area was a 3.3 mN event on 2018-12-13 in James Bay. The only felt earthquake was a 2.4 mN event under Kirkland Lake which was not associated with any nearby mines. The smallest measured earthquake, in the Severn Highlands, had an estimated magnitude of 1.0 mN.

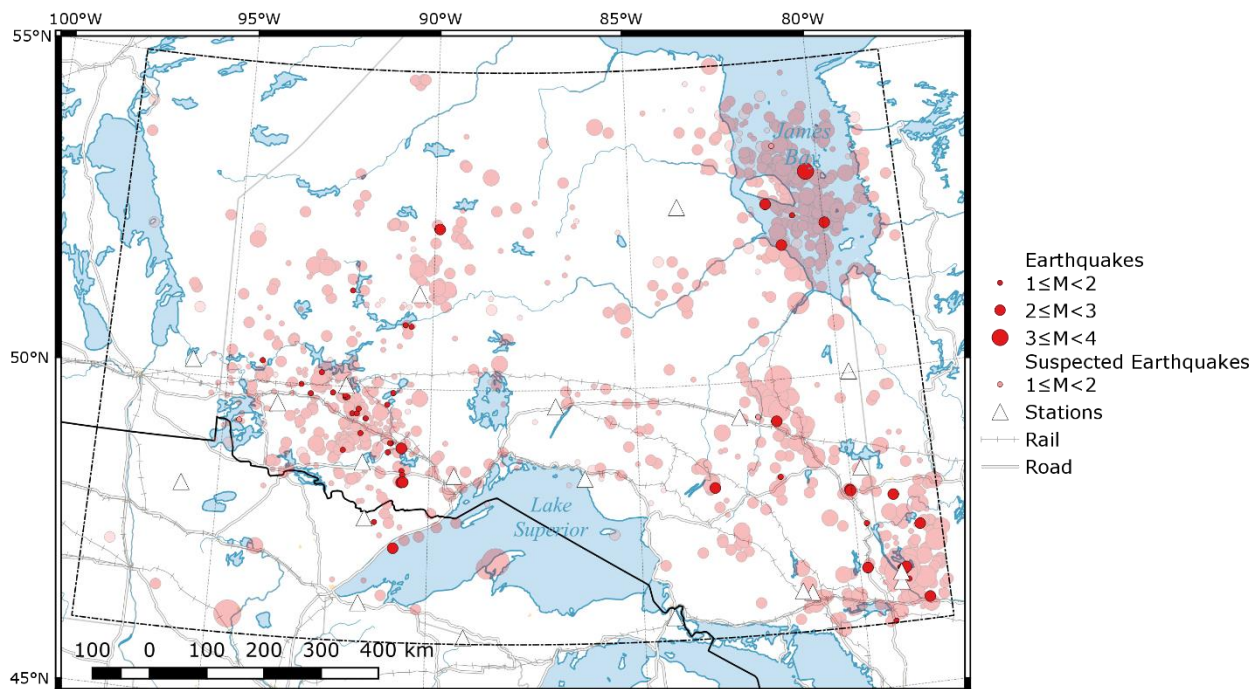


**Figure 4-4: Annual Seismic Activity on the Canadian Shield for 2018 (Red) with Historic Seismicity (Pink)**

#### 4.6 PALEOSEISMICITY

The seismic monitoring program described in the previous section provides information on current seismic activity. The NWMO also supports work to develop an understanding of ancient past seismic activity.

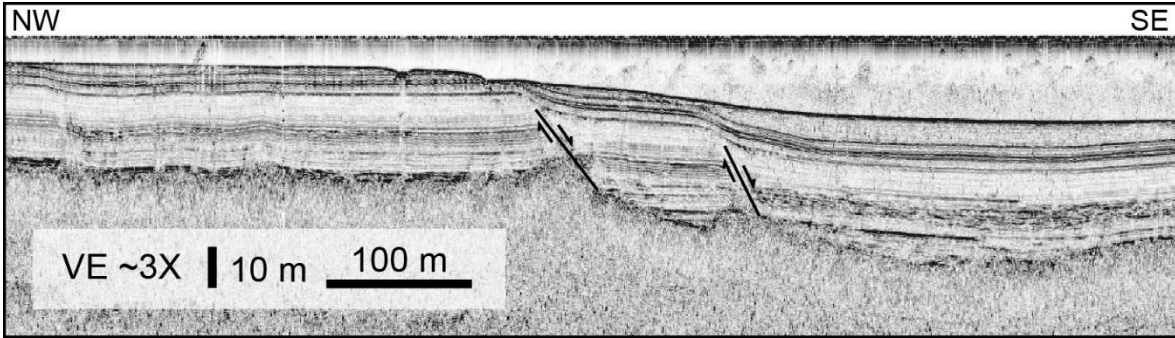
This work has included development and application of a method to detect past seismic events through studies of sediment layers in lakes. This research program involves several projects, which are summarised in the following sub-sections.

##### 4.6.1 Sediment Coring and Mapping in Lakes Duparquet and Dufresnoy, Quebec

This aspect of the research was completed during 2018. A final, peer-reviewed journal publication on this work is expected in 2020.

##### 4.6.2 Mapping and Dating a Fault Feature in Round Lake, Ontario

A potential fault feature has been identified in Round Lake, near Kirkland Lake, Ontario. In 2018, additional sub-bottom profiles were collected from Round Lake, using a seismic source mounted on the side of a boat in combination with a ~2 m long geophone array deployed beside the boat. Over 40 km of seismic lines were collected using this 'overwater seismic' equipment over the portion of the lake where fault-like structures had been mapped previously. An example of an overwater seismic line, which reveals offset (faulted) glaciolacustrine deposits, is shown in Figure 4-5. Work is ongoing on dating this feature.



Note: This line crosses two locations of offset glaciolacustrine deposits in the sub-bottom. The obvious step in the basal reflector underlies the offset on the left.

**Figure 4-5: Example of an Overwater Seismic Line Acquired from Round Lake**

#### 4.6.3 Estimating Magnitude and Epicentre of a Paleoearthquake Occurring ~9100 BP

Through paleoseismic research conducted at the Ontario- Quebec boarder, evidence for a potential, strong paleo-earthquake was identified. A consistent signal for a mass transport deposit (MTD) was observed in lake bottom sediments across a large area corresponding to the same sediment “varve year” (layer) or vyr 1483. Dating of sediment cores revealed that this varve year corresponds to a calendar year of about 9100 years before present (BP). The 2018 work focused on confirming this signal in other sediment cores, recovered from lakes across northwestern Quebec and northeastern Ontario.

##### 4.6.3.1 Core for Lakes Chassignole and Malartic, Quebec

As summarized previously (Brooks 2016; 2018), the vyr 1483 MTD is interpreted to be present in Lake Chassignolle and Malartic cores and thus the regional vyr 1483 signature extends eastward to at least Lac Malartic, Quebec. During 2018, the varve numbering was finalized for the intervals over- and underlying the 1485-1528 sequence in the cores collected in 2017 and 2018 from both lakes. In the cores, the post v1538 couplets match well with those of the Timiskaming varve series, similar to Lakes Dasserat, Dufresnoy and Duparquet. In the Lake Chassignolle core, the varve sequence 1236-1377 also matches well with the Timiskaming varve series, with the exception of a short ‘floating’ sequence tentatively assigned to numbers 1442-1471. Oddly, a large portion of the pre-1483 varves in the Malartic cores do not correlate well to the Timiskaming varve series. The interval of v1169-v1298 correlates well, but the numbering of v1304-1403 is provisional at best and regarded as ‘floating’. However, the uncertain numbering of these older varves does not affect the interpretation of the varve numbering in the post v1483 portion of the cores.

##### 4.6.3.2 The vyr 1483 MTD Signature in Northeastern Ontario

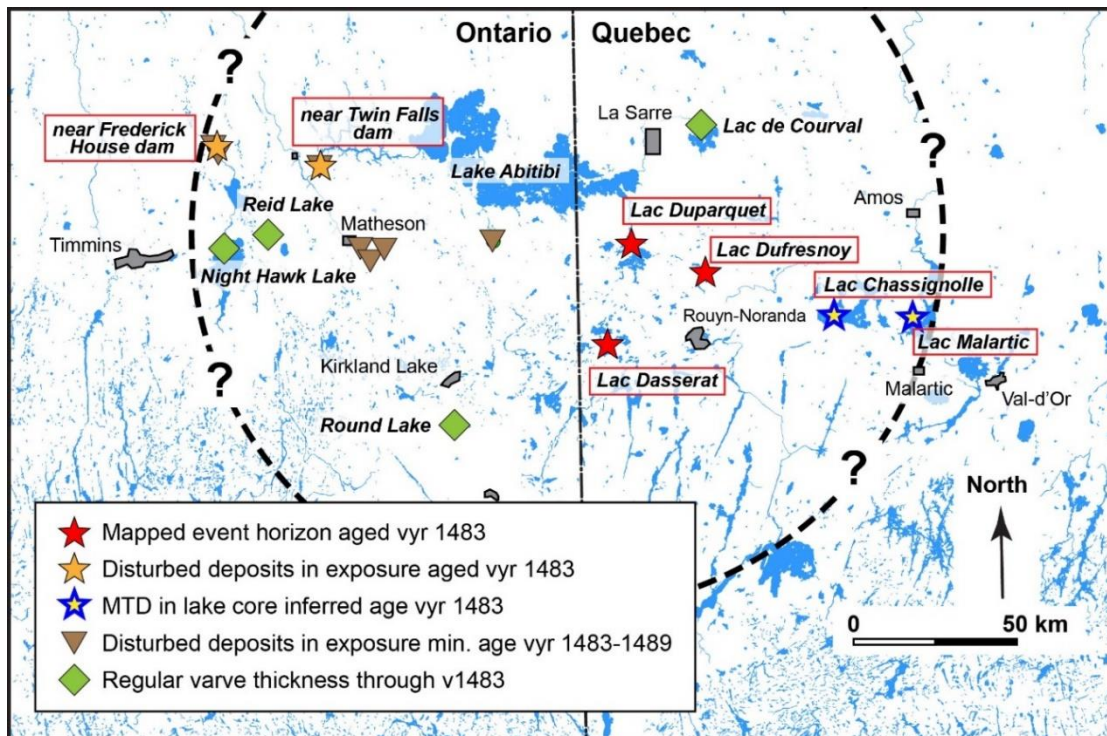
Brooks (2016, 2018) interpreted the presence of the vyr 1483 MTD signature in northeastern Ontario using summary logs of varve exposures in Antevs (1925, 1928) and Hughes (1959). These authors reported the occurrence of disturbed deposits at eight sites for which the inferred minimum varves ages are identical to or up to six varve years younger than vyr 1483 (Figure 4-6). Because of the high precision of the varve ages and the possibility of these deposits being closely, but differently aged, it was deemed necessary to verify that at least some of these

disturbed deposits actually have the same age as the vyr 1483 signature. Unlike northwestern Quebec, there are few readily accessible lakes in northeastern Ontario, aside from Night Hawk and Frederick House Lakes. In these two lakes, however, the combination of large zones of no penetration of the profiler acoustic energy into the sub-bottom and the lack of MTDs in the areas of useful returns inhibited identifying targets for coring. Hence, it was decided to investigate river bank exposures near the locations reported by Antevs (1925, 1928) and Hughes (1959).

River bank work was undertaken in August 2018 at four locations in Ontario. Excavations at natural exposures revealed disturbed deposits that formed in vyr 1483 along both Frederick House and Abitibi rivers (Figure 4-6 and Figure 4-7). These data verify that the vyr 1483 MTD signature also occurs in northeastern Ontario. They also indicate that reference to disturbed deposits the same or slightly younger than vyr 1483 in the summary logs of Antevs and Hughes can reasonably be inferred to be part of the regional vyr 1483 MTD signature.

Figure 4-6 illustrates the various locations studied and the indications at each whether there was evidence for an event corresponding to vyr 1483. Also shown is a circle representing the estimated area impacted by this event based on the measurements.

This regional pattern of disturbed lake sediments may be a record from a strong paleoearthquake that occurred about 9100 years before present. This time frame corresponds generally with the post glacial retreat from this area. Work was underway to estimate the magnitude of this presumed event.



Note: Dashed line represents the approximate extent of the known MTD-disturbed deposit signature. The shape of the signature is assumed to be circular.

**Figure 4-6: Map Showing the Study Sites (Marked by Stars) in Northeastern Ontario-Northwestern Quebec**

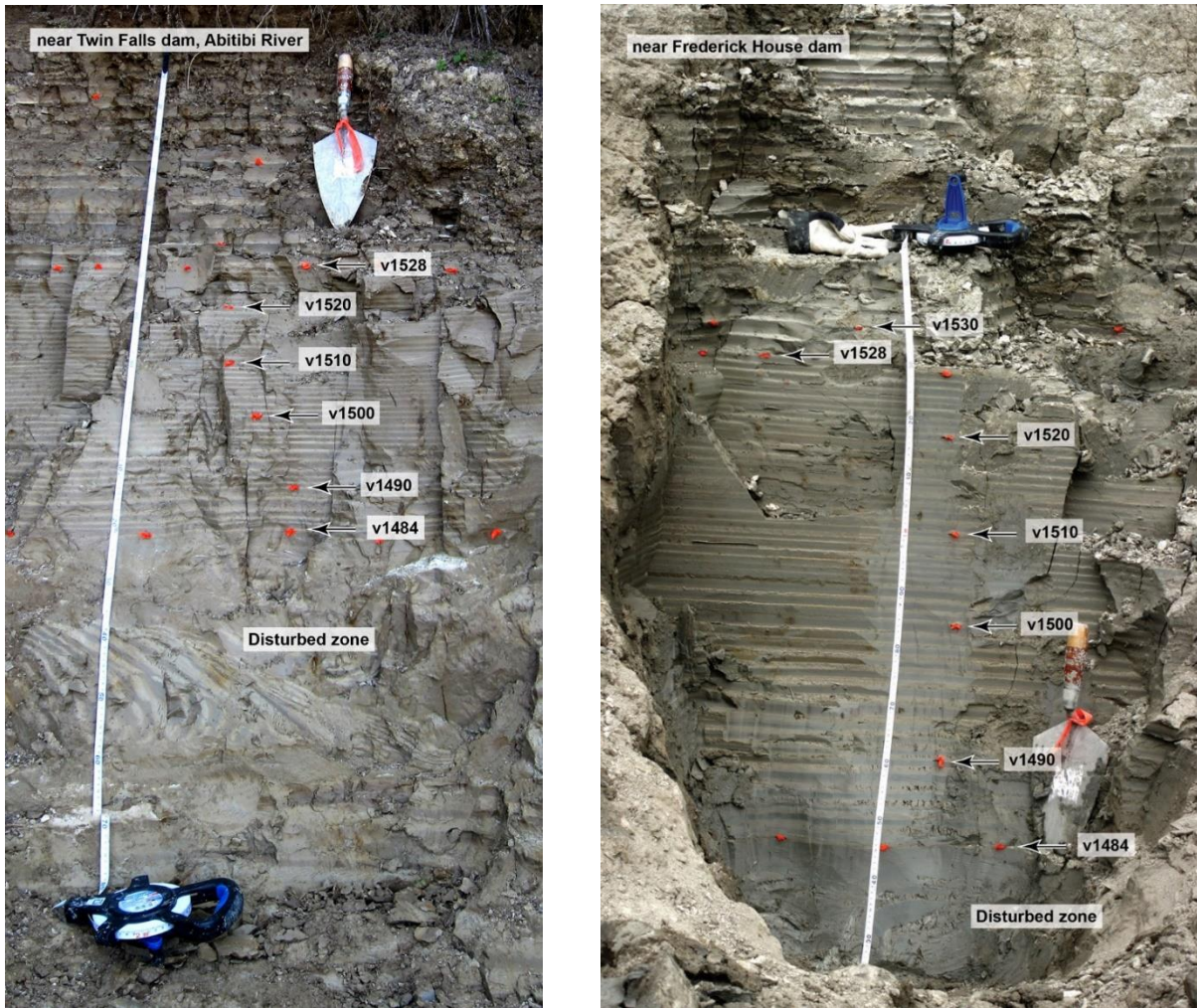


**Figure 4-7: Photograph of Varves Exposed along the Abitibi River, near Twin Falls Dam, Ontario**

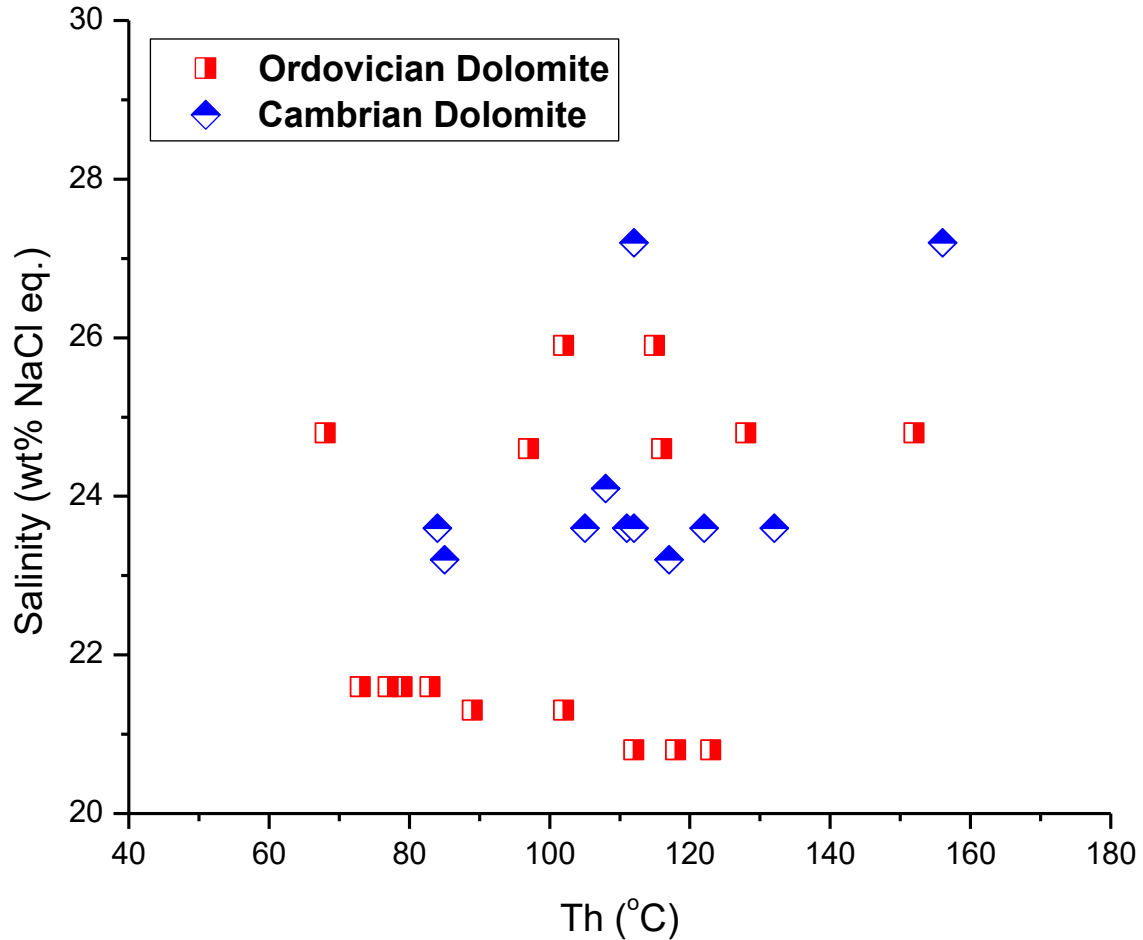
#### 4.7 DOLOMITE PALEOGENESIS

Research undertaken with the University of Windsor starting in 2015 has investigated the nature and origin of strata-bound near-horizontally layered dolomitized beds occurring within the bedrock formations of the Black River Group in the Huron Domain of southern Ontario. In 2018, the research program continued to look for evidence of fault-related dolomitization at a regional scale. Based on results to date, there is no evidence from the wells sampled within the Huron Domain for the presence of fault-controlled dolomites. A summary of the work conducted since 2015 is given in Al-Aasm and Crowe (2018).

A key finding from this research has been the identification of two distinct diagenetic fluid systems: An underlying permeable Cambrian system with a more radiogenic, high temperature and highly saline signature; and an overlying Ordovician system characterized by a less radiogenic, higher temperature and salinity signatures (Figure 4-8). The isotopic  $\delta^{18}\text{O}$  signatures determined for the Cambrian are different from those of the Ordovician carbonates suggesting that a different fluid was responsible for dolomitization. The results of  $^{87}\text{Sr}/^{86}\text{Sr}$  ratios for matrix

dolomite and later precipitated calcite cement demonstrate both a marine fluid composition for the Ordovician carbonates and an external, more radiogenic source for the Cambrian.

In 2019, the scope of the research will focus on the determination of Rare Earth Elements (REE) in both previously examined samples and new samples collected in 2018. The objective of this research is to better understand the provenance of the source material for the formations.



Note: this figure shows a bimodal distribution in the Ordovician and Cambrian formations. In both formations the salinity values for the measured fluid inclusions in both calcite and dolomite are high, suggesting dolomitization and calcite cementation resulted from highly saline (brine) fluids.

**Figure 4-8: Plot of Salinity vs Homogenization Temperatures for Samples in the Huron Domain**

#### 4.8 NATURAL RESOURCE ASSESSMENT – SOUTHERN ONTARIO

The Geological Survey of Canada is quantitatively assessing oil and gas resources in the proposed deep geologic repository and vicinity area of southern Ontario. In particular, it is considering self-sourced and -retained fine-grained shale reservoirs in the Upper Ordovician Collingwood and Rouge River members, as well as the potential for undiscovered oil and gas resource in Paleozoic conventional reservoirs. If the two Upper Ordovician shale units are treated as separate resource plays, both fail to meet the minimum criteria set out by the United States Geological Survey that define a hydrocarbon resource play. When combined however, the two units can be treated as a continuous sedimentary package and, therefore, can be treated as a single resource play.

The cut-off for the regional study (see Figure 4-9) is conservative and reflects the uncertainty in the region due to a low density of wells. The cut-off for the volumetric calculation is 0.5 meters of cumulative hydrocarbon-saturated rock column, which is calculated from hydrocarbon saturated porosity times gross thickness of combined Collingwood and Rouge River shale units. The 0.5 meter cut-off is equivalent to a hydrocarbon saturated porosity >2.5% and combined gross thickness >20 meters. The cut-off is in general consistent with the geological criteria for defining the shale play boundary discussed in the previous section. The total area defined by the reservoir cut-off is smaller than the area within the shale play boundary and is regarded as the risked prospective area by reservoir criterion.

Technically recoverable resources are to be calculated for both formations within the study area, with the results to be compared to similar conventional black-shale reserves in North America. A final report on this research is expected in 2019.

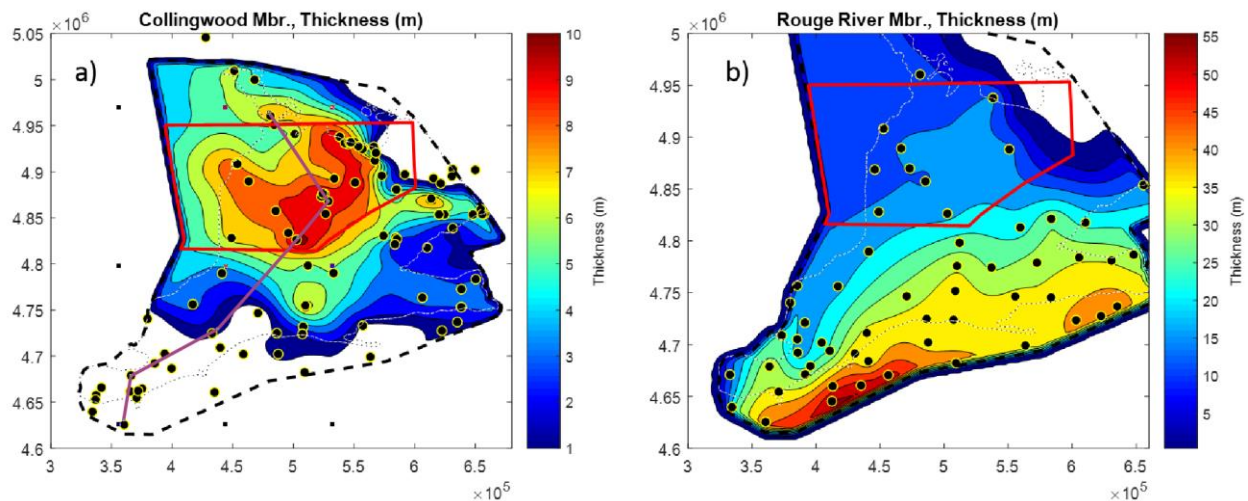


**Figure 4-9: Isopachs of the Upper Ordovician Shale Units (Collingwood and Rouge River Members) Showing Geographic Variation in Thickness of the Shale Units in Relation to the Study Area (Red Polygon)**

## 4.9 FRACTURE NETWORK MODELLING

Fracture network modelling involves using 3-dimensional (3D), geostatistical tools for creating realistic, structurally possible models of fracture zone networks within a geosphere that are based on field data. The ability to represent and manage the uncertainty in the geometry of fracture networks in numerical flow and transport models is a necessary element in the development of credible geosphere models. Fracture network modelling will also be used to inform repository siting and design. The NWMO is supporting the MoFrac code for this modelling. Creation of fracture network models in MoFrac is a multistep process that involves integrating interpretations of lineament data and other available field data to define fracture orientation sets and their parameterization.

In 2018, a new research program was initiated to further refine the MoFrac software. This enables model development and validation to occur in an iterative manner to support site characterization activities. Also during 2018, work commenced to build version 4.0 of the code. The following key development tasks were chosen to prepare the code for application to site-specific information:

- Propagate fractures in 3D: Rather than using an assigned 'mean orientation plane', fractures will be allowed to propagate freely in 3D.
- Vary fracture intensity spatially: Ability to define fracture density as a function of depth, or, more generally, by proximity to defined geometry. Stochastic fractures will be seeded at depth to achieve required intensities.
- Allow further propagation of a DFN model: Enable MoFrac to import existing DFNs to further propagate defined fractures, and to add additional fractures.
- Profiling MoFrac: MoFrac will be profiled to identify where performance enhancements would be most beneficial.
- Repeatability: To enable results that are reproducible, random number generator seed(s) will be stored. The random number generation strategy will have to accommodate algorithms that exploit parallelism.
- Fracture branching and clustering: Fracture branching will permit MoFrac to simulate either branching or coalescing fractures. Fracture clustering will allow for control of the spatial distribution of fractures.
- Time slicing: Time slicing will be used to propagate multiple fractures simultaneously. Propagation will no longer be a whole-fracture process, but instead will operate on extending a partially-complete-fracture mesh.
- Mapping attributes and generating apertures: Add a new feature to permit attribute data to be mapped to fracture mesh points and/or triangles. Variations in aperture across a fracture will be generated stochastically and be mapped on fracture mesh points.

Development work will continue during 2019, with the release of Version 4.0 scheduled for the following year.

#### 4.10 GLACIAL SYSTEMS MODELLING

Over the last one million years, the Canadian landmass has been subjected to nine glaciation events, each lasting for periods of approximately 100,000 years (Peltier 2002). Glaciation associated with long-term climate change is considered the strongest external perturbation to the geosphere at potential repository depths. Potential impacts of glacial cycles on a deep geological repository include: 1) increased stress at repository depth, caused by glacial loading; 2) penetration of permafrost to repository depth; 3) recharge of oxygenated glacial meltwater to repository depth; and 4) the generation of seismic events and reactivation of faults induced by glacial rebound following ice-sheet retreat. The ability to adequately predict surface boundary conditions during glaciation is an essential element in determining the full impact of glaciation on the safety and stability of a DGR site and will be a necessary component of site characterization activities. For NWMO's studies into the impact of glaciation, such boundary conditions have been defined based on the University of Toronto's Glacial Systems Model (GSM) predictions (Peltier 2002, 2006a,b; Stuhne and Peltier 2015a,b; 2016; 2017). The GSM is a state-of-the-art model used to describe the advance and retreat of the Laurentide ice-sheet over the North American continent during the Late Quaternary Period of Earth history.

Following the update to the GSM methodology and subsequent validation described in Stuhne and Peltier (2015a,b; 2016; 2017), a new phase of research has been undertaken to refine the representation of the evolution of paleolakes and surface drainage basins within the model.

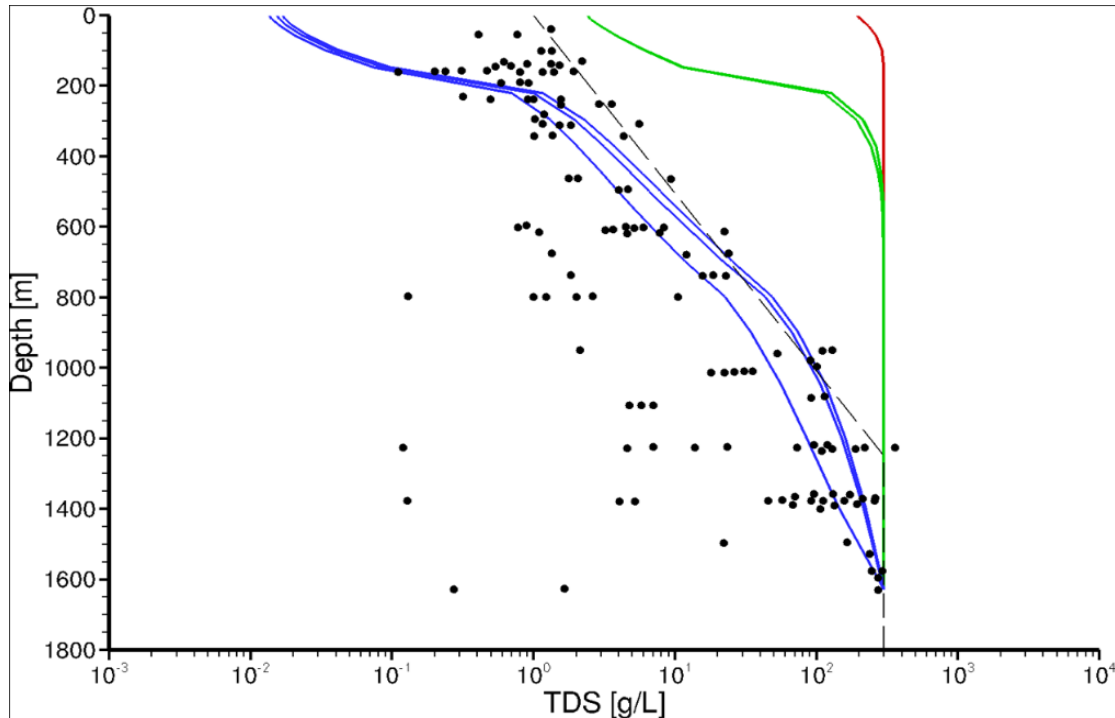
#### 4.11 GROUNDWATER SYSTEM EVOLUTION

Groundwater salinity (often expressed as Total Dissolved Solids or TDS) is relevant to the long-term behavior of the deep groundwater system. More saline fluids are denser. Including the currently measured salinity profiles with depth into groundwater models requires some analysis to ensure that the salinity profiles are consistent with the natural evolution of the site.

Research activities at the University of Waterloo focussed on the development of a conceptual model that allows for the in-situ generation of brine in a crystalline rock setting in groundwater models. Given that pore fluids at depth are in contact with the rock matrix for millions to billions of years, this approach allows for a steady-state equilibrium to be reached with the measured in-situ TDS being used as an upper bound concentration. A linear driving force source term for brine TDS is assigned in the groundwater model (HydroGeoSphere) using a mass transfer coefficient and the equilibrium brine TDS concentration. The rate of progress toward equilibrium is assumed proportional to the difference between the current state and the equilibrium state and the mass generated is linearly proportional to the driving force. This methodology has the benefit that at steady-state, the groundwater system would achieve equilibrium between the amount of brine mass produced in-situ and the amount removed from the groundwater system at discharge locations.

Various factors affect the steady-state brine TDS distribution, including the brine mass transfer coefficient and the hydraulic conductivity of the fracture zones and rock mass. A comparative analysis for nine models using a combination of three mass transfer rates and three fracture zone hydraulic conductivities ( $10^{-8}$ ,  $10^{-9}$ ,  $10^{-10}$  m/s) was developed (Normani et al. 2018). Figure 4-10 shows the average concentration vs average depth for all model domains. Data from the Canadian Shield is also plotted on the figure for comparison. The mass transfer rate of  $2 \times 10^{-18}$  s<sup>-1</sup> provides the best overall fit (blue lines) and the variation in TDS concentration is also more apparent with differing hydraulic conductivities as compared to the other scenarios.

An extensive review of the literature was begun to update hydraulic and geochemical properties of crystalline rock. This database will permit an update of both Equivalent Porous Medium rock mass and fracture zone properties with depth for Canadian Shield settings. This database contains data from over 200 studies covering 33 countries with over 30,000 permeability versus depth measurements. These measurements were collected by Ahtziger-Zupancic et al. (2017) and Ranjram et al. (2014). In addition, over 380 geochemical data for Canada are included. The permeability data were checked for duplicates in site location, depth, and permeability. This reduced the database to 23,760 unique permeability versus depth measurements for the global dataset. Additional data from Canadian Shield sites is being sought and added to the database.



Note: Red, green, blue are mass transfer coefficients of  $2 \times 10^{-12}$ ,  $2 \times 10^{-15}$  and  $2 \times 10^{-18} \text{ s}^{-1}$ , respectively.

**Figure 4-10: Average TDS Concentration vs Average Depth for Modelled Domains**

## 4.12 GEOMECHANICAL RESEARCH

The NWMO geomechanical work program concentrates on the near-field, defined as the rock mass in the immediate vicinity of any underground openings. The research can be divided into two branches: 1) characterization of rock properties at field and laboratory scales, and 2) numerical modelling of rock mass behavior. The following is a brief update on geomechanical research conducted during 2018. Much of this work was conducted at Queen's University.

### 4.12.1 Effects of Saturation on Mechanical Parameters

Building on past work conducted by Jaczkowski et al. (2017a,b) to explore scale effect, loading rate and saturation condition on EDZ damage parameters from unconfined compression testing involving Cobourg argillaceous limestone. Parameters examined include Crack initiation

threshold (CI), Critical Crack Damage (CD) and peak strength or Unconfined Compressive Strength (UCS). This new testing program utilized samples from the Point du Bois (PdB) batholith in Manitoba. Currently, Lac du Bonnet (LdB) granite is being also tested for saturation effects.

Different saturation conditions were achieved through use of RRH (relative room humidity of unconditioned samples), oven drying to achieve minimum saturation, and various saturation techniques (short and long-term immersion as well as vacuum saturation). For the limestones, it was observed that a dominant proportion of the water intake for a bulk sample was entirely within the argillaceous phases. For granite, re-saturation was limited (less than 0.1% water content achieved).

As depicted in Figure 4-11, Brazilian tensile strength (BTS) data shows a decreasing trend with water content in the limestone. On the other hand, Brazilian tensile strength of the granite appears unaffected by the saturation range achieved in these experiments.

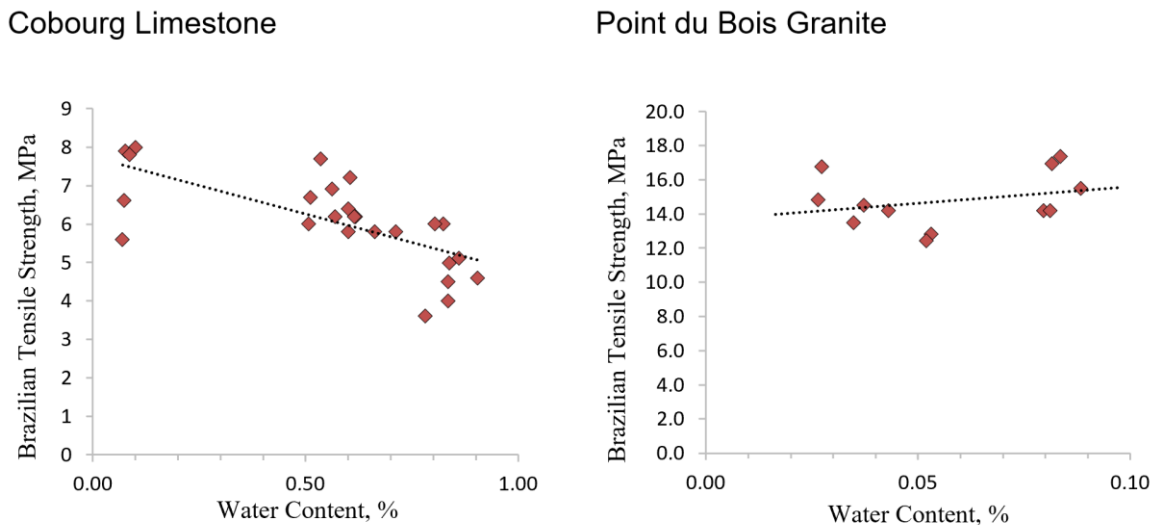


**Figure 4-11: Effects of Saturation on BTS for the Cobourg Limestone (Left) and Point du Bois Granite (Right)**

Unconfined Compressive Strength test data was used to determine the UCS, Young's modulus, Poisson's ratio, and CI and CD thresholds. Average CI is estimated using lateral strain, crack volumetric strain, inverse tangent lateral stiffness, instantaneous Poisson's ratio and acoustic emissions (Jaczkowski et al. 2017a,b). The methods used to determine an average CD are axial strain, volumetric strain, instantaneous Young's modulus, and acoustic emissions. While the limestone showed distinctive inverse trends for CD and UCS, there was less influence of saturation on the damage initiation threshold of the limestone (coincident with the long-term in situ strength limit as per Ghazvinian and Diederichs 2018). For the granite, conflicting trends were observed for the upper bound strength thresholds. This may be due to internal variability within the samples. Similar testing will be done with the more homogenous Lac du Bonnet granite. Water content, within the ranges achievable by re-saturation, had little effect on Poisson's ratio and an inverse influence on Young's modulus for both rock types.

Triaxial (confined compression or TCS) test data was used to determine confined CI, CD, and peak strength in RRH (room relative humidity) and SAT (saturated) conditions. Generalized Hoek-Brown envelopes (Hoek et al. 2002) were used for the three thresholds (Figure 4-12). For the Cobourg limestone, the triaxial testing results show a significant decrease of peak strength and CD envelopes with saturation, while CI remains relatively unaffected. There is minimal impact of saturation on the thresholds for the granite.

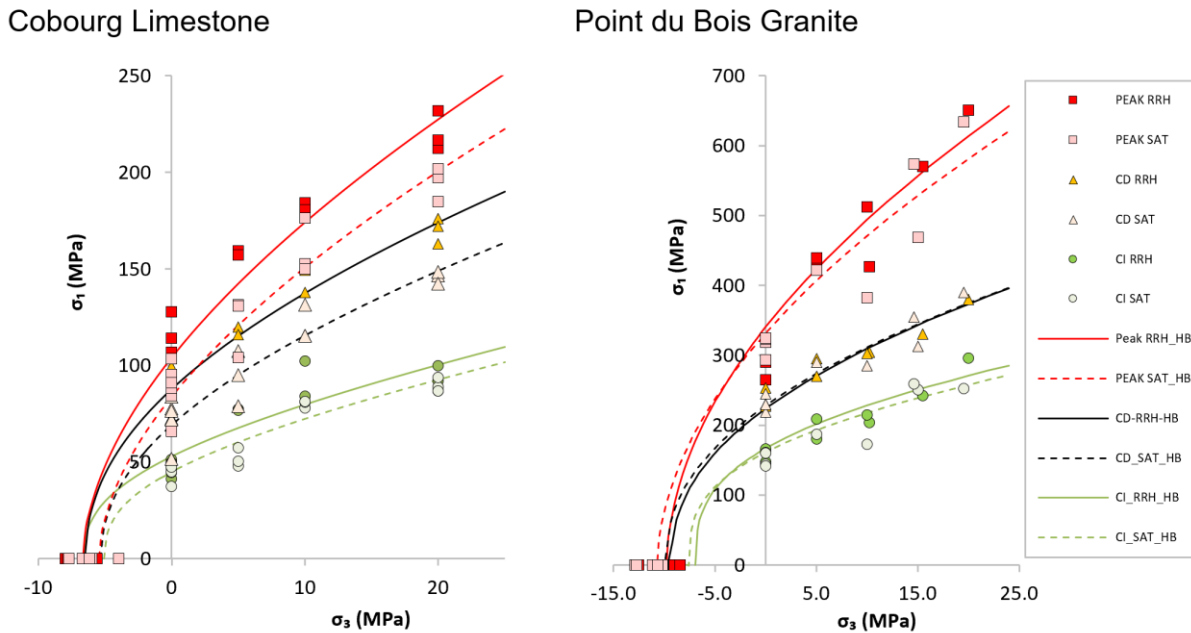


**Figure 4-12: Effects of Saturation on Damage Threshold and Strength Envelopes in the Cobourg Limestone (Left) and Point Du Bois Granite (Right)**

#### 4.12.2 Exploration of Boundary Condition Effects on Direct Shear Testing

Packulak et al. (2018a,b) completed a preliminary study on the impact of the normal boundary condition in direct shear testing. Conventional shear testing is performed on joints and fractures by maintaining a constant normal stress (in a test called constant normal load – CNL) on the shearing sample. In constant, normal stiffness (CNS) testing, the boundary condition normal to the sample simulates a spring responding to joint dilation by increasing confinement. The former condition is ideal for slope and surface work whereas the CNS condition is intended to replicate the confined condition around a joint in an underground situation. The aim of this research is to explore this method and produce guidance for its application.

#### 4.12.3 Assessment of Natural Variability of Mechanical Parameters Using Continuous Logging

Sampling for physical testing (UCS, BTS, TCS, etc.) is a discrete process. Samples are selected at defined intervals governed by the investigation scope (feasibility vs detailed design, for example). The resultant data may be sufficient to quantify mean values for formations and units within the rock but may not fully capture the inherent variability in laminated sedimentary rock or variable metamorphic rock. A continuous logging process was validated using a 500 m length of continuous drill core through sedimentary rock (Gull River Formation) and the

basement metamorphic rocks beneath Kingston, Ontario. Additional experimental data was obtained from a horizontal probe hole from mine development in the Sudbury area. Further work is needed to adapt this technique for downhole logging in addition to on-surface core analysis. Nevertheless, this could be a powerful tool for site investigation and reliability analysis ( Figure 4-13).

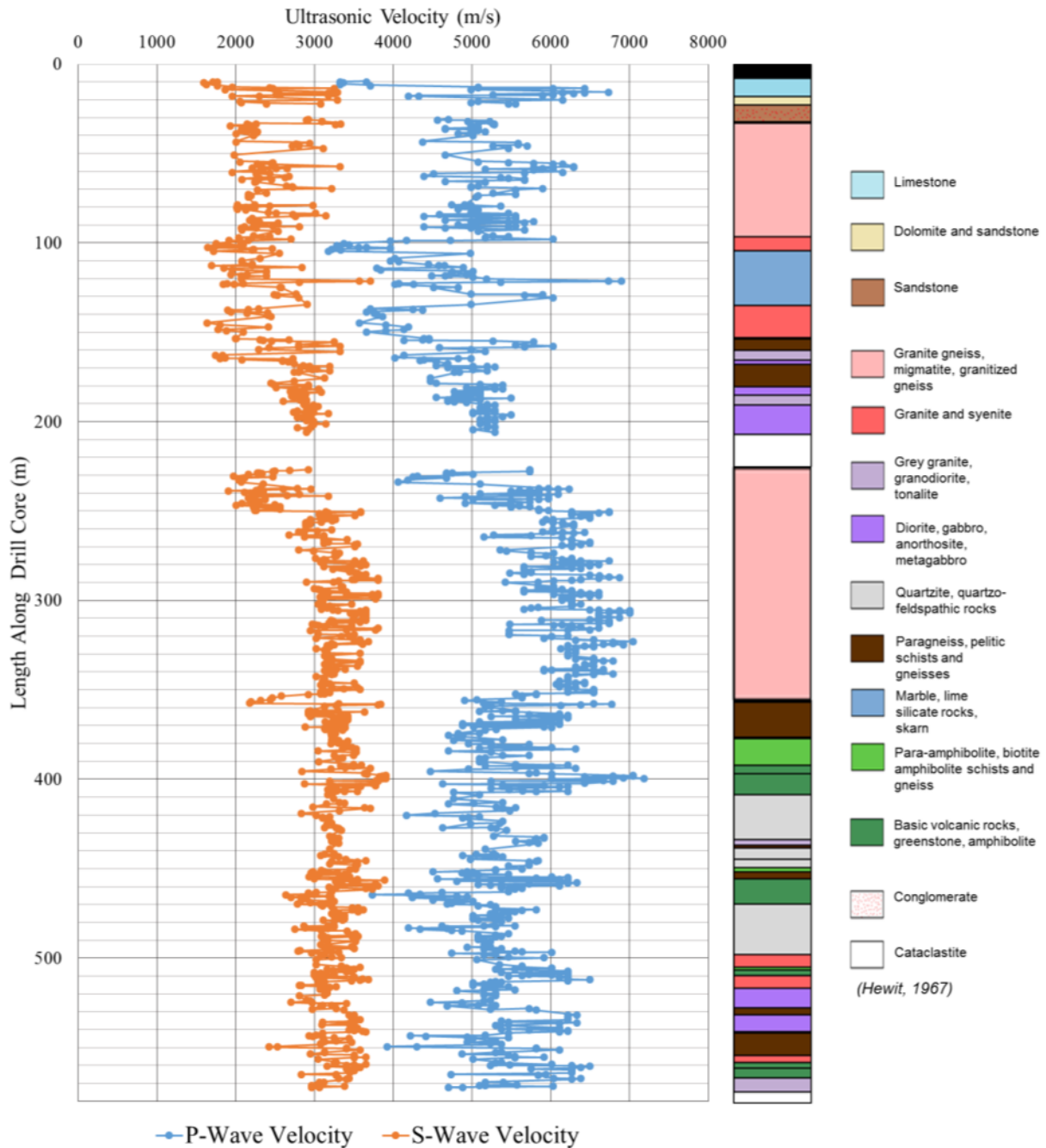


Figure 4-13: Example Data from Continuous Acoustic Logging of Drill Core

#### 4.12.4 Parametric Variability and Reliability of EDZ Predictions

Ongoing research relates to quantifying the reliability of EDZ prediction, in brittle rocks, from numerical models, and includes both continuum and discontinuum approaches. The following two continuum approaches are used:

- Damage Initiation Spalling Limit (DISL) approach using finite element analysis (RS2 by Rocscience Inc.)
- Cohesion Weakening Friction Strengthening (CWFS) using finite difference analysis (FLAC by Itasca Consulting Group, Inc.)

Two discontinuum approaches for Grain Based Models (GBM) are used, as follows:

- Discrete Element Models (DEM) using UDEC (Itasca Consulting Group, Inc.)
- Finite-Discrete Element Models (FDEM) using IRAZU (Geomechanica Inc.)

A comparison of continuum analysis of EDZ (DISL in RS2) and discontinuum analysis (FDEM using Irazu) is underway using the example of the Mine-by Experiment from the AECL Whiteshell Underground Research Laboratory. The first step in this analysis for each method is to establish indicators for EDZ prediction and delineation. This was done for DISL models by Perras and Diederichs (2016), for CWFS models by LeRiche et al. (2017) and Walton and Diederichs (2015). The delineation of EDZ zones (HDZ, EDZ<sub>i</sub>, EDZ<sub>o</sub>, EIZ) in discontinuum codes requires a different approach: work in progress by other members of the research team using FDEM; and using DEM by Vazaios et al. (2018c), Farahmand et al. (2018) and by Dadashzadeh and Diederichs (2018a,b). The next steps involve reliability analyses (Dadashzadeh and Diederichs 2018c, for example) relating model input uncertainty to predictive variability and reliability. The research plan for this study is shown in Figure 4-14 with significant progress in 2018 and completion expected in 2019.

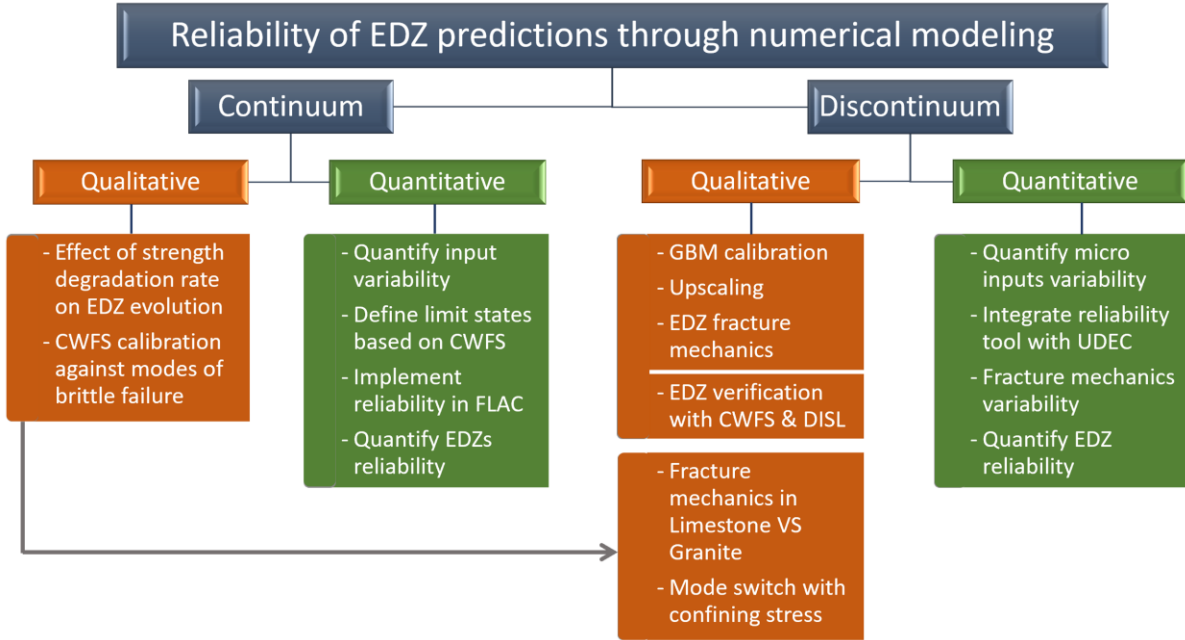


**Figure 4-14: Workflow for Comprehensive Study of EDZ Reliability from Continuum and Discontinuum Models**

The influence of sparse and non-persistent jointing (pre-existing fractures) on the development of EDZ using discontinuum models has been the subject of research by Vazaios et al. (2018a,b) and Farahmand et al. (2018). An example of the impact of non-persistent structure, generated using a DFN engine (MoFrac) combined with FDEM (Irazu) can be seen in Figure 4-15.

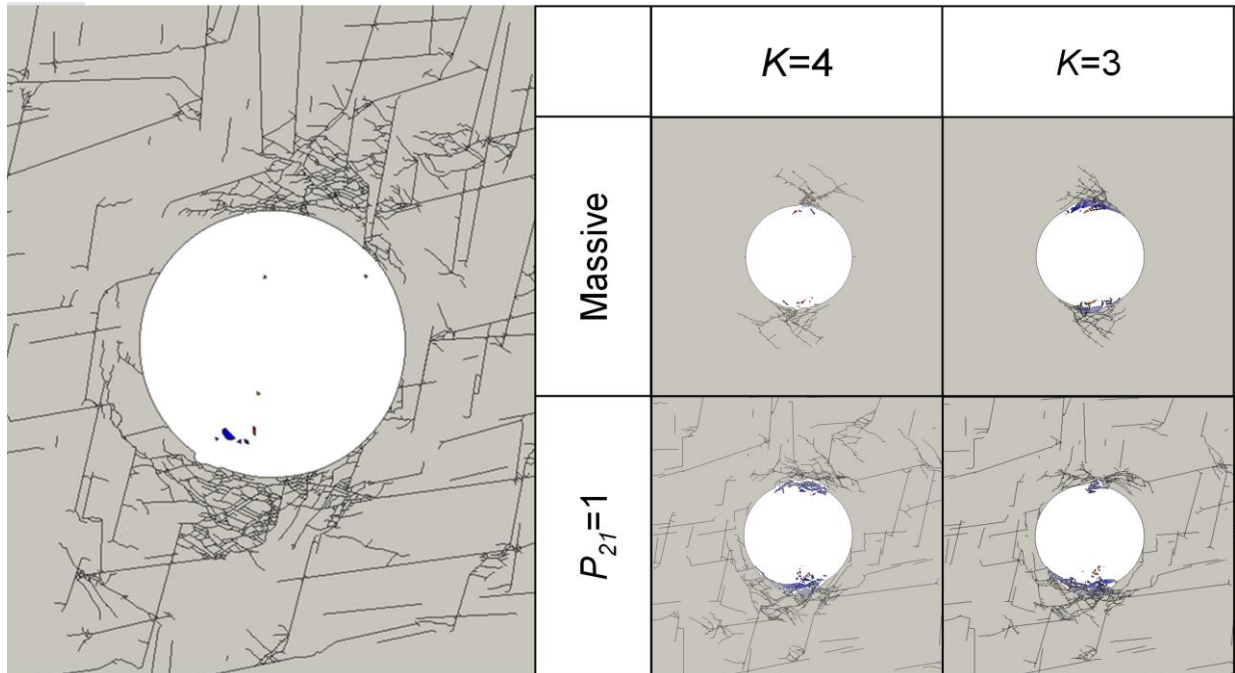


**Figure 4-15: Influence of Sparse, Non-persistent Jointing on EDZ Development**

Ongoing research is aimed at providing a methodology for similar analyses using discontinuum methods. The effect of different in situ stress ratios and magnitudes, relationships between damage initiation and peak compressive or tensile strength (lithological factors) and geometry are currently being explored.

#### 4.13 THERMO-HYDRO-MECHANICAL PROPERTIES OF LOW-POROSITY ROCKS

##### 4.13.1 Permeability of Cobourg Limestone

Measurement of the permeability characteristics of the Cobourg limestone presents a challenge because of the heterogeneity of the rock at the decimeter scale, which requires testing of samples of sufficient dimensions that will encompass a Representative Volume Element (RVE). The RVE should contain the nodular lighter components (consisting of calcite and dolomite) and the darker phase argillaceous partings (consisting of calcite, dolomite, quartz and a nominal amount of clay). The nodular regions can vary in dimensions up to 75 mm. Both lighter and darker components have low permeabilities. In order to perform steady state tests, the sample dimensions in the direction of flow need to be small, which is not feasible if the RVE constraint is to be satisfied. Therefore, research was conducted to develop a multi-phasic approach to estimate permeability of the Cobourg limestone, based on the permeability measurements of the separate components from either local permeability measurements, or by small sample testing.

The permeabilities of the lighter and darker components were determined in the studies performed by Selvadurai and Głowacki (2018) and Głowacki (2017), which used mini-water entry ports located in regions with visually identified lighter and darker components. The permeabilities of the two components were estimated as:

$$K_{DR} \approx 8.00 \times 10^{-19} \text{ m}^2 \quad ; \quad K_{LR} \approx 0.62 \times 10^{-19} \text{ m}^2$$

Gas permeability testing of the two components performed at CYDAREX (Paris, France) resulted in:

$$K_{DR}^G \approx 0.127 \times 10^{-19} \text{ m}^2 \quad ; \quad K_{LR}^G \approx 0.026 \times 10^{-19} \text{ m}^2$$

The higher values for the mini-water entry port tests could be attributed to the sample disturbance during installation of the entry ports. These values can be used as possible upper and lower limits for the permeability values of the different components within the Cobourg limestone. The trends in the experimental values are consistent in the sense that the darker component has a higher value of permeability than the lighter component.

Research to estimate the bulk permeability of the Cobourg limestone was extended to mapping of the spatial distribution of the separate components of the rock by dissecting a cuboidal region of the Cobourg limestone measuring 80 mm x 120 mm x 300 mm into ten samples measuring 80 mm x 120 mm x 8 mm. The surface features of the sections were digitally imaged and the interior distribution was estimated using either extrusion over the 8 mm thickness or by using the LOFT command in AUTOCAD. The mapped regions of the thick sections were used to construct finite element models of the fabric. Permeabilities of the sections in three orthogonal directions were estimated using the estimates for the component permeabilities (light and dark components). Both the weighted mean and weighted harmonic mean were used to obtain the directional permeabilities of the cuboidal region in three orthogonal directions. The effective

permeability of the cuboid was estimated using the geometric mean concept. Using the permeability estimates for the light and dark components from the mini- water entry ports testing (Selvadurai and Głowacki 2018; Głowacki 2017), the effective permeability is estimated to be

$$2.031 \leq \left( \frac{K^*}{10^{-19} \text{ m}^2} \right) \leq 2.266$$

However, using the component gas permeability estimates, the effective permeability is estimated to be

$$0.0602 \leq \left( \frac{K^*}{10^{-19} \text{ m}^2} \right) \leq 0.0728$$

Additional one-dimensional steady state tests on samples of the lighter and darker rock components will be conducted to resolve the discrepancy between the above two estimates.

#### 4.13.2 Thermal Conductivity of Cobourg Limestone

Experiments were conducted to estimate thermal conductivity of the Cobourg limestone using one-dimensional (1D) transient tests. Cylindrical test specimens 50.8 mm in diameter and 250 mm long were cored normal to the nominal planes of argillaceous partings and oven dried. The test specimens were insulated on the side. Heat was applied on one end and the other uninsulated end was maintained at a constant room temperature by providing an insulating layer material to minimize effects of convection (Figure 4-16). The temperatures were measured at two locations on the cylindrical surface of the specimen using Type K thermocouples. The time history of the temperature evolution in the middle and quarter of the specimen height from the hot plate were used in conjunction with a finite element approach (COMSOL software) to estimate the thermal diffusivity and consequently the thermal conductivity. Deviations from the purely 1D heat conduction through the test specimen can occur as a result of heat conduction through the insulation. A PID controller was used to maintain a constant temperature at the base of the sample (i.e. by the hot plate). An optimization technique was used to minimize the error between the theoretical predictions based on the finite element technique and the experimental results. The experiments were performed at three boundary temperatures; i.e. 50°C, 100°C and 150°C.

The preliminary results from this research do not indicate any specific trend of thermal conductivity with temperature, and correspond well with those reported by Pitts (2017) and AECL (2011), as shown in Table 4-1.

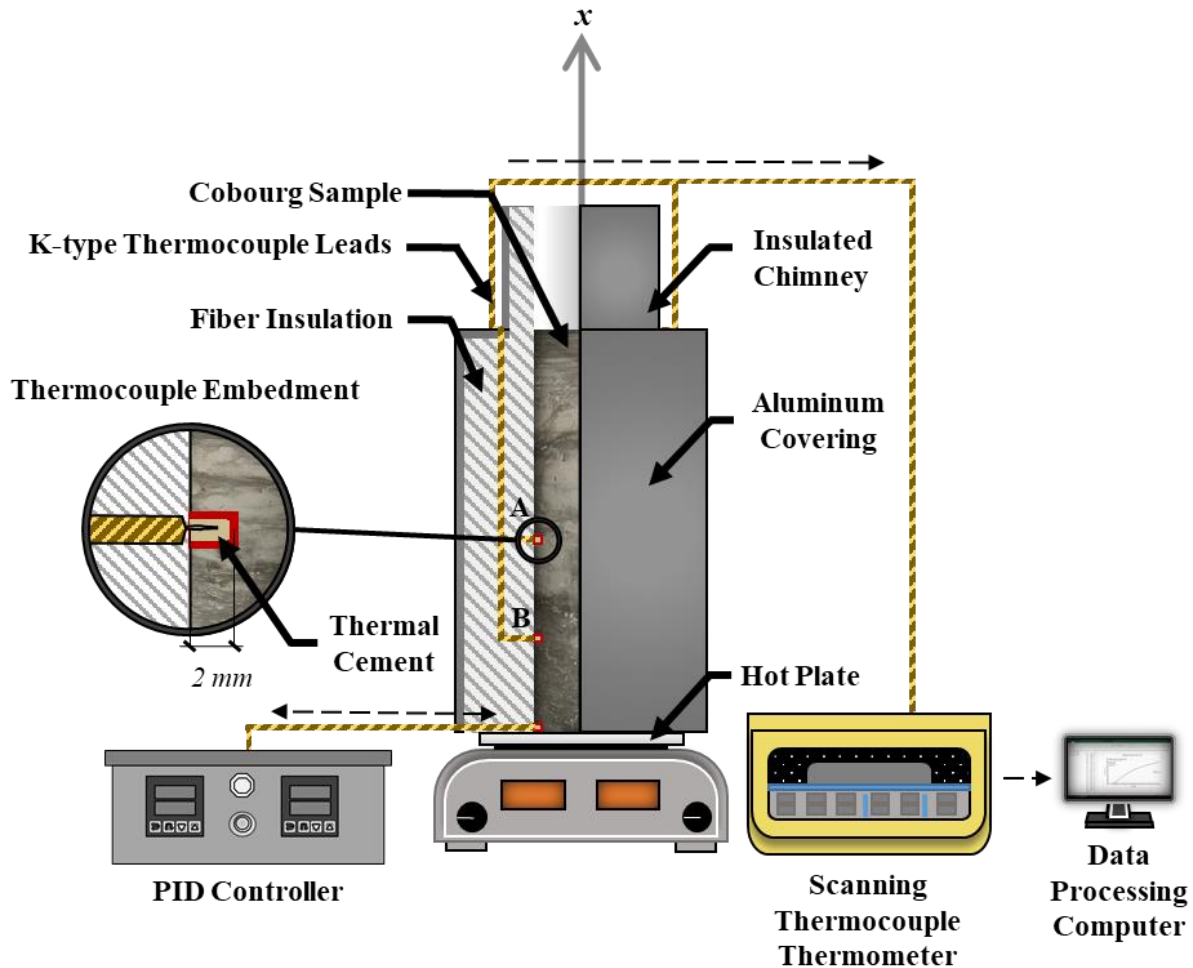


**Figure 4-16: Details of 1D Thermal Conductivity Experiment of the Cobourg Limestone**

**Table 4-1: Preliminary Thermal conductivity of the Cobourg limestone from McGill University compared to published literature [W/mK]**

Study	Temperature (°C)			
	25	50	100	150
Current testing at McGill University		2.14	1.98	2.12
Pitts (2017)	3.04±0.9	2.50±0.9	1.43±0.9	-
AECL (2011)	2.56	-	-	-

#### 4.13.3 Physical and Mineralogical Characteristics of Stanstead and Lac du Bonnet Granites

In the past, researchers at McGill University have studied the thermal and fluid transport characteristics of the Stanstead granite (from the eastern flank of the Canadian Shield in the province of Quebec) including permeability (Selvadurai et al. 2005; Selvadurai and Najari 2015, 2016), THM response (Najari and Selvadurai 2014), and recent complementary studies (e.g.

XRD analysis). During 2018, the research team began testing the Lac du Bonnet granite. This is a new initiative from NWMO to further characterize the Lac du Bonnet granite as a reference crystalline rock from the western flank of the Canadian Shield. Detailed studies on these reference rocks will provide context for the characteristics of crystalline rock from the candidate repository site.

XRD analyses employing a Bruker D8 Discovery X-ray Diffractometer were used to estimate the mineralogical composition of the Stanstead granite. The testing requirements include finely ground rock powder sieved to finer than 75 micrometers. Particles with grain size greater than 75 micrometer grain size were also separately tested, and revealed that XRD results were independent of grain size. The preliminary results indicate the presence of quartz, feldspar (mainly albite, oligoclase, and microcline), and mica (mainly biotite) in the Stanstead granite and are compared to published literature in Table 4-2.

The ongoing research will investigate physical and mineralogical characteristics of the Lac du Bonnet granites to understand its similarities to the Stanstead granite and to compare THM properties of both granites.

**Table 4-2: Mineralogical Compositions of the Stanstead Granite**

Study	Quartz (%)	Feldspar (%)	Mica (%)	Other (%)
Current testing at McGill University	38.6	58.9	2.5	-
Nasseri and Mohanty (2008)	24.7	66.7	0.6	8

#### 4.13.4 Permeability of Stanstead and Lac du Bonnet Granites

Researchers at McGill University have extensively studied the permeability of low-porosity and/or heterogeneous rocks (e.g. Selvadurai and Selvadurai 2010, 2014; Głowacki and Selvadurai 2016; Selvadurai et al. 2005; Selvadurai and Najari 2015). For the Stanstead granite, the method described by Selvadurai and Selvadurai (2010, 2014) was adopted to estimate the surface permeabilities of a cuboid measuring 300 mm x 300 mm x 300 mm. To ensure that there is no interface leakage between the annular sealing region and the granitic rock, the sealing efficiency was confirmed through the application of a constant pressure to the permeameter in contact with a stainless steel plate. A preliminary surface permeability test resulted in a value of  $3.35 \times 10^{-18} m^2$  for permeability of the Stanstead granite whose porosity determined from dry and water- saturated densities was 0.77%.

Building on recent permeability works (e.g. Głowacki and Selvadurai 2016), using plugs of the Stanstead granite 50 mm in diameter and with lengths between 25 mm and 150 mm, steady-state and hydraulic pulse permeability tests were performed in a GDS Triaxial Cell following the procedures described by Selvadurai and Głowacki (2008) and Selvadurai et al. (2011). One-dimensional steady state tests were performed by maintaining a constant inlet pressure and estimating the flow rate using the time history of the volume being pumped through the sample. A preliminary test resulted in a permeability value of  $0.057 \times 10^{-18} m^2$ .

A schematic of the equipment currently being used to test the permeability of the Lac du Bonnet block is shown in Figure 4-17. Future research will investigate effect of sample dimension on the permeability of the Lac du Bonnet granite.

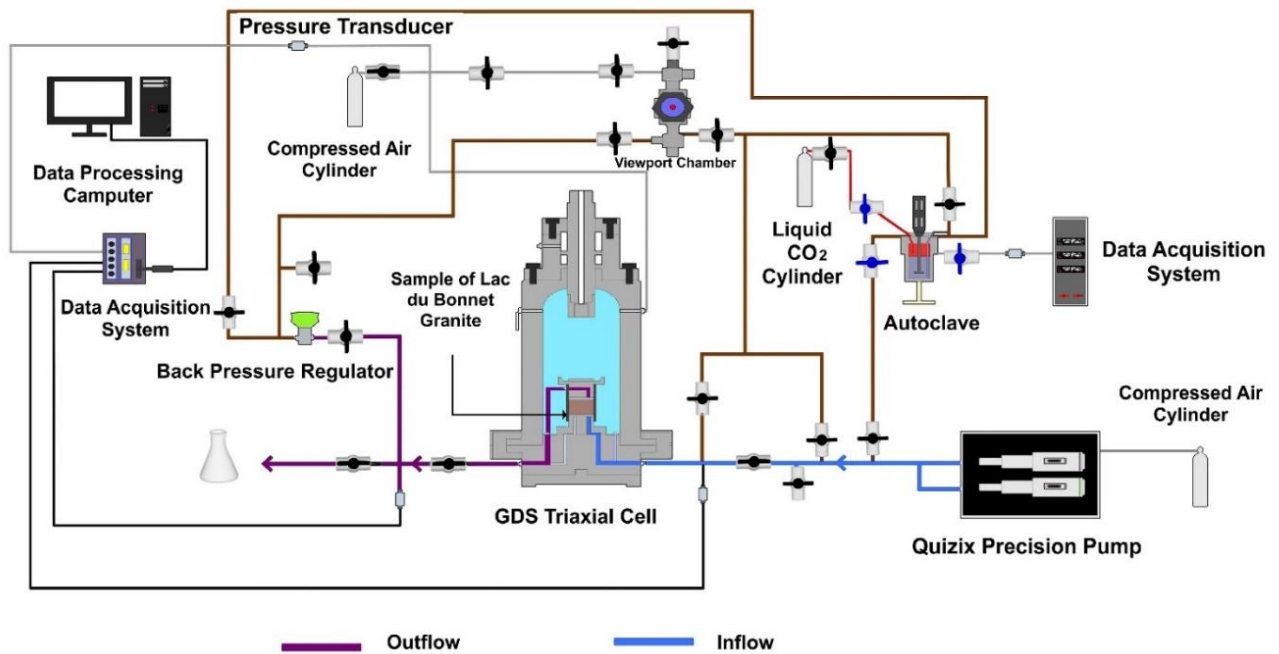


**Figure 4-17: A Schematic View of GDS Cell Used in Permeability Testing of the Granitic Samples**

#### 4.14 NUMERICAL DEVELOPMENT OF ROCK MASS EFFECTIVE PROPERTIES

The primary objective of this collaborative, international project with SKB is to design a methodology and a software tool to predict the evolution of rock mass effective properties with scale, using a multiscale DFN approach. Expected outcomes are constitutive relationships between initial fractured system models (DFN and fracture mechanical models) and the rock mass mechanical parameters such as: Elastic properties, young's Modulus ( $E$ ) and Poisson's ratio ( $\nu$ ) (equivalently the shear and bulk modulus,  $G$  and  $K$ , respectively). The evolution of fracture aperture, and therefore rock mass permeability, with evolving stress conditions will be examined. In a later phase of the project, failure envelope parameters (tensile strength, UCS, friction angle) will be addressed. The second objective is to apply the methodology developed to rock mass models in various settings, including an effective/explicit representation of fractures in modelling applications.

During 2018, research progress included the development of analytical equations and numerical solutions for elastic properties and stress aperture (e.g. Davy et al. 2018, Darcel et al. 2018), development of a new software tool (PyRockMass), including the ability to import a MoFrac-format DFN. Future research includes developing the ability to analyze and quantify stress fluctuations due to the presence and interaction of fractures of different sizes.

#### 4.15 FRACTURE PARAMETRIZATION AND UPSCALING - POST PROJECT

During the development of a nuclear waste repository, it is anticipated that discontinuities that range in scale from natural or induced microcracks to regional deformation zones will be encountered. Regardless of scale, these fractures must be considered in the design and safety assessment of the repository. In order to locate suitable rock masses for waste deposition, specific rock suitability classification criteria have been established by SKB and Posiva for their repository site developments (SKB 2009; Posiva 2012).

Current research within this collaborative project (POST 2016) between SKB, Posiva and NWMO is a continuation of an earlier study on fracture parameterization for repository design and post-closure analysis (namely POST 2014), which ran from 2014 to 2016 (Siren et al. 2017). The objectives of the POST 2016 project are to continue to develop a strategy and guidelines for determining the parameters necessary for assessing fracture stability at the deposition tunnel scale for repository design and safety assessment. Investigations under thermal and dynamic conditions are not within the scope of the current study. POST 2016 has also explored the influence of scale effect on fracture shear resistance due to the topography roughness of fracture surfaces by means of testing fracture replicas.

To achieve the study objectives, the research involves the following three tasks:

1. Construct fracture shear equipment to conduct large-scale laboratory testing in accordance to the original project plan (Siren et al. 2017) to support numerical model and constitutive model development.
2. Carry out a program of normal and shear testing of natural rock fracture samples and fracture replicas of different sizes under Constant Normal Stress (CNS) and Constant Normal Load (CNL) conditions. The intent is to improve current understanding of confinement and upscaling on the shear resistance of rock fractures.
3. Using the results of various scale shear tests from Task 2, perform back-analyses to develop and verify numerical models and constitutive relations to simulate and estimate large-scale shearing behaviour of a natural clean fracture (no mineral infill) that can be practically used to support rock suitability decision process for deposition hole selection. All findings from the analyses from both organizations will be synthesized to develop or improve a constitutive model of rock fractures.

Key progress to date includes:

1. The methodology for manufacturing and quality control of replica samples has been developed and tested.
2. Proof of concept shear testing with intermediate size samples has been successfully carried out. Several 100 mm x 70 mm natural fracture and replica samples have been tested. They have undergone 10 mm shear displacement under different CNL and CNS boundary conditions. The whole characterization package including laser scanning before and after testing, pressure film, and AE measurements has been successfully implemented (see for example Figure 4-18 and Figure 4-19).

In the next steps of this research, the experimental data will be used to reproduce the shear tests results numerically. The experimental will be also used as input into various analytical and

semi-analytical criteria to assess their applicability. It is expected that the large shear test equipment will be assembled, tested and that calibration will begin during 2019.

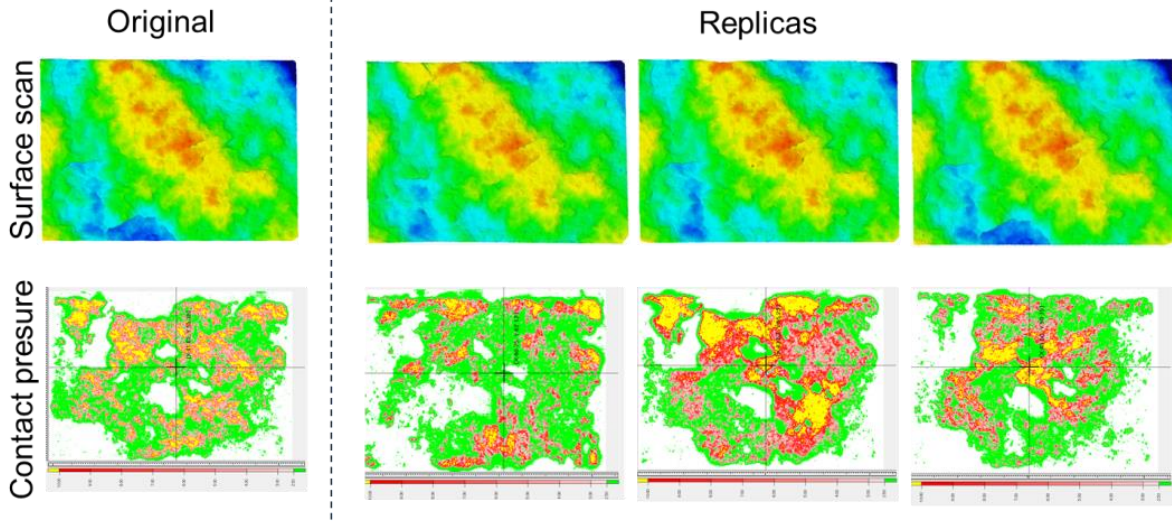
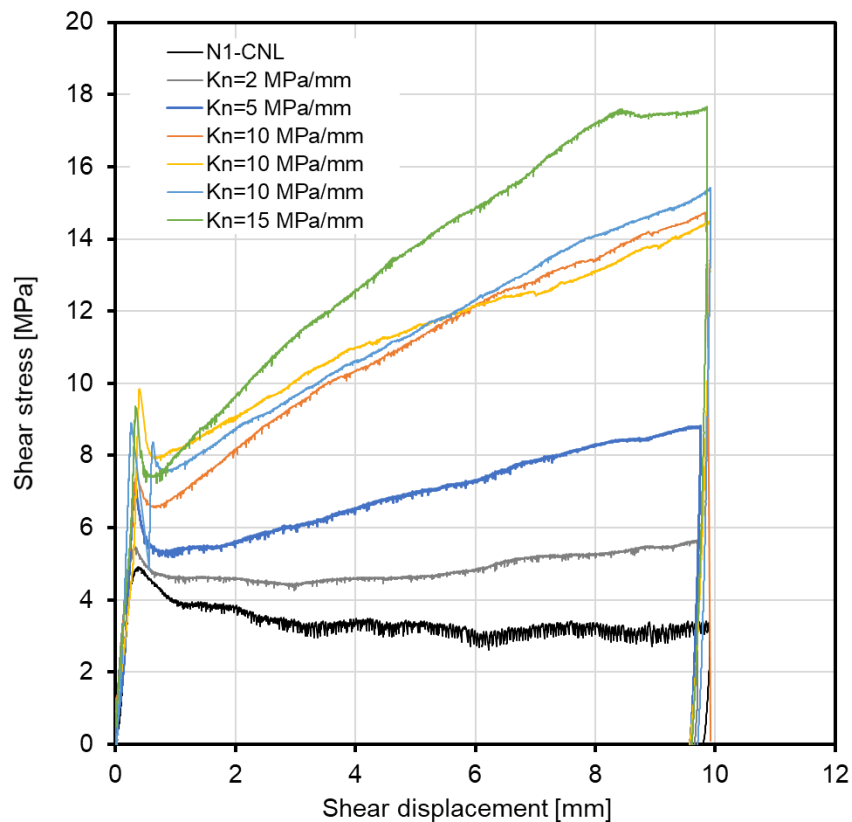


**Figure 4-18: Surface Scan and Contact Pressure Measurements of a Natural Fracture and its Three Replicas**



Note: the initial normal stress on the fracture plane is 5 MPa in all of the tests.

**Figure 4-19: Shear Stress vs. Shear Displacement Plots of a Natural Sample under CNL Conditions (N1-CNL) and Replicas under Different CNS Conditions**

#### 4.16 FIELD EXPERIMENTS IN MONT TERRI, SWITZERLAND

In 2018, the NWMO was a project partner in three experiments involving geomechanical research at the Mont Terri Rock Laboratory, Switzerland: the Full-scale Emplacement Experiment included the geomechanical aspects (FE-M) and gas monitoring (FE-G), and Geomechanical Characterization (GC-A). Updates on these experiments are provided in the following sections.

##### 4.16.1 Long-Term Monitoring of the Full Scale Emplacement Experiment (FE-M)

The FE-M experiment, a 1:1 horizontal heating test, is on-going - the heating phase commenced in December 2014. This experiment was designed to demonstrate the feasibility of: (1) constructing a full-scale 50 m long and 3 m in diameter deposition tunnel using standard construction equipment; (2) heater emplacement and backfilling procedures; and (3) early post-closure monitoring to investigate repository-induced thermo-hydro-mechanical (THM) coupled effects on the host rock and validation of THM models (Muller et al. 2017). A schematic of this experiment is shown in Figure 4-20.

The main objectives of this experiment were to understand the response of backfill material and the host rock (i.e. Opalinus Clay) to the elevated temperatures by using several hundred sensors to record temperature, pore-water pressure, humidity/water content and suction, and thermal conductivity, as well as deformations and stresses throughout the entire experiment duration. The monitoring program has completed its fourth year and measurements will continue in the coming years. Coupled THM modelling using the data collected is currently underway by two modelling teams contracted by Andra. Calibrations of the THM parameters of bentonite backfill and host rock are currently in progress in order to gain understanding of the underlying processes.

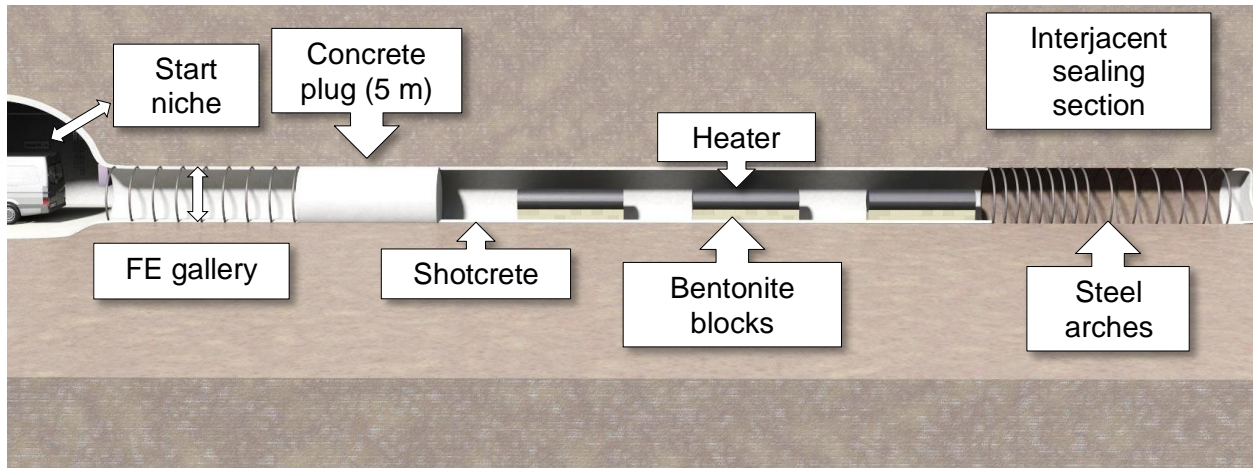


**Figure 4-20: Visualization of Final Arrangement of FE-M Experiment at Mont Terri Rock Laboratory (Muller et al. 2017)**

#### **4.16.2 Gases in an Unsaturated SF/HLW Emplacement Drift Experiment (FE-G)**

Gas monitoring in FE-G was on-going in 2018 and included gas composition studies, numerical modelling and complementary table-top experiments. The gas composition in the FE-G, similar to a potential DGR, is controlled by different biological, hydrogeochemical and transport processes. Analysis of aerobic conditions after backfilling, gas advection through the tunnel EDZ and plug, gas exchange with the clay host rock and other bio-chemical processes continued during 2018. Composition of the bentonite pore space has been monitored since construction in 2014 to capture long term behaviour of, for example, unsaturated transport of corrosive species (ex. O<sub>2</sub> and H<sub>2</sub>S) and gas generation (e.g. H<sub>2</sub>). An important observation from the test was the faster reduction in oxygen (weeks to months) compared with the previously estimated years to decades (Giroud et al. 2018).

#### **4.16.3 Characterization of EDZ Development - Sandy Facies Experiment (GC-A)**

This main objective of this experiment is to understand the geomechanical in-situ response of the Opalinus clay during excavation, with a focus on mineralogical variabilities (i.e. at the transition from shaly to sandy facies).

This experiment includes multiple components including:

- Monitoring of the excavation response: Geodetic techniques will be used to measure excavation convergence with high-frequency at the facies transition. Pore pressure response will be recorded by three grouted-in piezometers placed at variable distances along a 15 m long borehole;
- Laboratory and field testing to quantify the scaling factor between static and dynamic elastic properties of the Opalinus clay;
- In-situ stress measurements using different techniques (overcoring, pressuremeter, hydraulic fracturing) followed by 3D numerical modelling to investigate the effects of topography and larger tectonic structures on in-situ stress state.

These studies will be complemented by drilling radial boreholes and injecting resins to assess the extent of EDZ around the GC-A tunnel.

### **4.17 LONG-TERM STABILITY ANALYSIS OF DGR**

Building on past long-term stability analyses of repository configurations in both sedimentary and crystalline geological settings (Itasca 2015), research activities in this year included complementary numerical simulations as part of an updated study on long-term stability analysis of a DGR (to be published as Itasca 2019 report).

## 5. REPOSITORY SAFETY

The objective of the repository safety program is to evaluate and improve the operational and long-term safety of any candidate deep geological repository. In the near-term, before a candidate site has been identified, this objective is addressed through case studies and through improving the understanding of important features and processes. Activities conducted in 2018 are described in the following sections.

The NWMO has completed studies that provide a technical summary of information on the safety of repositories located in a hypothetical crystalline Canadian Shield setting (NWMO 2012; 2017) and the sedimentary rock of the Michigan Basin in southern Ontario (NWMO 2013; 2018). The reports summarize key aspects of the repository concept and explain why the repository concept is expected to be safe in these locations (see Table 5-1).

**Table 5-1: Typical Physical Attributes Relevant to Long-term Safety**

Repository depth provides isolation from human activities
Site low in natural resources
Durable wasteform
Robust container
Clay seals
Low-permeability host rock
Spatial extent and durability of host rock formation
Stable chemical and hydrological environment

### 5.1 MODEL AND DATA DEVELOPMENT

#### 5.1.1 Used Fuel Characterization

The inventories of radionuclides and potential hazardous contaminants in CANDU (Canada Deuterium Uranium) used fuel are important parameters in safety assessment and design of a DGR facility. The radionuclide inventories include fission products and actinides in the used fuel, and neutron activated impurities in the UO<sub>2</sub> pellets and Zircaloy tubing. A compilation of CANDU inventory data was produced in 2000/ 2001 (Tait et al. 2000; Tait and Hanna 2001). A compilation of the bundle inventory as of June 2018 is in Ion (2018).

##### 5.1.1.1 Used Fuel Inventory Update

Updating the 2000/2001 inventory continued throughout 2018. Calculations have been carried out using the most recent Industry Standard Tool version of the ORIGEN-S code and the latest CANDU specific nuclear data (e.g., cross-sections, decay data, and fission product yields) for a range of used fuel burnups of interest to the safety assessment or design. Similar calculations have also been performed for specific used fuel bundles with known burnups and power histories, for which radionuclide inventories have been experimentally measured. These latter calculations are for code validation and to provide confidence in the ORIGEN-S results. This work is expected to be completed in 2019.

### 5.1.1.2 Unirradiated Fuel Bundle Trace Element Composition

Measured data on main and trace elemental composition from 21 unirradiated CANDU fuel bundles ( $\text{UO}_2$  pellets, Zircaloy end caps, Zircaloy tubing, Zircaloy tubing with a braze and spacer, and Zircaloy tubing with CANLUB coating), which encompassed a range of manufacturers, bundle types and manufacture dates, were combined with available data from literature to develop a recommended elemental composition value for  $\text{UO}_2$  pellets and Zircaloy cladding (which includes the tubing as well as end caps, braze region and CANLUB). The results were used to support the code validation exercise and for the inventory update mentioned in Section 5.1.1.1.

### 5.1.1.3 Irradiated End Plate Analysis

The analysis of a sample of an irradiated CANDU fuel bundle end plate continued in 2018 at Kinectrics. The purpose was to obtain data on the radionuclide content of the Zircaloy, in order to help validate source term calculations. Figure 5-1 shows sample pieces prior to analysis.

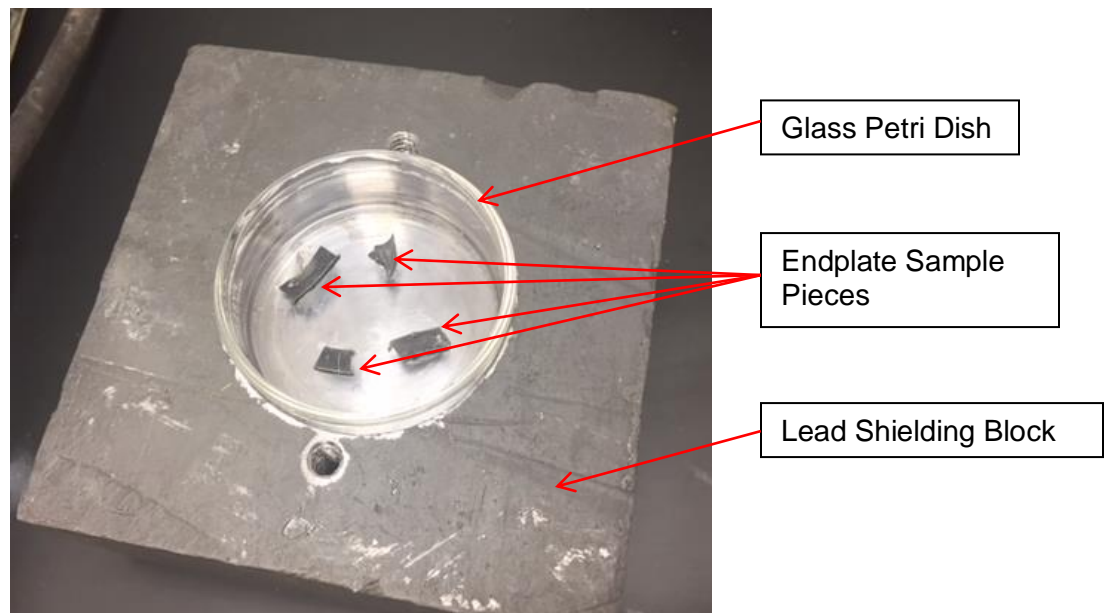


**Figure 5-1: Endplate Sample Pieces Prior to Analysis**

A 2- $\mu\text{m}$  thick zirconium oxide ( $\text{ZrO}_2$ ) layer was present on the outer surface of the endplate. The oxide layer was observed to be very thin and strongly adherent. The oxide layer was mechanically removed, along with adjacent surface base metal, to create a surface layer sample for analysis.

Both the surface layer and base metal samples were analyzed for elemental composition and radionuclide activity, which includes gamma and difficult-to-measure (DTM) radionuclides. Comparison of the radionuclide activities in the base metal and surface samples demonstrated that for most radionuclides, the activity agreed within an order of magnitude. The results of this analysis were used to support the code validation exercise mentioned in Section 5.1.1.1.

### 5.1.2 Wasteform Modelling

The first barrier to the release of radionuclides is the used fuel matrix. Most radionuclides are trapped within the  $\text{UO}_2$  grains and are only released as the fuel itself dissolves (which in turn only occurs if the container fails). The rate of fuel dissolution is therefore an important parameter for assessing long-term safety.

$\text{UO}_2$  dissolves extremely slowly under reducing conditions similar to those that would be expected in a Canadian deep geological repository. However, in a failed container that has filled with groundwater, used fuel dissolution may be driven by oxidants, particularly hydrogen peroxide ( $\text{H}_2\text{O}_2$ ) generated by the radiolysis of water. The mechanistic understanding of the corrosion of  $\text{UO}_2$  under used fuel container conditions is important for long-term predictions of used fuel stability.

Research on  $\text{UO}_2$  dissolution continued at Western University, with a focus on the development of an improved database for the model developed to describe the fuel behaviour inside a failed container. Results of this research are described in the following sections.

#### 5.1.2.1 Validation of Mechanistic Model of $\text{UO}_2$ Fuel Corrosion

Alpha-radiolysis of water is the dominant mechanism for used fuel dissolution inside a failed used fuel container, with the alpha-radiolysis product  $\text{H}_2\text{O}_2$  being the major fuel oxidant. For this reason, the influence of the alpha-dose rate on corrosion of  $\text{UO}_2$  materials has been extensively studied (Poinssot et al. 2005). Measurements have been made on a wide variety of specimens including U-233 doped  $\text{UO}_2$ , Pu-238 doped  $\text{UO}_2$ , Ac-225 doped  $\text{UO}_2$ ,  $\text{UO}_2$  fuel pellets, SIMFUEL and some spent fuel. Although there is wide variability in the measured corrosion/dissolution rates (see Figure 5-2), a clear trend of increasing corrosion rate with increasing alpha-dose rate is apparent.

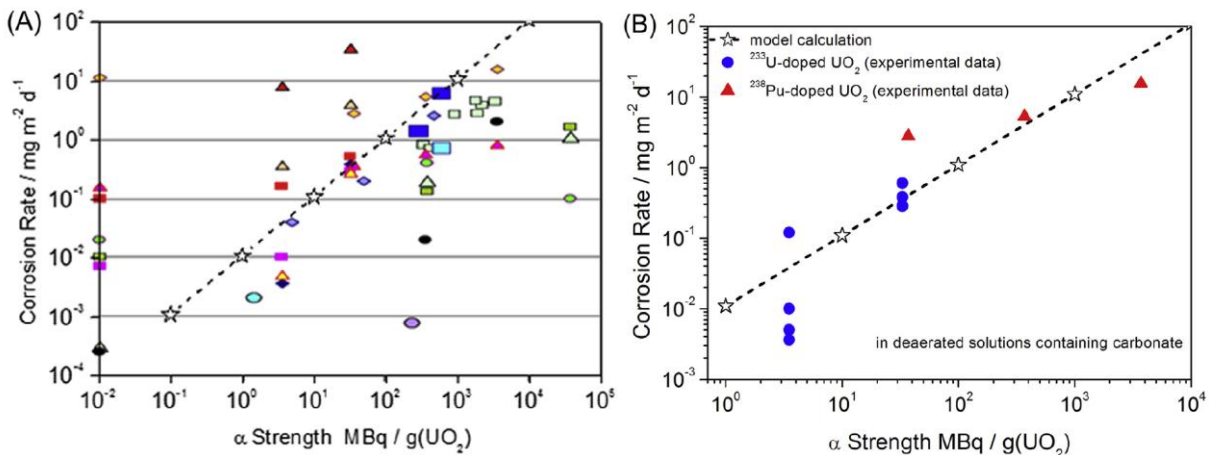


**Figure 5-2: Comparison of Experimental Corrosion Rates from Poinssot et al. (2005) with Simulation Results (Stars Connected by a Dashed Line): (A) Full Experimental Data Set; (B) Only Data Measured under Similar Experimental Conditions (i.e., for  $\alpha$ -doped  $\text{UO}_2$ , in Deaerated Solutions Containing Carbonate)**

A model was developed to predict the corrosion rate of used nuclear fuel ( $\text{UO}_2$ ) inside a failed waste container (Wu et al. 2014a,b; Liu et al. 2016a,b). It was shown that the model reproduced the internationally available data on fuel dissolution rates measured as a function of alpha radiation source strength (Figure 5-2).

Efforts to further validate the model were undertaken by adapting it to calculate the rates measured in various published studies (Liu et al. 2017a). These calculations demonstrated that the production of  $\text{O}_2$  by the decomposition of  $\text{H}_2\text{O}_2$  can influence the fuel dissolution rate if it is retained in the vicinity of the fuel and  $\text{H}_2$  is ineffective in controlling fuel oxidation rates. When the influence of  $\text{H}_2$ , acting as a reductant on noble metal particles, is included in the calculations no steady-state can be established due to the accumulation of radiolytic  $\text{H}_2$  with time. As a consequence the fuel corrosion rate decreases eventually to a negligible value.

It was shown that the alpha radiation dose rate, the extent of  $\text{H}_2\text{O}_2$  decomposition, and the availability of noble metal particles (which would be determined by the extent of in-reactor burnup) will all influence the time required for the corrosion rate to be suppressed to a negligible level but should not prevent suppression (Liu et al. 2017a). Extension of these sensitivity calculations is underway.

#### 5.1.2.2 Kinetics of Anodic and Cathodic Reactions

The reactivity of  $\text{UO}_2$  fuel and how it is modified by in-reactor irradiation is important in determining fuel corrosion rates under disposal conditions. The key changes likely to influence the reactivity of the fuel are fission-product doping (in particular the rare earth elements, for example,  $\text{Gd}^{\text{III}}$ ) of the  $\text{UO}_2$  matrix, the presence of noble metal particles, and the development of non-stoichiometry (Razdan and Shoesmith 2014a,b; He et al. 2012, 2009, 2007).

These influences have all been studied, but separately in specimens which are either  $\text{RE}^{\text{III}}$ -doped or non-stoichiometric, and either do or do not contain noble metal particles (Kim et al. 2017; Liu et al. 2017b,c; Lee et al. 2017). The question remains, however, on the relative importance of these effects on the anodic reactivity and the kinetics of cathodic reactions (in particular, the reduction of radiolytically-produced  $\text{H}_2\text{O}_2$ ) which can support fuel corrosion and, hence, radionuclide release. To clarify these issues, two studies have been undertaken: (1) a comparison of the anodic reactivity of close-to-stoichiometric  $\text{UO}_{2.002}$ , SIMFUEL ( $\text{RE}^{\text{III}}$ -doped with noble metal particles), and  $\text{Gd}^{\text{III}}$  and  $\text{Dy}^{\text{III}}$ -doped  $\text{UO}_2$  ( $\text{RE}^{\text{III}}$ -doped  $\text{UO}_2$  with no noble metal particles) (Liu et al. 2017b,c); and (2) a comparison of  $\text{Gd}$ -doped hyperstoichiometric  $\text{UO}_2$  ( $\text{U}_{1-y}\text{Gd}_y\text{O}_{2+x}$ ) and  $\text{Gd}$ -doped hypostoichiometric  $\text{UO}_2$  ( $\text{U}_{1-y}\text{Gd}_y\text{O}_{2-x}$ ) (Kim et al. 2017).

The first study demonstrated that anodic oxidation of the  $\text{UO}_2$  matrix and its dissolution were both suppressed by doping, with the anodic reactivity (i.e., susceptibility to corrosion) in the order  $\text{UO}_{2.002} > \text{SIMFUEL} > \text{Gd-UO}_2, \text{Dy-UO}_2$ . Dissolution of  $\text{UO}_{2.002}$  was facilitated by the slight degree of non-stoichiometry which was shown to be inhomogeneously distributed on the  $\text{UO}_{2+x}$  surface, while the  $\text{RE}^{\text{III}}$ -doping clearly suppressed both  $\text{UO}_2$  surface oxidation ( $\text{UO}_2 \rightarrow \text{UO}_{2+x}$ ) and dissolution ( $\text{UO}_{2+x} \rightarrow \text{UO}_{22+}$ ). There is no evidence that the presence of noble metal particles has any influence on the anodic reactivity, which is not unexpected. For the  $\text{RE}^{\text{III}}$ -doped specimens (which includes the SIMFUEL), the onset of dissolution was found to be initiated by tetragonal distortions of the cubic  $\text{UO}_2$  matrix and was accompanied by a deeper and more extensive oxidation of the  $\text{UO}_2$  matrix. This could be important since the balance between  $\text{H}_2\text{O}_2$  (which will be present inside a failed container due to the alpha radiolysis of  $\text{H}_2\text{O}$ ) decomposition and  $\text{UO}_2$  dissolution may depend on whether or not such distortions have

occurred.  $\text{H}_2\text{O}_2$  decomposition would be expected to be the preferred reaction if such distortions do not occur (Liu et al. 2017b, 2017c).

In the second study, electrochemical experiments showed that a variation in Gd content (extent of  $\text{RE}^{\text{III}}$  doping) had only a minor influence on the reactivity of stoichiometric  $\text{UO}_2$  ( $\text{U}_{1-y}\text{Gd}_y\text{O}_2$ ). By contrast the reactivity of hypostoichiometric  $\text{UO}_2$  ( $\text{U}_{1-y}\text{Gd}_y\text{O}_{2-x}$ ) increased and hyperstoichiometric  $\text{UO}_2$  ( $\text{U}_{1-y}\text{Gd}_y\text{O}_{2+x}$ ) decreased with Gd content. Since hyperstoichiometric  $\text{UO}_2$  is anticipated in spent nuclear fuel, this fuel under disposal conditions should not experience any increase in corrosion rate (Kim et al. 2017).

Two studies are presently underway. The first is a study of the decomposition kinetics of  $\text{H}_2\text{O}_2$ . Sensitivity calculations using the developed fuel dissolution model (Liu et al. 2016a, 2016b; Liu et al. 2017a) show  $\text{H}_2\text{O}_2$  decomposition to be a key reaction in causing fuel dissolution. Preliminary results on  $\text{H}_2\text{O}_2$  decomposition show this reaction tends to be dominant with  $\text{UO}_2$  corrosion being only a minor reaction. However, since  $\text{O}_2$  is the product of the decomposition reaction, this does not rule out the possibility of fuel corrosion since  $\text{O}_2$  is also expected to cause corrosion, albeit at a much reduced rate. X-ray photoelectron spectroscopic analyses of the  $\text{UO}_2$  surface after exposure to a solution containing  $\text{H}_2\text{O}_2$  show that  $\text{H}_2\text{O}_2$  first accelerates the decomposition reaction by creating a catalytic  $\text{U}^{\text{IV}}_{1-2x}\text{U}^{\text{V}}_{2x}\text{O}_{2+x}$  surface. The importance of the formation of this layer indicating the balance between  $\text{H}_2\text{O}_2$  decomposition and fuel dissolution is presently under study.

The second study is of the kinetics of  $\text{H}_2\text{O}_2$  reduction on a range of SIMFUELS,  $\text{RE}^{\text{III}}$ -doped  $\text{UO}_2$  and non-stoichiometric  $\text{UO}_{2+x}$ . This reaction can support either/or/both  $\text{UO}_2$  corrosion and  $\text{H}_2\text{O}_2$  oxidation (leading to  $\text{H}_2\text{O}_2$  decomposition) and could be the rate-determining step in the overall  $\text{UO}_2$  corrosion process. Preliminary results on the electrochemical reduction of  $\text{H}_2\text{O}_2$  suggest that the overall mechanism of the reaction may not change with the changes in composition of the  $\text{UO}_2$  (i.e., non-stoichiometry, SIMFUEL,  $\text{RE}^{\text{III}}$ -doped) but the kinetics of the reaction do.

The research work is currently focussed on the development of an improved database for the model developed to describe the fuel behaviour inside a failed container, including establishing the variability of  $\text{UO}_2$  reactivity for CANDU fuel pellets. This work continued in 2018.

### 5.1.3 Near-Field Modelling

The repository, or near-field, region includes the container, the surrounding buffer and backfill, other engineered barriers, and the adjacent host rock. Almost all radioactivity associated with the used fuel is expected to be isolated and contained within this area over the lifetime of the repository. On-going work with respect to repository safety in the near-field region is aimed at improving understanding of the transport-limiting processes around a failed container. Work on container corrosion models, carried out under the Repository Engineering program, is described in Section 3.2.

#### 5.1.3.1 Thermodynamic Database Review

NWMO continues to support the joint international Nuclear Energy Agency (NEA) effort on developing thermodynamic databases for elements of importance in safety assessment (Mompeán and Wanner 2003). Phase V of the Thermodynamic Database (TDB) Project, which started in 2014, has been extended for one more year (until March 2019). Phase VI of the project, expected to start in 2019, which will provide (1) an update of the chemical thermodynamics of complexes and compounds of U, Np, Pu, Am, Tc, Zr, Ni and Se with

selected organic ligands, (2) a review of the chemical thermodynamics of lanthanides or weak complexes, and (3) a state-of-the-art review on thermodynamics at high temperatures.

The reviews of the thermodynamic data for iron (Volume 2) and the second updates of the actinides and technetium thermodynamic data are expected for publication in 2019. The reviews of molybdenum thermodynamic data are expected for completion in 2020. The state-of-the-art reports on the thermodynamics of cement materials and high-ionic strength systems (Pitzer model) are expected in 2020. The implementation of the new interactive TDB electronic database was completed in 2018 and a PHREEQC format thermodynamic database was available.

The NEA TDB project provides high-quality datasets. This information is important, but is not sufficient on its own, as it does not address the full range of conditions of interest. For example, the NEA TDB project has focused on low-salinity systems in which activity corrections are described using Specific Ion Interaction Theory (SIT) parameters. Due to the high salinity of porewaters observed in some deep-seated sedimentary and crystalline rock formations in Canada, a thermodynamic database including Pitzer ion interaction parameters is needed for radionuclide solubility calculations.

The state-of-the-art report on high-ionic strength systems (Pitzer model) will be useful to identify the data gap for Pitzer ion interaction parameters. The THEREDA (THERmodynamic REference DAtabase) Pitzer thermodynamic database (Altmaier et al. 2011) is a relevant public database for high-salinity systems. It has been assessed by the NWMO and found to provide a good representation of experimental data for many subsystems.

The NWMO is also co-sponsoring the NSERC/UNENE Senior Industrial Research Chair in High Temperature Aqueous Chemistry at the University of Guelph, where there is capability to carry out various thermodynamic measurements at high temperatures and high salinities. This Chair program initiated in April 2016. New equipment needed to carry out experiments of interest to the NWMO has been purchased and progress has been made in several areas. Formation constants for uranyl sulfate complexes in saline solutions at 25-375 °C have been determined by Raman spectroscopy approach (Alcorn 2018). Thermodynamic properties of uranyl chloride, hydroxide and carbonate complexes as well as lanthanum chloride complexes are being studied at 25-300 °C by Raman spectroscopy, titration calorimetry and conductivity. Thermodynamic properties of ion pairing of lanthanum with hydroxide as well as thorium with chloride and hydroxide in saline solutions will also be studied by Raman spectroscopy, AC conductivity and titration calorimetry.

#### 5.1.3.2 Gas-Permeable Seal Test (GAST)

Potential high gas pressure within the emplacement room due primarily to corrosion of metals and microbial degradation of organic materials is a significant safety concern for long term repository performance. To address this potential problem, Nagra initiated the GAST project at Grimsel Test Site, Switzerland in late 2010. The main objective of GAST is to demonstrate the feasibility of the Engineered Gas Transport System which enables a preferable flow path for gas at over-pressures below 20 bars where the transport capacity for water remains very limited. NWMO has been part of the GAST project since its inception.

Presently the experimental facility is still in the saturation phase. The delay is due to a major leak event occurring in 2014 and due to the significantly underestimated speed of the saturation process in the sand bentonite mixture.

### 5.1.3.3 Shaft Seal Properties

The shaft seal for a deep geological repository will include various materials with different functions. The reference materials are 70/30 (wt%) bentonite/sand mixture, Low-Heat High-Performance Concrete (LHHPC), and asphalt.

In 2018, NWMO completed a series of basic physical and mechanical tests on 70/30 bentonite-sand shaft seal material and 100% MX-80 bentonite in order to establish the effect of groundwater salinity on their behaviour (Dixon et al., 2018). The pore fluids are defined in reference to total dissolved solids (TDS) concentrations: deionized water, approximately 11 g/L TDS, approximately 223 g/L TDS, and approximately 335 g/L TDS.

The tests evaluate the following:

1. Compaction/fabrication properties of the materials (to Modified Proctor density);
2. Consistency limits (Atterberg Limits) and free swell tests;
3. Density of as-fabricated material;
4. Moisture content of as-fabricated material;
5. Mineralogical/chemical composition, including three independent measurements of montmorillonite content using different laboratories;
6. Swelling pressure;
7. Saturated hydraulic conductivity;
8. Two-phase gas/water properties, specifically the capillary pressure function (or soil-water characteristic curve, SWCC) and relative permeability function, measured over a range of saturations that include the as-fabricated and fully-saturated condition;
9. Mineralogical/chemical composition of the materials exposed to brine for an extended period of time;
10. Thermal properties including thermal conductivity and specific heat capacity; and
11. Mechanical parameters including Shear Modulus (G), Bulk Modulus (K) and Young's Modulus (E).

The measurements are consistent with anticipated values, based on literature information available for similar materials (Priyanto et al. 2013; Barone et al. 2014).

In 2018, a scope of work was initiated to identify an optimized bentonite/seal mixture by evaluating the seal behavior of bentonite/sand mixtures having composition ratios other than 70:30. This work builds on ongoing shaft seal program by strengthening the database on seal properties, including providing information on batch-to-batch variability. In this study, the use of a crushed limestone based sand material will be studied in addition to granitic sand. Composition ratios of bentonite/sand mixture of 50:50, 60:40, 70:30, 80:20 and 90:10 (by weight) will be assessed.

#### 5.1.3.4 Thermal Response of a Conceptual DGR in Sedimentary Rock

The NWMO is designing and assessing the thermal-mechanical performance of a DGR in a sedimentary rock environment, in which used fuel containers are horizontally placed in buffer boxes perpendicular to the placement room axis. This study assesses the thermal performance of the conceptual DGR and its placement concept.

A series of conceptual design studies for a DGR has been carried out in the past (Acres et al. 1985, 1993; Mathers 1985; Tsui and Tsai 1985; Baumgartner et al. 1994; Park et al. 2000; Guo 2008; 2016; Hökmark et al. 2010). These include two- and three-dimensional thermal transient and thermo-mechanical analyses for the far-field and near-field regions. In the near-field models, an adiabatic thermal boundary condition is applied on the four vertical outside boundaries for a unit cell of the repository, and as such, this represents a repository with an infinite horizontal dimension.

The results from such models are accurate at early times, with the thermal response overestimated at longer times (Guo 2007). To correct for this, Guo (2007, 2017) proposed a method for modifying near-field thermal results. This approach was applied to estimate the thermal performance of a conceptual repository in sedimentary rock.

In this study, Near-Field and Far-Field Models are developed using the COMSOL code and used to perform thermal modelling. Near-field model results are then corrected to erase the influence of the adiabatic boundary condition using the method describing in Guo (2017). These corrected near-field results can be used as input to near-field coupled thermal-mechanical modelling simulations.

For this particular study (Guo 2018), the modelling results showed that the temperature of container surface at the centre of panels reaches its peak of 93°C after 43 years and then decreases to 81°C after 600 years. After 200,000 years, the container surface temperature approaches 18°C (the ambient temperature is 17°C). Example near-field results are shown in Figure 5-3.

The model also showed that presence of a ventilated access tunnel remaining open for 100 years has a small effect on repository temperatures at locations close to the tunnel (due to heat removal with the air), but there is no effect on the maximum temperatures quoted above.

The influence of the saturation of the buffer material on the container temperature (through the thermal conductivity change) was also studied. The bounding value of the container surface temperature is 97°C, considering the process of clay-based buffer saturation.

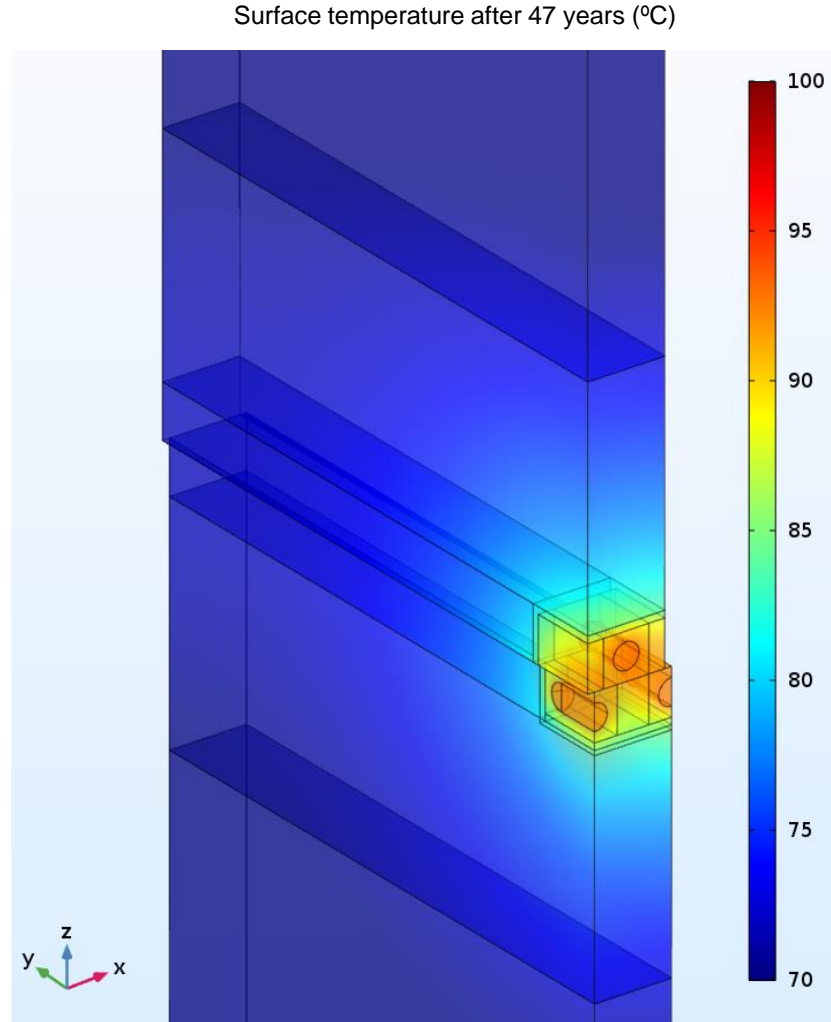


**Figure 5-3: Temperatures in the Rock along the Vertical Surfaces near the Tunnel at 47 Years after Placement**

#### 5.1.3.5 Reactive Transport Modelling of Concrete-Bentonite Interactions

The multi-component reactive transport code MIN3P-THCm (Mayer et al. 2002; Mayer and MacQuarrie 2010) has been developed at the University of British Columbia for simulation of geochemical processes. Prior reactive transport modelling work related to engineered barriers (e.g. bentonite) included the Äspö EBS TF-C benchmark work program (Xie et al. 2014), and the geochemical evolution at the interface between clay and concrete (Marty et al. 2015).

MIN3P-THCm has been used to investigate the long-term geochemical evolution and radionuclide (i.e. I-129) migration across interfaces of highly compacted bentonite (HCB), bentonite pellets as gap filling material (GFM), low-heat high-performance concrete (LHPC) and granite (for crystalline host rock) or limestone (for sedimentary host rock). Two types of reactive transport simulations have been performed to investigate the influence of porosity changes due to mineral dissolution/precipitation on reactive transport and radionuclide migration: (1) constant porosity (as well as tortuosity and diffusion coefficients), and (2) evolving porosity accounting for the mineral dissolution/precipitation. The simulation results indicate pore

clogging at the HCB/LHHPC and/or LHHPC/host rock interfaces due to mineral precipitation. Significant porosity reduction could result in notable delay of radionuclide migration, especially in cases where the release of radionuclides happens after pore clogging.

Reactive transport simulations with excavation damaged zones (EDZs) are also included to investigate the effect of EDZs on reactive transport and radionuclide migration. Simulation results will be compared for scenarios with and without including EDZs. Results for both scenarios show that the chemical interactions near the material interfaces and their effects on radionuclide migration are consistent. However, the time required to reach clogging is prolonged if EDZs are considered because the increased pore volume in the EDZs can accommodate more precipitated minerals. A technical report on this work is expected in 2019.

#### **5.1.4 Biosphere Modelling**

##### **5.1.4.1 Chemical Toxicity**

A number of postclosure safety assessments have been completed that examine the long-term safety implications of a hypothetical deep geological repository for used fuel. These safety assessments focused on radiological consequences. However, because a repository contains other materials, some of which are chemically toxic in large enough quantities, analyses of non-radiological consequences have also been included in these safety assessments.

A set of interim acceptance criteria are documented in a report issued in early 2015 (Medri 2015). Criteria are referred to as “interim” because they have not been formally approved for use in a used fuel repository licence application. The report presents the comprehensive set of interim acceptance criteria for all relevant elements in a used fuel repository. It also documents the basis for the interim acceptance criteria for five environmental media: groundwater, surface water, soil, sediment and air.

However, Medri (2015) does not contain information on all elements for all media. Consequently, work was initiated in 2016 to perform a literature review and to develop interim non-radiological acceptance criteria for the subset of potentially important elements that are missing from NWMO’s compilation. The results of the literature search revealed that data were lacking in all media (except air) for the platinum group elements. In the absence of data, conservatively low criteria could be adopted. Consequently, a set of laboratory toxicity tests were performed to obtain additional toxicity endpoints for Rhodium and Ruthenium, and to strengthen the data available for criteria derivation.

The report, which uses the results of the toxicity tests as well as the results of the literature search to derive supplementary criteria for the elements and media missing from Medri (2015), will be published in 2019.

##### **5.1.4.2 Participation in BIOPROTA**

BIOPROTA is an international collaborative program created to address key uncertainties in long-term assessments of contaminant releases into the environment arising from radioactive waste disposal. Participation is aimed at national authorities and agencies with responsibility for achieving safe radioactive waste management practices. Overall, the intention of BIOPROTA is to make available the best sources of information to justify modelling assumptions made within radiological assessments constructed to support radioactive waste management. In 2018, the NWMO co-sponsored the following projects.

### C-14 Project

Over the past decade, BIOPROTA has undertaken a number of projects relating to the behavior of C-14 in the biosphere. In 2014, refereed paper on this work was published in the Radiocarbon Journal (Limer et al. 2013). In 2016, another workshop was held to discuss model-data and model-model comparisons for three C-14 scenarios covering atmospheric deposition, release to sub-soil and modelling of contamination from an historical near-surface disposal. This led to a new project being initiated in 2017 to encompass model-data and model-model comparisons for two scenarios (one relating to C-14 from a historical near-surface disposal facility at Duke Swamp at the Chalk River Laboratory Site in Canada and the second to C-14 behaviour in a Finnish boreal forest).

The project also included a task to review the behaviour of carbon and C-14 in aquatic environments, with particular focus on where fish obtain their carbon from. Specifications for the data sets were circulated and modelling participation was invited. A fish review specification was also circulated. Reports on these studies were published in 2018 (Thorne et al. 2018). A workshop is planned for 2019 to share understanding, take stock of progress over recent years and to explore the potential for further collaborative research.

### BIOMASS 2020 Update

The International Atomic Energy Agency (IAEA) BIOMASS report on reference biospheres for solid radioactive waste disposal was published in 2003. BIOPROTA has undertaken to review and enhance the BIOMASS methodology. The work programme is being co-ordinated with IAEA MODARIA II working group 6 (WG6). To this end, BIOPROTA held two workshops in 2016, two workshops in 2017, and published workshop reports identifying key areas of review and update of the BIOMASS methodology (Smith 2016, 2017a, 2017b). In 2018, an interim report on the BIOPROTA / BIOMASS project was published, along with three workshop reports and a journal publication on climate change and landscape development with respect to the BIOMASS update (Lindborg et al. 2018). The update is planned to be completed by the end of 2019.

#### **5.1.5 System Modelling**

The postclosure safety assessment of a used fuel repository uses several complementary computer models, as identified in Table 5-2. These are either commercially maintained codes, or codes maintained by the NWMO software quality assurance program.

In late 2018, the NWMO initiated development of a new system modelling tool known as the Integrated System Model or ISM. The ISM tool will consist of a connected series of models developed in commercially available codes each representing a specific portion of the repository system. COMSOL has been selected for the ISM near field (fuel, container, engineered barrier system) model, HydroGeoSphere for the geosphere model and AMBER for the ISM biosphere model. All ISM submodels will be linked together using a linking and data pre-processing tool called LINKER. At this point, the ISM is in the preliminary stages of development and a proof-of-concept or beta version of the software is expected to be available in 2019.

**Table 5-2: Main Safety Assessment Codes**

<b>Software</b>	<b>Version</b>	<b>Description / Use</b>
SYVAC3-CC4	4.09.3	Reference system model
RSM	1.1	Radionuclide / chemical element screening code
FRAC3DVS-OPG	1.3	Reference 3D groundwater flow and transport code
HYDROGEOSPHERE	1540	3D groundwater / surface water flow and transport code
T2GGM	3.2.1	3D two-phase gas and water flow code
AMBER	6.3	Generic compartment modelling software
COMSOL	5.4	3D multi-physics finite element modelling software
PHREEQC	3.0.6	Geochemical calculations code
MICROSHIELD	9.07	Radioactive shielding and dose code
ORIGEN (SCALE)	4.2	Used fuel inventory calculations
MCNP	6.1	Criticality and shielding assessments

#### 5.1.5.1 Updates to T2GGM

T2GGM is a three-dimensional simulator that couples the Gas Generation Model (GGM) and TOUGH2. GGM models the detailed generation of gas within the repository due to corrosion and microbial degradation of the metals and organics present. TOUGH2 models the subsequent two-phase transport of the gas through the repository and geosphere. The coupling of GGM and TOUGH2 allows T2GGM to simulate the interactions between gas generation/pressure and water saturation in the repository.

A revised T2GGM, version 3.2.1, was released in 2018 to include three minor updates. Since the updates are minor, the user manual and verification report are not reissued.

## 5.2 SAFETY STUDIES

The objective of safety case studies is to provide illustrative examples of repository safety under various conditions and to test and/or demonstrate NWMO's safety assessment approach.

The focus of these studies is primarily on the postclosure period; however, some work activities on the preclosure period also are underway. The following sections describe work undertaken in both of these subject areas.

### 5.2.1 Preclosure Studies

#### 5.2.1.1 Preliminary Accident Dose Analysis

In 2017, preliminary radiological public dose calculations were carried out for accident scenarios identified in the preliminary hazard identification study (Reijonen et al. 2016). The presence or absence of ventilation system HEPA filters was also considered in combination with specific accident scenarios. A Gaussian dispersion model considering the most stable atmospheric condition (Pasquill stability category F) was used to estimate the exposure of a member of the public in the direct plume path at the location of maximum airborne radionuclide concentrations in a generic site. The public dose was calculated via the inhalation, air immersion and ground exposure pathways at various distances from the UFPP, ventilation shaft and main shaft.

The results of the preliminary radiological public dose calculations were presented at the WM2018 conference (Liberda and Leung 2018). For all accidents considered, the calculated public doses were below the 1 mSv criterion. The maximum calculated dose reached approximately 0.8 mSv, for the fall and breach of a UFTP, even at the minimum 100 m distance from the release location. Sensitivity cases were also carried out to determine the effect of stack release height, the effluent exit velocity, and the release orientation on the calculated public dose. As expected, lower stack release height, lower effluent exit velocities, and horizontal stack release all lead to lower atmospheric dispersion resulting in higher calculated public doses.

#### 5.2.1.2 Climate Change Impacts Study

A study was initiated in 2018 to review anticipated climate change impacts on climate conditions (e.g., temperature and precipitation) and develop a methodology to incorporate these climate changes into probable maximum precipitation (PMP) estimation appropriate for the five DGR candidate siting areas (Ignace, Hornepayne, Manitouwadge, South Bruce, and Huron-Kinloss) in Ontario. A report documenting this study is expected to be issued in early 2019.

The next phase of this study is to apply the preferred method to assess the PMP amounts for two or three study sites under changing climate conditions.

#### 5.2.1.3 Knowledge Management

The NEA Repository Metadata (RepMet) Management Project (NEA 2014) is aiming to create sets of metadata that can be used by national programmes to manage their repository data, information and records in a way that is harmonized internationally and suitable for long-term management. RepMet deals with the period before closure. In 2018, the NWMO continued to participate in this program.

The NEA initiative on the Preservation of Records, Knowledge and Memory across Generations (NEA 2015) was launched to minimise the risk of losing records, knowledge and memory, with a focus on the period of time after repository closure. In 2018, the NWMO continued to participate in this program.

### 5.2.2 Postclosure Studies

#### 5.2.2.1 Features, Events, and Processes

Features, Events and Processes (FEPs) refers to those factors that may need to be considered as part of a safety assessment. As part of each assessment, NWMO reviews each of these factors and provides a screening analysis indicating whether or not it should be included within the detailed safety assessment. This helps provide a completeness check on the assessment, i.e., that all relevant factors are being considered.

The FEPs assessment for the 6th Case Study has been completed (Garisto 2017). This assessment is, in many respects, similar to that for the 4th Case Study (Garisto 2012). Major differences arise due to adoption of the smaller copper coated used fuel container for the 6th Case Study and the repository design. The FEPs assessment for the 7th Case Study has been completed (Garisto 2018). This assessment in many respects is similar to that for the 5th Case Study (Garisto 2013). As with the 6th Case Study, major differences arise due to adoption of the smaller copper coated used fuel container for the 7th Case Study and the repository design.

### 5.2.2.2 Sedimentary Rock Case Study

In 2018, the NWMO completed an assessment of the postclosure performance of a conceptual repository design for sedimentary host rock. Results of this study are documented in a technical report (NWMO 2018, Gobien et al 2018). The main differences relative to the Fifth Case Study (NWMO 2013) are the Mark II engineered barrier system and the adaptive underground layout. This study describes the reference design for a deep geological repository in sedimentary rock and provides an illustrative postclosure safety assessment approach which is structured, systematic and consistent with CNSC REGDOC-2.11.1, Volume III (CNSC 2018). The illustrative assessment includes a description of the repository system, systematically identifies scenarios, models and methods for evaluating safety, uses different assessment strategies, addresses uncertainty, and compares the results of the assessment with interim acceptance criteria.

This postclosure safety assessment shows, for the Normal Evolution Scenario and associated sensitivity cases, that all radiological and non-radiological interim acceptance criteria are met with substantial margins during the postclosure period. This result is consistent with previous assessments of a deep geological repository in Canada, as well as with safety assessment studies by other national radioactive waste management organizations.

## 6. SITE ASSESSMENT

As of 2018, potential repository siting areas were being considered within three regions in Ontario (Figure 6-2): the Ignace Wabigoon area, North of Superior, and Southern Ontario. The status of the geological and environmental studies underway in these regions is described below.

### 6.1 IGNACE WABIGOON

#### 6.1.1 Geological Investigation

In January 2018 the Geoscience Site Assessment team and their contractors completed the drilling of a 1001 m deep vertical borehole in crystalline rock in the Revell Batholith west of Ignace, Ontario, that was started in late fall of 2017. The drilling, coring, logging, core sampling and opportunistic groundwater sampling took 44 days to complete. Each 3 m core run retrieved underwent a standard work flow that included core photography, core sampling, as well as geological and geotechnical logging of lithology, alterations and structures into an acQuire GIM Suite borehole data management system.

The borehole drilling plan included taking water samples opportunistically from any locations where flowing groundwater was intersected. One groundwater sample was successfully collected in the upper 50 m of the borehole. Water inflow was low enough in the remainder of the borehole that no additional groundwater samples were able to be collected below 50 m.



Figure 6-1: 1001 Metres of Core from Borehole IG\_BH01

Down-hole geophysical logging of the borehole (i.e. measurements taken within the borehole) was completed in January 2018. Sixteen geophysical logs were collected, including Optical & Acoustic Televiwer, Flowing Fluid Electrical Conductivity (FFEC), Natural Gamma, Gamma-Gamma Density, and Neutron and Borehole Deviation. Geophysical logging, specifically the optical and acoustic televiwer logs, were used to orient structures logged in the unoriented core. Natural Gamma, Neutron, and Density logs provided additional information to refine the distribution and characterization of lithological units and alteration. Other down-hole geophysical logs (e.g., FFEC) provided key inputs into the planning of subsequent borehole tests including hydraulic testing and the installation of a long-term WestBay monitoring system.

Hydraulic testing of the borehole was carried out using a double inflatable packer tool with a 20 m interval. Testing was carried out along the length of the borehole, but focussed on the 400 to 600 m interval of the borehole. A total of 10 hydraulic tests were completed. Tests were designed to test the intact rock and areas where structures and potential water flow were indicated by core and geophysical logs.

Following the hydraulic testing, a Westbay MP38 Multi-Level system was installed. The Westbay system comprised 20 packered intervals where pressure and temperature can be measured. This system will allow for the monitoring of the evolution of formation pressures, for potential to sample groundwater, and will provide information on vertical gradients at the site.

Approximately 200 rock core samples were sent to offsite laboratories for various analyses including Geomechanics (strength), Petrophysics (density, porosity, permeability and effective diffusion), Geochemistry (porewater composition, sorption) and Microbiology. In addition, a suite of general archive samples was collected and preserved, to be available for future testing.

Planning and consultation are underway for the next boreholes. Permission from Ontario Ministry of Natural Resources and Forestry for boreholes 2 and 3 in the area was received in November 2018, and construction of the temporary access routes for these boreholes began in December.

### **6.1.2 Environmental Assessment**

In 2018, the NWMO and its contractor (Tulloch Engineering Inc.) undertook its third year of field studies to collect abiotic and biotic data in the Ignace Wabigoon siting area. The 2018 study area included a collection of points (i.e. borehole site) and linear (i.e. road) features (Figure 6-2). Three confirmed Borehole sites (Borehole 1, 2, and 3) and access road servicing those three borehole have been investigated in the past years and their inclusion represents a continuation of previous work. Three additional confirmed borehole sites (Borehole 4, 5, and 6) and two Area of Interests (AOI 1 and 2) and associated access routes were newly identified for 2018. Collectively, these areas are referred to herein as the 2018 Study Area and were designed to include a 120 m buffer around the above-described locations (Figure 6-2).

During this stage, studies included the continuation of water and soil quality monitoring as well as Natural Heritage investigations at newly identified locations. Ecological Land Classification surveys, bird surveys for various guilds, bat potential maternity roosting habitat surveys, rare plants survey and wildlife visual encounter surveys were completed to characterize the terrestrial environment. Aquatic habitat surveys were conducted to confirm surface water quality during multiple seasonal sampling events, presence of fish (incidental observations and non-lethal targeted sampling), general fish habitat classification, as well as stream sediment quality

and benthic macroinvertebrate community sampling at locations where aquatic habitat was identified in study area.

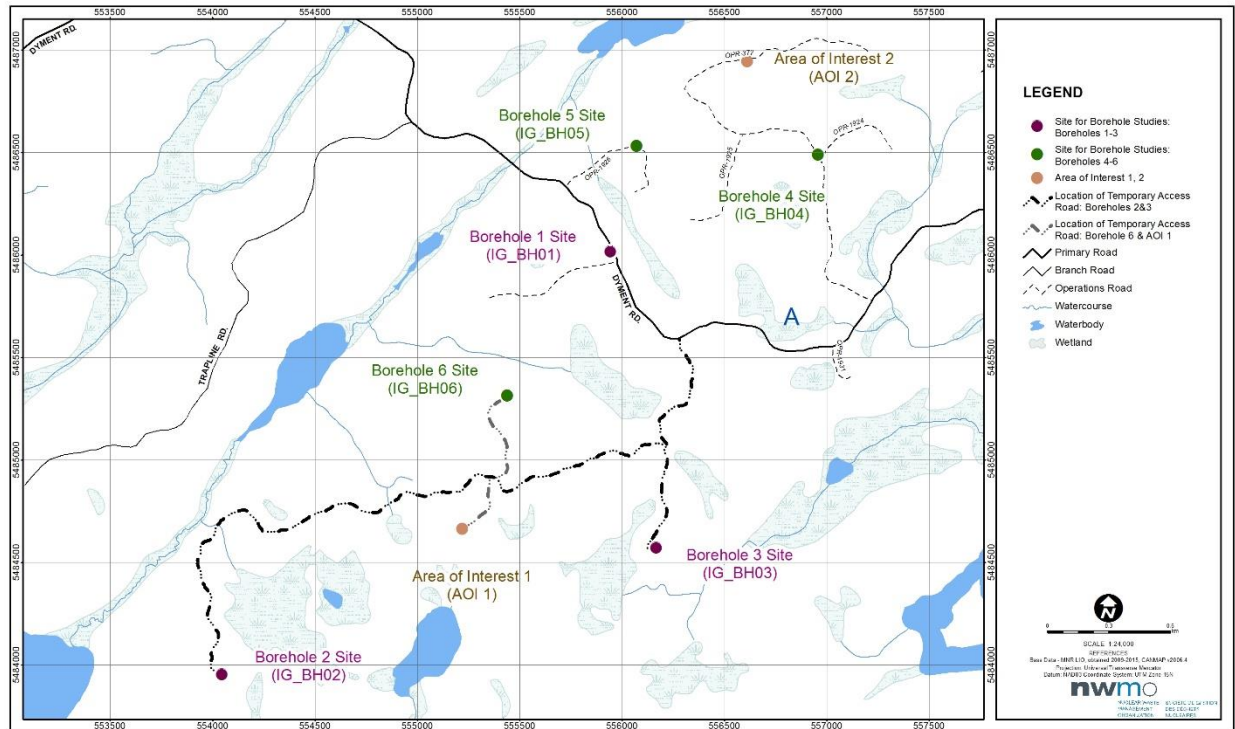


**Figure 6-2: Ignace Wabigoon - Location of Borehole Sites 1 to 6 and Area of Interest 1 and 2**

All surface water sampling sites from 2017 were re-visited in 2018, as well as an additional two new sites. These new sampling sites were established to act as additional up-stream reference sites and to provide greater resolution regarding water quality and chemistry from minor tributaries feeding into the larger Mennin Lake system. In-situ water measurements and surface water sample collection occurred in June, August and October 2018. Sediment sampling occurred at all surface water sites in October 2018. Sediment composition at every site was a combination of either sand, clay, organic material and/or mud. Soil samples were collected at Boreholes 1, 2 and 3 in August 2018. Sampling followed a 3 x 3 grid pattern with approximately 10 m spacing between sites. The soils at Borehole 1 consisted of outsourced gravel and sand used to establish the laydown area. Borehole 2 soils had a high volume of organics mixed throughout them dominated by fine sand. Borehole 3 soils were primarily sand and loamy sand atop of unconsolidated bedrock.

Access roads servicing Boreholes 2 and 3 were delineated in-field during summer 2018. No large stick nests indicative of raptor nesting were observed along the finalized right-of-way. No evidence of nesting by migratory bird species was observed within the right-of-way. No high quality habitat for colonial bat roosting was observed within the road right-of-way. Access road for Borehole 4, 5 and Area of Interest 2 are either overgrown or partly overgrown with Speckled Alder. The route was assessed in the field for potential water crossings; all potential water crossings assessed were classified as indirect and/or not fish habitat, apart from one, which was identified as direct fish habitat. A self assessment of this habitat was submitted to the Department of Fisheries and Oceans, and was approved to carry-on as described in the

submission. Access roads to Borehole 6 and AOI 1 are not established, and field verification was deferred to a future date once preliminary routing has been established.

The findings from the 2018 field surveys demonstrated that the confirmed drilling area IG-BH04 is centered on a cleared forest access road intersection and dominated mostly by tall shrubs of Speckled Alder. The area within 120 m of IG\_BH04 is dominated by a low regenerating canopy of planted Jack pine on moderately deep soils that vary from fresh to moist. IG\_BH04 supports suitable nesting habitat for two Species at Risk (SAR) but the Nightjar Acoustic surveys confirmed the absence of both within the study area. The site supports suitable nesting habitat for many migratory bird species. One SAR was recorded outside the study area, but somewhere within a 1000 m radius. Songmeters and incidental observations documented 14 species of migratory bird on location in 2018 and indicated that two species breed in the vicinity.

IG\_BH05 is centered on a former forestry staging area on access road. IG\_BH05 and the area within 120 m are dominated by low regenerating canopy of planted Jack Pine on fresh, moderately deep soil. IG\_BH05 supports suitable nesting habitat for two SAR, but the species-specific surveys confirmed the absence of both within the study area. The site supports suitable nesting habitat for migratory bird species. Songmeters and incidental observations documented 15 species of migratory bird on location in 2018. One special concern species was recorded from 100 north of the location center. Retention of this wooded habitat is advised in order to preserve its ecological function. No suitable amphibian breeding habitat was found on location, but songmeters recorded three species may breed in the vicinity.

IG\_BH06 is located in an undeveloped and mature conifer stand. IG\_BH06 and the area within 120 m are dominated by Black spruce and Jack Pine on moderately deep fresh soils. The location does not support suitable nesting habitat for SAR. The site supports suitable nesting habitat for migratory bird species. Songmeters and incidental observations documented 14 species of migratory bird on location. No suitable amphibian breeding habitat were found on location, but songmeters observed three species may breed in the vicinity.

Area of Interest 1 is located in an undeveloped and mature conifer stand. The majority of the site is Black Spruce and Jack Pine on moderately deep fresh soils. The site supports suitable nesting habitat for migratory bird species. Songmeters and incidental observations documented 13 species of migratory bird on location in 2018.

Area of Interest 2 is centered on a clear staging area of forest access road. The location is dominated to the north by a mix of young Trembling Aspen and Jack Pine and to the south by a near pure plantation of young Jack Pine. The site supports suitable nesting habitat for two SAR. Species specific surveys confirmed the absence of one SAR. One of the species was observed (an individual) foraging over the site. The location supports suitable nesting habitat for many migratory bird species. Songmeters and incidental observations recorded 16 species of migratory birds at this location.

It is the opinion of the NWMO and its contractor that the proposed drilling activities would not negatively impact the natural features identified in any of the six confirmed drilling area, with the implementation of appropriate mitigation methods and monitoring. Additional information is required to confirm there are no negative impacts to migratory birds and endangered bat species if work is conducted during sensitive timeframes. Disruptive work to date has avoided these sensitive time frames. Water crossing design plans will be required to confirm no impact on Fisheries resources, and to identify if additional regulator review is required through the Department of Fisheries and Oceans self-assessment process. With appropriate mitigation

measures, including avoiding sensitive areas, there is no indication that the sitting work would result in measureable risk to the environment.

## **6.2 NORTH OF SUPERIOR**

### **6.2.1 Geological Investigation**

In 2018, the Geoscience Site Assessment team continued planning activities for fieldwork in the Hornepayne and Manitouwadge areas located to the north of Lake Superior. An RFP for borehole drilling and testing was issued and awarded. In addition, in 2018, plans for acquiring LiDAR data were finalized, although data acquisition was delayed to 2019 due to environmental conditions (smoke from forest fires in the region). Ongoing work includes planning for drilling of initial boreholes in the area (Figure 6-3 and Figure 6-4).

### **6.2.2 Environmental Assessment**

In 2018, the NWMO and its contractor (Wood) undertook field studies to collect abiotic and biotic data related to the potential borehole drilling areas (Figure 6-3 and Figure 6-4). Each potential drilling area consists of a 78.5 hectare (ha) circle (500 m radius) within which the specific borehole locations would be placed. The preliminary monitoring program surveys completed in 2018 specifically targeted areas within each potential drilling area, and were designed to cover an additional 200 m beyond the boundaries of the potential drilling areas as a precautionary approach to survey potential zones of influence that may extend outside of the 75.8 ha in the event that the borehole is located at the edge of the potential drilling area.

During this stage, Ecological Land Classification surveys, bird surveys for various guilds, aerial surveys for stick nests and larger mammals, bat acoustic and potential maternity roosting habitat surveys, and wildlife visual encounter surveys were completed to characterize the terrestrial environment. Aquatic habitat surveys were conducted to confirm surface water quality during multiple seasonal sampling events, presence of fish (incidental observations and non-lethal targeted sampling), general fish habitat classification, as well as stream sediment quality and benthic macroinvertebrate community sampling at locations where aquatic habitat was identified near the identified potential drilling areas.

#### **6.2.2.1 Hornepayne**

The findings from the 2018 field surveys demonstrated that the potential drilling area labelled as HP-BH01 was composed of 71% upland habitat. Three species at risk (SAR) were confirmed using or passing through the potential drill area and there was potential for five types of significant wildlife habitat (SWH) in the study area, although none were confirmed.

Approximately 10% of potential drilling area HP-BH01 was considered suitable for supporting SAR bat maternity roosts. The study area associated with potential drilling area HP-BH02 was composed of 51% upland habitat, with two SAR confirmed using or passing through the potential drilling area. Four types of SWH had potential to occur within the potential drilling area, although none were confirmed. Approximately 6% of the total area within potential drilling area HP-BH02 had potential to support SAR bat maternity roosts. Within the potential drilling area HP-BH03, 68% of the area was composed of upland habitat. Three SAR were confirmed either using or passing through the potential drilling area, and one SAR was recorded using habitat adjacent to the potential drilling area. Six types of SWH had potential to occur, although none were confirmed within the HP-BH03 study area. Approximately 74% of the available habitat within potential drilling area HP-BH03 has potential to support SAR bat maternity roosts.

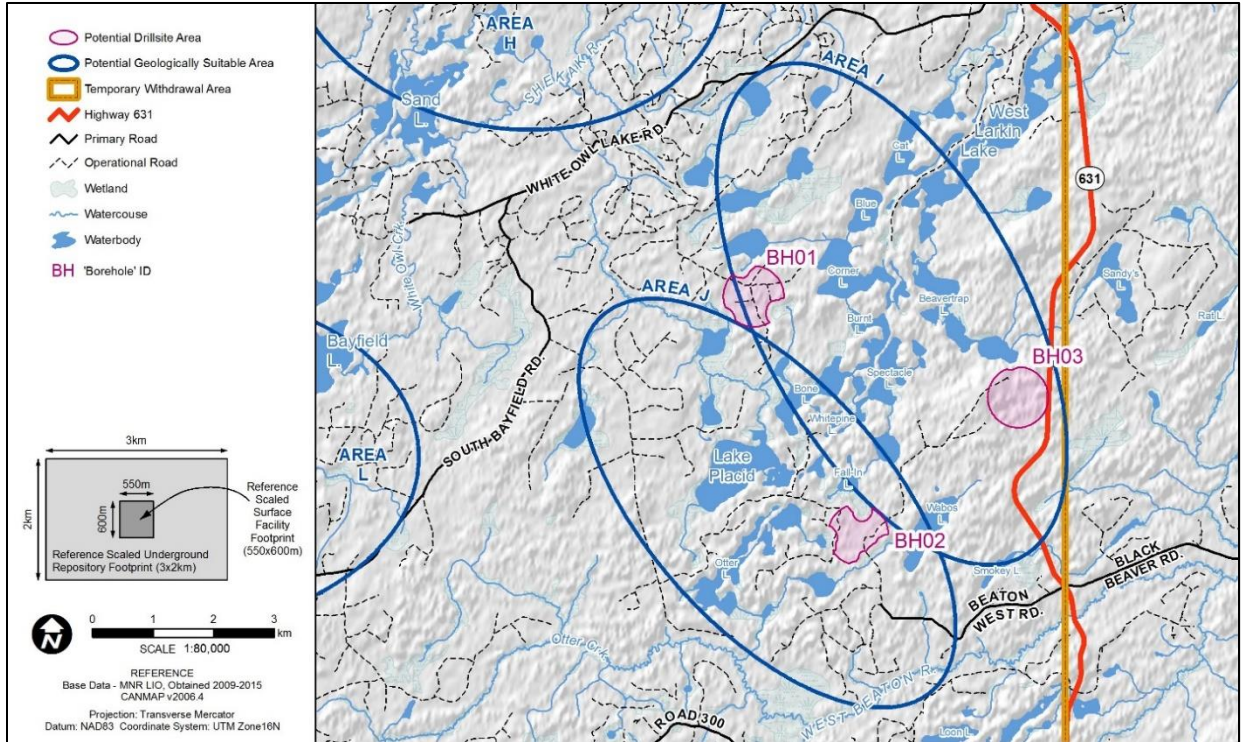


**Figure 6-3: Hornepayne - Location of Borehole 1, 2, and 3 – For Discussion with People in the Area**

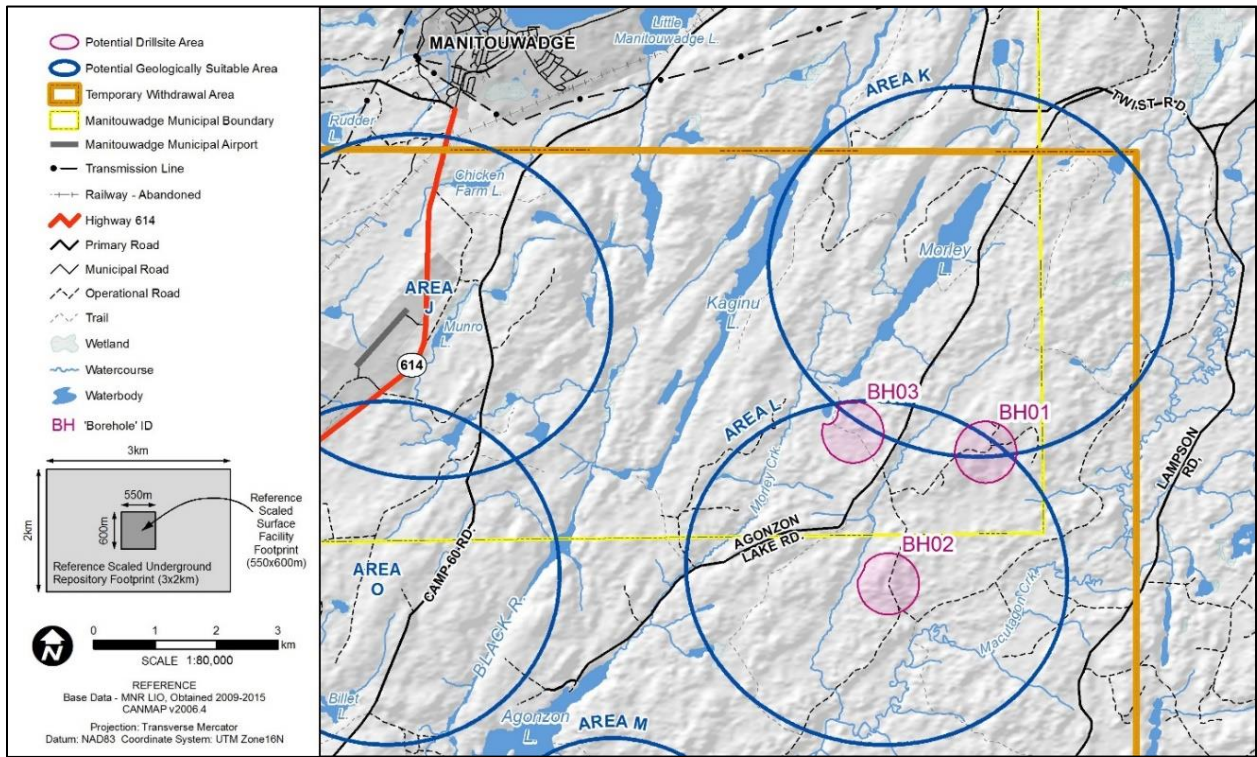


**Figure 6-4: Manitowadge - Location of Borehole 1, 2, and 3 – For Discussion with People in the Area**

The 2018 field surveys related to aquatic studies also suggest that the three potential borehole locations are suitable for borehole drilling, with limited presence of open water habitat within the areas of investigation. It is noted that access to HP-BH02 may require the reinstatement of an access road crossing at the Wabos Lake outlet stream; however, environmental management of potential risks to aquatic habitat related to the water crossings are well understood and best management practices are available to control potential effects of these activities.

#### 6.2.2.2 Manitouwadge

The findings from the 2018 field surveys demonstrated that the potential drilling area labelled as MN-BH01 was composed of 82% upland habitat. Two species at risk (SAR) were confirmed using or passing through the potential drilling area and there was potential for five types of significant wildlife habitat (SWH) in the study area, although none were confirmed. Approximately 8% of potential drilling area MN-BH01 was considered suitable for supporting at-risk bat maternity roosts. The study area associated with potential drilling area MN-BH02 was composed of 59% upland habitat, with two SAR confirmed using or passing through the potential drilling area. Five types of SWH had potential to occur within the potential drilling area, and 0.18 ha of Open Rock Barren was confirmed present. Approximately 51% of the total area within potential drilling area MN-BH02 had potential to support SAR bat maternity roosts. Within the potential drilling area MN-BH03, 43% of the area was composed of upland habitat. No SAR were confirmed using or passing through the study area. Five types of SWH had potential to occur, although none were confirmed within the MN-BH03 study area. None of the available habitat within potential drilling area MN-BH03 has potential to support SAR bat maternity roosts.

The 2018 aquatic field survey findings suggest that MN-BH01 has no open water habitat present, and therefore, limited pathways of potential effects to surrounding watercourse or waterbodies are available. The MN-BH02 aquatic habitat are limited to an unnamed watercourse near the eastern edge of the area, consequently, a borehole could be positioned away from the watercourse with limited potential aquatic habitat interaction. MN-BH03 is mostly a low-lying area that may provide subsurface water flow connectivity to adjacent waterbodies (e.g., Morley Lake) under high flow conditions or periods of prolonged precipitation or melting (spring freshet). However, best management practices and site-specific erosion and sediment control measures are available to mitigate potential pathways of effects from borehole drilling activities.

### 6.3 SOUTHERN ONTARIO

The candidate siting areas are the Huron-Kinloss and South Bruce areas of Southern Ontario. As of 2018, specific siting areas were in the process of being identified. Site assessment activities in Southern Ontario mainly related to planning for drilling of initial boreholes in the area.

Regionally, information on the geology is available from the deep boreholes and detailed studies undertaken at the Bruce nuclear site in the adjacent Municipality of Kincardine. Ongoing studies of the southern Ontario geology have been noted in the previous Section 5.



## REFERENCES

- Achtziger-Zupancic, P., S. Loew and G. Mariethoz. 2017. A new global database to improve predictions of permeability distribution in crystalline rocks at site scale. *Journal of Geophysical Research: Solid Earth*, 122:3513-3539. doi:10.1002/2017JB014106.
- Acres Consulting Services Limited in conjunction with RE/SPEC Ltd. 1985. A feasibility study of the multilevel vault concept. Atomic Energy of Canada Limited Report, AECL TR 297. Pinawa, Canada.
- Acres Consulting Services Ltd. 1993. A preliminary study of long-hole emplacement alternatives. Atomic Energy of Canada Limited Report, AECL TR-346. Pinawa, Canada
- AECL. 2011. Summary of thermal properties tests on DGR4 rock samples. Whiteshell Laboratories. Atomic Energy of Canada Limited Report. Pinawa, Canada.
- Al, T., I. Clark, L. Kennell, M. Jensen and K. Raven. 2015. Geochemical evolution and residence time of porewater in low-permeability rock of the Michigan Basin, Southwest Ontario. *Chemical Geology*, 404: 1-17.
- Al-Aasm, I.A. and R. Crowe. 2018. Fluid compartmentalisation and dolomitization in the Cambrian and Ordovician Successions of the Huron Domain, Michigan Basin. *Marine and Petroleum Geology*. 92: 160-178.
- Alcorn, C.D. 2018. A quantitative Raman and density functional theory investigation of uranyl sulfate complexation and liquid-liquid phase separation under hydrothermal conditions. Ph.D. Thesis, University of Guelph, Ontario, Canada.
- Altmaier, M., V. Brendler, C. Bube, V. Neck, C. Marquardt, H.C. Moog, A. Richter, T. Scharge, W. Voigt, S. Wilhelm, T. Willms and G. Wollmann. 2011. THEREDA Thermodynamische Referenz-Datenbasis. Abschlussbericht (dt. Vollversion). Gesellschaft für Anlagen und Reaktorsicherheit, GRS-265. Germany.
- Antevs, E. 1925. Retreat of the last ice-sheet in eastern Canada. Geological Survey of Canada, Memoir 146. Ottawa, Canada.
- Antevs, E. 1928. The last glaciation with reference to the retreat in northeastern North America. American Geographical Society Research Series, No. 17, New York, United States.
- Barone, F., J. Stone and A. Man. 2014. Geotechnical properties of candidate shaft backfill. Nuclear Waste Management Organization Report NWMO TR-2014-12. Toronto, Canada.
- Baumgartner, P., T.V. Tran and R. Burgher. 1994. Sensitivity analyses for the thermal response of a nuclear fuel waste disposal vault. Atomic Energy of Canada Limited Technical Report, TR-621, COG-94-258. Pinawa, Canada.

- Bea Jofre, S.A., K.U. Mayer and K.T.B. MacQuarrie. 2011a. Modelling reactive transport in sedimentary rock environments – Phase II, MIN3P code enhancements and illustrative simulations for a glaciation scenario. Nuclear Waste Management Organization Report NWMO TR-2011-13. Toronto, Canada.
- Bea Jofre, S.A., K.U. Mayer and K.T.B. MacQuarrie. 2011b. Modelling of reactive transport in a sedimentary basin affected by a glaciation/deglaciation event. Proceedings of Waste Management, Decommissioning and Environmental Restoration for Canada's Nuclear Activities, Canadian Nuclear Society, Toronto, Canada.
- Bea, S.A., K.U. Mayer and K.T.B. MacQuarrie. 2015. Reactive transport and thermo-hydro-mechanical coupling in deep sedimentary basins affected by glaciation cycles: model development, verification, and illustrative example. *Geofluids*. doi:10.1111/gfl.12148.
- Bea, S.A., D. Su, K.U. Mayer and K.T.B. MacQuarrie. 2018. Evaluation of the potential for dissolved oxygen ingress into deep sedimentary basins during a glaciation event. *Geofluids*, Article ID 9475741. doi: 10.1155/2018/9475741.
- Bertetti, F.P. 2016. Determination of sorption properties for sedimentary rocks under saline, reducing conditions – key radionuclides. Nuclear Waste Management Organization Technical Report NWMO-TR-2016-08. Toronto, Canada.
- Blacklock, N. and M. Diederichs. 2017. Applications of scout hole programs in tunnelling operations under high stress. Proceedings World Tunnelling Conference, Bergen, Norway.
- Bouchard, L., J. Veizer, L. Kennell-Morrison, M. Jensen, K.G. Raven and I.D. Clark. 2018. Origin and  $^{87}\text{Rb}/^{87}\text{Sr}$  age of porewaters in low permeability Ordovician sediments on the eastern flank of the Michigan basin, Tiverton, Ontario, Canada. *Canadian Journal of Earth Sciences*, Special Issue in honour of Ján Veizer. dx.doi.org/10.1139/cjes-2018-0061.
- Bradbury, M.H. and B. Baeyens. 2005. Modelling the sorption of Mn(II), Co(II), Ni(II), Zn(II), Cd(II), Eu(III), Am(III), Sn(IV), Th(IV), Np(V) and U(VI) on montmorillonite: Linear free energy relationships and estimates of surface binding constants for some selected heavy metals and actinides. *Geochimica et Cosmochimica Acta* 69: 875-892.
- Brooks, G.R. 2016. Evidence of late glacial paleoseismicity from mass transport deposits within Lac Dasserat, northwestern Quebec, Canada. *Quaternary Research*, 86: 184-199. doi.org/10.1016/j.yqres.2016.06.005.
- Brooks, G.R. 2018. Deglacial record of paleoearthquakes interpreted from mass transport deposits at three lakes near Rouyn-Noranda, northwestern Quebec, Canada. *Sedimentology*, 65(7). doi.org/10.1111/sed.12473.
- Carter, T.R. 2012. Regional groundwater systems in southern Ontario. *Ontario Oil & Gas*, 44-48.

- Celejewski, M., L. Scott and T. Al. 2014. An absorption method for extraction and characterization of porewater from low-permeability rocks using cellulosic sheets. *Applied Geochemistry* 49: 22-30.
- Celejewski, M., D. Barton and T. Al. 2018. Measurement of Cl:Br Ratios in the Porewater of Clay-Rich Rocks – A Comparison of the Crush-and-Leach and the Paper-Absorption Methods. *Geofluids*, Article ID 9682042. doi:10.1155/2018/9682042.2018.
- Clark, I. D., T. Al, M. Jensen, L. Kennell, M. Mazurek, R. Mohapatra and K.G. Raven. 2013. Paleozoic-aged brine and authigenic helium preserved in an Ordovician shale aquiclude. *Geology*, 41(9): 951-954.
- Clark, I., D. Ilin, R. Jackson, M. Jensen, L. Kennell, H. Mohammadzadeh, A. Poulain, Y. Xing and K. Raven. 2015. Paleozoic-aged Microbial Methane in an Ordovician Shale and Carbonate Aquiclude of the Michigan Basin, Southwestern Ontario. *Organic Geochemistry*, 83-84: 118-126.
- CNSC. 2018. Assessing the Long-Term Safety of Radioactive Waste Management. Canadian Nuclear Safety Commission Regulatory Document CNSC REGDOC-2.11.1 Volume III. Ottawa, Canada.
- Dadashzadeh, N. and MS. Diederichs. 2018a. Effect of Rock Strength Components' Evolution Rate on the Mechanism of Failure in Brittle Rocks. *Proceedings Tunneling and Trenchless Conference (TT2018 – TAC/NASTT-NW)*, Edmonton, Canada.
- Dadashzadeh, N, and M. Diederichs. 2018b. Reliability of Prediction for Tunnel Excavation Damage Zone Depth in Brittle Rocks. *Proceedings 10th Asian Rock Mechanics Symposium*, Singapore.
- Dadashzadeh, N and M. Diederichs. 2018c. Prediction of Excavation Damage Zone Depth Variability in Brittle Rocks. *Proceedings of Geomechanics and geodynamics of rock masses, ISRM-EUROCK 2018*, Saint-Petersburg, Russia.
- Darcel, C., P. Davy, R. Le Goc and D. Mas Ivars, 2018. Rock mass effective properties from a DFN approach. *Second International Discrete Fracture Network Engineering Conference*, Seattle, USA.
- Darcel, C., P. Davy, and R. Le Goc. 2015. Onkalo POSE experiment - Effective elastic properties of fractured rocks. *Posiva Report 2015-17*. Eurajoki, Finland.
- Davy, P., C. Darcel, R. Le Goc and D. Mas Ivars. 2018. Elastic properties of fractured rock masses with frictional properties and power-law fracture size distributions. *J Geophysical Research: Solid Earth*, 123(8).
- Diamond, L.W., L. Aschwanden and R. Caldas. 2016. Fluid Inclusion Study of Drill Core and Outcrop Samples from the Bruce Nuclear Site, Southern Ontario. *Nuclear Waste Management Organization Technical Report NWMO-TR-2015-24*. Toronto, Canada.

- Dixon, D., A. Man, S. Rimal, J. Stone, and G. Siemens. 2018. Bentonite seal properties in saline water. Nuclear Waste Management Organization Report NWMO-TR-2018-20. Toronto, Canada.
- Farahmand, K., I. Vazaios, MS. Diederichs and N. Vlachopoulos. 2018. Investigating the scale-dependency of the geometrical and mechanical properties of a moderately jointed rock using a synthetic rock mass (SRM) approach. *Computers and Geotechnics*. 95: 162-179.
- Garisto, F. 2018. Seventh Case Study: Features, Events and Processes. Nuclear Waste Management Organization Technical Report NWMO-TR-2018-15. Toronto, Canada.
- Garisto, F. 2017. Sixth Case Study: Features, Events and Processes. Nuclear Waste Management Organization Technical Report NWMO-TR-2017-08. Toronto, Canada.
- Garisto, F. 2013. Fifth Case Study: Features, Events and Processes. Nuclear Waste Management Organization Technical Report NWMO-TR-2013-06. Toronto, Canada.
- Garisto, F. 2012. Fourth Case Study: Features, Events and Processes. Nuclear Waste Management Organization Technical Report NWMO-TR-2012-14. Toronto, Canada.
- Ghazvinian, E. and M. Diederichs. 2018. Progress of brittle microfracturing in crystalline rocks under cyclic loading conditions. *Journal of the South African Institute of Mining and Metallurgy*, 118(3): 217-226.
- Giroud, N., Y. Tomonaga, P. Wersin, S. Briggs, F. King, T. Vogt and N. Diomidis. 2018. On the fate of oxygen in a spent fuel emplacement drift in Opalinus Clay. *Applied geochemistry*, 97: 270-278.
- Głowacki, A. 2017. Stress-induced permeability evolution in limestone rocks, PhD Thesis, McGill University, Quebec, Canada.
- Głowacki, A. and A.P.S. Selvadurai. 2016. Stress-induced permeability changes in Indiana Limestone. *Engineering Geology*, 25: 122-130.
- Grigoryan, A.A., D.R. Jalique, P. Medihala, S. Stroes-Gascoyne, G.M. Wolfaardt, J. McKelvie and D.R. Korber. 2018. Bacterial diversity and production of sulfide in microcosms containing uncompacted bentonites. *Heliyon* 4(8).
- Guo, R. 2007. Numerical modelling of a deep geological repository using the in-floor borehole placement method. Nuclear Waste Management Organization Report NWMO-TR-2007-14. Toronto, Canada.
- Guo, R. 2008. Sensitivity analyses to investigate the influence of the container spacing and tunnel spacing on the thermal response in a deep geological repository. Nuclear Waste Management Organization NWMO-TR-2008-24. Toronto, Canada.

- Guo, R. 2016. Thermal response of the Mark II conceptual deep geological repository in crystalline rock. Nuclear Waste Management Organization Report NWMO-TR-2016-03. Toronto, Canada.
- Guo, R. 2017. Thermal response of a Canadian conceptual deep geological repository in crystalline rock and a method to correct the influence of the near-field adiabatic boundary condition. *Engineering Geology*, 218: 50-62.
- Hall, D., T.E. Standish, M. Behazin and P.G. Keech. 2018. Corrosion of copper-coated used nuclear fuel containers due to oxygen trapped in a Canadian deep geological repository, *Corrosion Engineering, Science and Technology*, 53(4): 309-315. doi: 10.1080/1478422X.2018.1463009
- He, H., M. Broczkowski, K. O'Neil, D. Ofori, O. Semenikhin and D.W. Shoesmith. 2012. Corrosion of nuclear fuel (UO<sub>2</sub>) inside a failed nuclear waste container. Nuclear Waste Management Organization Report NWMO TR-2012-09. Toronto, Canada.
- He, H., R.K. Zhu, Z. Qin, P. Keech, Z. Ding and D.W. Shoesmith. 2009. Determination of local corrosion kinetics on hyper-stoichiometric UO<sub>2+x</sub> by scanning electrochemical microscopy. *J. Electrochemical Society* 156: C87-C94.
- He, H., P. Keech, M. E. Broczkowski, J.J. Noel and D.W. Shoesmith. 2007. Characterization of the influence of fission product doping on the anodic reactivity of uranium dioxide. *Canadian J Chemistry*, 85: 702-713.
- Hoek, E., C. Carranza-Torres and B. Corkum. 2002. Hoek-Brown failure criterion-2002 edition. *Proceedings of NARMS-Tac*, 1(1): 267-273.
- Hökmark, H., M. Lönngqvist and B. Fälth. 2010. THM-issues in repository rock. Thermal, mechanical, thermo-mechanical and hydromechanical evolution of the rock at the Forsmark and Laxemar sites. Swedish Nuclear Fuel and Waste Management Report SKB TR-10-23. Stockholm, Sweden.
- Hughes, O.L. 1959. Surficial geology of Smooth Rock and Iroquois Falls map areas, Cochrane District, Ontario. Ph.D. thesis, Department of Geology, University of Kansas, USA.
- Ion, M. 2018. Nuclear fuel waste projections in Canada – 2018 Update. Nuclear Waste Management Organization Technical Report NWMO-TR-2018-18. Toronto, Ontario, Canada.
- Itasca. 2012. FLAC3D (Fast Lagrangian Analysis of Continua in 3 Dimensions) Version 5.2. Itasca Consulting Group Inc. Minneapolis, USA.
- Itasca. 2013. 3DEC - Three Dimensional Discrete Element Code, Version 5.0. Itasca Consulting Group, Minneapolis, USA.
- Itasca. 2014a. PFC suite - Particle Flow Code in 3 dimensions, Version 5.0. Itasca Consulting Group, Minneapolis, USA.

- Itasca. 2014b. Universal Distinct Element Code (UDEC) Version 6.00. Itasca Consulting Group Inc. Minneapolis, USA.
- Itasca. 2015. Long-Term stability analysis of APM conceptual design in sedimentary and crystalline rock settings. Nuclear Waste Management Organization Report NWMO-TR-2015-27. Toronto, Canada.
- Jaczkowski, E., E. Ghazvinian and M. Diederichs. 2017a. Uniaxial compression and indirect tensile testing of Cobourg limestone: Influence of scale, saturation and loading rate. Nuclear Waste Management Organization Report NWMO-TR-2017-17. Toronto, Canada.
- Jaczkowski, E., E. Ghazvinian and M. Diederichs. 2017b. The influence of scale and loading rate on the crack damage thresholds of Cobourg limestone. Proceedings World Tunnelling Conference, Bergen, Norway.
- Jautzy, J.J., J.M.E. Ahad, M. Jensen and I.D. Clark. 2018. Molecular and isotopic evaluation of the maturation history of the organic matter in an Ordovician aquiclude (Michigan Basin): Evidence for late diagenetic biodegradation. *Organic Geochemistry* 125: 129-141.
- Kim, J-D., J-M. Lee, Y-S. Youn, N. Liu, J-G. Kim, Y-H. Ha, S-E. Bae, D.W. Shoesmith and J-Y. Kim. 2017. The combined influence of Gd-doping and Non-stoichiometry on the structural and electrochemical properties of uranium dioxide; *Electrochimica Acta* 247: 942-948.
- King F. 2005a. Overview of the corrosion behaviour of copper and steel used fuel containers in a deep geologic repository in the sedimentary rock of the Michigan basin, Ontario. Ontario Power Generation Report OPG 06819-REP-01300-10101-R00. Toronto, Canada.
- King F. 2005b. Evolution of environmental conditions in a deep geologic repository in the sedimentary rock of the Michigan Basin, Ontario Power Generation Report 06819-REP-01300-10102-R00. Toronto, Canada.
- Kwong GM. 2011. Status of corrosion studies for copper used fuel containers under low salinity conditions. Nuclear Waste Management Organization NWMO TR-2011-14. Toronto, Canada.
- Lee, J-M., J-D. Kim, N. Liu, Y-K. Ha, D.W. Shoesmith, Y-S. Youn and J-G. Kim. 2017. Raman study of the structure of  $U_{1-y}Gd_yO_{2-x}$  ( $y = 0.005, 0.01, 0.03, 0.05, 0.1$ ) solid solutions. *J. Nuclear Materials*, 486: 216-221.
- LeRiche A., K. Kalenchuk and M. Diederichs. 2017. Estimation of in situ stress from borehole breakout in brittle rock for the prediction of shaft overbreak. Proceedings World Tunnelling Conference, Bergen, Norway.

- Liberda, K. and H. Leung. 2018. Preliminary preclosure accident consequence analysis for the APM conceptual design. Proceedings Waste Management WM2018 Conference, Phoenix, USA.
- Limer, L., R. Klos, R. Walke, G. Shaw., M. Nordén, S. Xu. 2013. Soil-plant-atmosphere modeling in the context of releases of  $^{14}\text{C}$  as a consequence of nuclear activities. *Radiocarbon* 55(2-3), 804-813.
- Lindborg, T., M.Thorne, E.Andersson, J.Becker, J.Brandefelt, T.Cabianca, M.Gunia, A.T.K.Ikonen, E.Johansson, V.Kangasniemi, U.Kautsky, G.Kirchner, R.Klos, R.Kowe, A.Kontula, P.Kupiainen, A.-M.Lahdenperä, N.S.Lord, D.J.Lunt, J.-O.Näslund, M.Nordén, S.Norris, D.Pérez-Sánchez, A.Proverbio, K.Rieki, A.Rübel, L.Sweeck, R.Walke, S.Xu, G.Smith, G.Pröhl. 2018. Climate change and landscape development in post-closure safety assessment of solid waste disposal: Results of an initiative of the IAEA. *Journal of Environmental Radioactivity*. 183: 41-83.
- Liu, N., Z. Qin, J.J. Noel and D.W. Shoesmith. 2017a. Modelling the Radiolytic Corrosion of  $\alpha$ -Doped  $\text{UO}_2$  and Spent Nuclear Fuel; *J. Nuclear Materials* 494: 87-94.
- Liu, N., H. He, J.J. Noel and D.W. Shoesmith. 2017b. The electrochemical study of  $\text{Dy}_2\text{O}_3$  doped  $\text{UO}_2$  in slightly alkaline sodium carbonate/bicarbonate and phosphate solutions, *Electrochimica Acta* 235: 654-663.
- Liu, N., J. Kim, J-M Lee, Y-S. Youn, J-G. Kim, J-Y. Kim, J.J. Noel and D.W. Shoesmith. 2017c. Influence of Gd Doping on the Structure and Electrochemical Behavior of  $\text{UO}_2$ , *Electrochimica Acta* 247: 496-504.
- Liu, N., L. Wu, Z. Qin and D.W. Shoesmith. 2016a. Roles of radiolytic and externally generated  $\text{H}_2$  in the corrosion of fractured spent nuclear fuel. *Environ. Sci. Tech.* 50: 12348-12355.
- Liu, N., L. Wu, Z. Qin and D.W. Shoesmith. 2016b. Modelling the radiolytic corrosion of nuclear fuel inside a failed waste container. Proceedings Third Canadian Conference on Nuclear Waste Management, Decommissioning and Environmental Restoration. Ottawa, Canada.
- Marty, N.C.M., P. Blanc, O. Bildstein, F. Claret, B. Cochapin, D. Su, E.C. Gaucher, D. Jacques, J.-E. Lartigue, K.U. Mayer, J.C.L Meeussen, I. Munier, I. Pointeau, S. Liu and C.I. Steefel. 2015. Benchmark for multicomponent reactive transport codes across a cement/clay interactions. *Computational Geosciences, Special Issue on: Subsurface Environmental Simulation Benchmarks*, 19(3). doi:10.1007/s10596-014-9463-6.
- Mathers, W.G. 1985. HOTROK, a program for calculating the transient temperature field from an underground nuclear waste disposal vault. Atomic Energy of Canada Limited Technical Report, TR-366. Pinawa, Canada.
- Mayer, K.U., E.O. Frind and D.W. Blowes. 2002. Multicomponent reactive transport modelling in variably saturated porous media using a generalized formulation for kinetically controlled reactions. *Water Resources Research* 38: 1174. doi: 10:1029/2001WR000862.

- Mayer, K.U. and K.T.B. MacQuarrie. 2010. Solution of the MoMaS reactive transport benchmark with MIN3P - Model formulation and simulation results, *Computational Geosciences* 14: 405-419. doi: 10.1007/s10596-009-9158-6.
- Mazurek, M., T. Al, M. Celejewski, I.D. Clark, A.M. Fernández, L. Kennell-Morrison, J.M. Matray, S. Murseli, T. Oyama, S. Qiu, D. Rufer, G. St-Jean, H.N. Waber and C. Yu. 2017. Mont Terri Project: Mont Terri DB-A Experiment: Comparison of pore-water investigations conducted by several research groups on core materials from the BDB-1 borehole. Nuclear Waste Management Organization Report NWMO-TR-2017-09. Toronto, Canada. (also published as Mont Terri TR 2017-01)
- Medri, C. 2015. Non-Radiological Interim Acceptance Criteria for the Protection of Persons and the Environment. Nuclear Waste Management Organization NWMO-TR-2015-03. Toronto, Canada.
- Michaela, H., M. Marshall and M.J. Simpson. 2014a. State of Science Review: Natural organic matter in clays and groundwater. Nuclear Waste Management Organization Report NWMO-TR-2014-05. Toronto, Canada.
- Michaela, H., M. Marshall and M.J. Simpson. 2014b. Characterization of natural organic matter in bentonite clays. Nuclear Waste Management Organization Report NWMO-TR-2014-10. Toronto, Canada.
- Mompeán, F.J and H. Wanner. 2003. The OECD Nuclear Energy Agency thermodynamic database project. *Radiochimica Acta*, 91: 617-622.
- Muller, H.R., B. Garitte, T. Vogt, S. Kohler, T. Sakaki, H. Weber, T. Spillman, M. Hertrich, J. Becker, N. Giroud, V. Cloet, N. Diomidis and T. Vietor. 2017. Implementation of the full-scale emplacement (FE) experiment at the Mont Terri rock laboratory. *Swiss Journal of Geosciences* 110(1): 287-306.
- Nagasaki, S. 1994. Influence of pseudocolloid generation on migration of nuclides and diffusion of charged colloids. The University of Tokyo, UTNL-R-0312. Tokai, Japan.
- Nagasaki, S. 2018. Sorption properties of Np on shale, illite and bentonite under saline, oxidizing and reducing conditions. Nuclear Waste Management Organization Report NWMO-TR-2018-02. Toronto, Canada.
- Nagasaki, S., J. Riddoch, T. Saito, J. Goguen, A. Walker and T. Yang. 2017. Sorption behavior of Np(IV) on illite, shale and MX-80 in high ionic strength solutions. *J Radioanalytical and Nuclear Chemistry*, 313(1): 1-11.
- Nagasaki, S., T. Saito and T. Yang. 2016. Sorption Behavior of Np(V) on Illite, Shale and MX-80 in High Ionic Strength Solutions. *J Radioanalytical and Nuclear Chemistry*, 308(1): 143-153.

- Najari, M. and A.P.S. Selvadurai. 2014. Thermo-hydro-mechanical response of granite to temperature changes, *Environmental Earth Sciences*, 72: 189-198.
- Nasseri, M.H.B. and B. Mohanty. 2008. Fracture toughness anisotropy in granitic rocks. *International J Rock Mechanics and Mining Science*, 45: 167-193.
- NEA. 2014. Vision Document for the Radioactive Waste Repository Metadata Management (RepMet) Project. OECD Nuclear Energy Agency. Paris, France.
- NEA. 2015. Preservation of Records, Knowledge and Memory Across Generations (RK&M): Phase-II Vision Document. OECD Nuclear Energy Agency. Paris, France.
- Normani, S., A. Snowdon and J. Sykes. 2018. Using geochemistry to inform hydraulic properties of fractured crystalline rock settings. *Proceedings AGU Fall Meeting 2018*, Washington, DC, United States.
- Nunn, J.A., Y. Xiang and T.A. Al. 2018. Investigation of partial water saturation effects on diffusion in shale. *Applied Geochemistry* 97: 93–101.
- NWMO. 2012. Used fuel repository conceptual design and postclosure safety assessment in crystalline rock. Nuclear Waste Management Organization Report NWMO-TR-2012-16. Toronto, Canada.
- NWMO. 2013. Postclosure safety assessment of a used fuel repository in sedimentary rock, Pre-Project Report. Nuclear Waste Management Organization Report NWMO-TR-2013-07. Toronto, Canada.
- NWMO. 2017. Postclosure safety assessment of a used fuel repository in crystalline rock. Nuclear Waste Management Organization Report NWMO-TR-2017-02. Toronto, Canada.
- NWMO. 2018. Postclosure safety assessment of a used fuel repository in sedimentary rock. Nuclear Waste Management Organization Report NWMO-TR-2018-08. Toronto, Canada.
- NWMO. 2019. Implementing Adaptive Phased Management 2019 to 2023. Nuclear Waste Management Organization. Toronto, Canada.
- Packulak, T., J. Day and M. Diederichs. 2018a. Role of rock direct shear testing in determining geomechanical properties of fractures. *Tunnels and Tunnelling*, 2: 32-36.
- Packulak, T., J. Day and M. Diederichs. 2018b. Practical aspects of boundary condition selection on direct shear laboratory tests. *Proceedings Geomechanics and Geodynamics of Rock Masses, ISRM-EUROCK 2018*, Saint-Petersburg, Russia.
- Park, J.H., J.E. Kuh, S. Kwon and C.H. Kang. 2000. Thermal analysis of high level radioactive waste repository using a large model. *J Korean Nuclear Society*, 32(3): 244-253.

- Peltier, W.R. 2002. A design basis glacier scenario. Ontario Power Generation Report 06819-REP-01200-10069-R01. Toronto, Canada.
- Peltier, W.R. 2006a. Boundary conditions data sets for spent fuel repository performance assessment. Ontario Power Generation Report 06819-REP-01200-10154-R00. Toronto, Canada.
- Peltier, W.R. 2006b. Laurentide glaciation: Simulation of sub-glacial hydrology. Ontario Power Generation Report 06819-REP-01200-10162-R00. Toronto, Canada.
- Perras, M. and M. Diederichs. 2016. Predicting excavation damage zone depths in brittle rocks. *J Rock Mechanics and Geotechnical Engineering*, 8(1): 60-74. doi:10.1016/j.jrmge.2015.11.004.
- Pitts, M. 2017. Thermal properties of the Cobourg limestone. Master's thesis, Department of Geological Sciences and Geological Engineering. Queen's University, Ontario, Canada.
- Poinssot, C., C. Ferry, M. Kelm, B.Grambow, A. Martinez-Esparza, L. Johnson, Z.Andriambololona, J. Bruno, C. Cachoir, J-M. Cavendon, H. Christensen, C.Corbil, C. Jegou, K.Lemmens, A. Loida, P. Lovera, F. Miserque, J. de Pablo, A. Poulesquen, J. Quinones, V. Rondinella, K. Spahiu and D.Wegen. 2005. Final report of the European project spent fuel stability under repository conditions. European Commission Report CEA-R-6093. Brussels, Belgium.
- Posiva. 2012. Rock Suitability Classification RSC 2012. Posiva Report 2012-24. Olkiluoto, Finland.
- Priyanto, D.G., C-S. Kim and D.A. Dixon. 2013. Geotechnical characterization of a potential shaft backfill material. Nuclear Waste Management Organization Report NWMO TR-2013-03. Toronto, Canada.
- Ranjram, M., T. Gleeson and E. Luijendijk. 2014. Is permeability of crystalline rock in the shallow crust related to depth, lithology or tectonic setting? *Geofluids*, 15. doi:10.1111/gfl.12098.
- Razdan, M. and D. Shoesmith. 2014a. The electrochemical reactivity of 6.0 wt% Gd-Doped  $\text{UO}_2$  in aqueous carbonate/bicarbonate solutions. *J. Electrochemical Society*, 161: H225-H234.
- Razdan, M. and D. Shoesmith. 2014b. Influence of trivalent-dopants on the structural and electrochemical properties of uranium dioxide ( $\text{UO}_2$ ). *J. Electrochemical Society*, 161: H105-H113.
- Reijonen, H., T. Karvonen and J.L. Cormenzana. 2016. Preliminary hazard identification for the Mark II conceptual design. Nuclear Waste Management Organization Report NWMO-TR-2016-02. Toronto, Canada.

- Selvadurai, A.P.S. and A. Głowacki. 2008. Evolution of permeability hysteresis of Indiana Limestone during isotropic compression. *Ground Water*, 46: 113-119.
- Selvadurai, A.P.S. and A. Glowacki. 2018. Estimates for the local permeability of the Cobourg limestone. *J Rock Mechanics and Geotechnical Engineering*, 10(6): 1009-1019.
- Selvadurai, A.P.S. and M. Najari. 2015. Laboratory-scale hydraulic pulse testing: Influence of air fraction in the fluid-filled cavity in the estimation of permeability. *Geotechnique*, 65: 124-134.
- Selvadurai, A.P.S. and M. Najari. 2016. Isothermal permeability of the argillaceous Cobourg Limestone, *Oil and Gas Science and Technology, Special Issue on Low Permeability Geomaterials*, 71: 53-69.
- Selvadurai, A.P.S. and P.A. Selvadurai. 2010. Surface permeability tests: Experiments and modelling for estimating effective permeability. *Proceedings Royal Society, Mathematical and Physical Sciences Series A*, 466: 2819-2846.
- Selvadurai, A.P.S., M.J. Boulon and T.S. Nguyen. 2005. The permeability of an intact granite. *Pure and Applied Geophysics*, 162: 373-407.
- Selvadurai, A.P.S., A. Letendre and B. Hekimi. 2011. Axial flow hydraulic pulse testing of an argillaceous limestone, *Environmental Earth Sciences*. , 64:2047-2058. doi 10.1007/s12665-011-1027-7.
- Selvadurai, P.A. and A.P.S. Selvadurai. 2014. On the effective permeability of a heterogeneous porous medium: the role of the geometric mean. *Philosophical Magazine*, 94: 2318-2338.
- Siren, T., M. Hakala, J. Valli, R. Christiansson, D. Mas Ivars, T. Lam, J. Mattila and J. Suikkanen. 2017. Parametrisation of Fractures – Final report. Posiva Report 2017-01. Eurajoki, Finland.
- SKB. 2009. Design premises for a KBS-3V repository based on results from the safety assessment SR-Can and some subsequent analyses. *Svensk Kärnbränslehantering Report SKB TR-09-22*. Stockholm, Sweden.
- Smith, K. 2016. Update and Review of the IAEA BIOMASS-6 Reference Biosphere Methodology. Report of the first programme workshop. BIOPROTA, UK.
- Smith, K. 2017a. Update and Review of the IAEA BIOMASS Methodology. Report of the second workshop held in parallel with the first meeting of MORARIA II Working Group 6. BIOPROTA, UK.
- Smith, K. 2017b. Update and Review of the IAEA BIOMASS Methodology. Summary of the third workshop held in parallel with the first interim meeting of MORARIA II Working Group 6. BIOPROTA, UK.

- Spiessl, S.M., K.U. Mayer and K.T.B. MacQuarrie. 2009. Reactive transport modelling in fractured rock - Redox Stability Study. Nuclear Waste Management Organization Report NWMO TR-2009-04, Toronto, Canada.
- Stuhne, G. and W. Peltier. 2015a. Reconciling the ICE-6G C reconstruction of glacial chronology with ice sheet dynamics: the cases of Greenland and Antarctica. *J Geophysical Research: Land Surface* 120: 1841–1865.
- Stuhne, G. and W. Peltier. 2015b. Surface boundary conditions during long-term climate Change. Nuclear Waste Management Organization Report NWMO-TR-2015-16. Toronto, Canada.
- Stuhne, G. and W. Peltier. 2016. Sensitivity analyses of surface boundary conditions during long-term climate change. Nuclear Waste Management Organization Report NWMO-TR-2016-19. Toronto, Canada.
- Stuhne, G. and W. Peltier. 2017. Assimilating the ICE-6G C reconstruction of the latest Quaternary ice age cycle into numerical simulations of the Laurentide and Fennoscandian ice sheets. *J Geophysical Research: Earth Surface*, 122(12): 2324–2347.
- Su, D., K.U. Mayer and K.T.B. MacQuarrie. 2015. Parallelization of reactive transport program MIN3P-THCm. Nuclear Waste Management Organization Report NWMO-TR-2015-23, Toronto, Canada.
- Su, D., K.U. Mayer and K.T.B. MacQuarrie. 2017. Parallelization of MIN3P-THCm: A high performance computational framework for subsurface flow and reactive transport simulation. *Environmental Modelling & Software*, 95: 271-289.
- Tait, J.C., H. Roman and C.A. Morrison. 2000. Characteristics and radionuclide inventories of used fuel from OPG nuclear generating stations - Volume 1 - Main Report. Ontario Power Generation Report 06819-REP-01200-10029-R00. Toronto, Canada.
- Tait, J.C. and S. Hanna. 2001. Characteristics and radionuclide inventories of used fuel from OPG Nuclear Generating Stations, Volume 3 - Radionuclide inventory data. Decay times 10 to 300 years. Ontario Power Generation Report 06819-REP-01200-10029-R00. Toronto, Canada.
- Thorne, M., K. Smith, I. Kovalets, R. Avila and R. Walke. 2018. Terrestrial model-data comparisons and review of carbon uptake by fish. BIOPROTA Report, Henley-on-Thames, UK.
- Tsui, K.K. and A. Tsai. 1985. Thermal analyses for different options of nuclear fuel waste placement. Atomic Energy of Canada Limited Report, AECL-7823. Pinawa, Canada.
- Turnbull, J., R. Szukalo, M. Behazin, D. Hall, D. Zagidulin, S. Ramamurthy, J.C. Wren and D.W. Shoesmith. 2018. The effects of cathodic reagent concentration and small solution volumes on the corrosion of copper in dilute nitric acid solutions. *Corrosion*, 74(3).

- Vazaios, I., N. Vlachopoulos and M. Diederichs. 2018a. A multidisciplinary approach in modelling hard rocks with natural discontinuities: From data collection to numerical simulation. Proceedings ARMA 2018 Conference, Seattle, USA.
- Vazaios, I., N. Vlachopoulos and M. Diederichs. 2018b. The effect of jointing in massive highly interlocked rockmasses under high stresses by using a FDEM approach. Proceedings IAEG 2018 Conference, San Francisco, USA.
- Vazaios, I., K. Farahmand, N. Vlachopoulos and M. Diederichs. 2018c. The effects of confinement on the rockmass modulus: A synthetic rockmass modelling (SRM) study. *J Rock Mechanics and Geotechnical Engineering*, 10(3): 436-456.
- Vilks, P. 2011. Sorption of selected radionuclides on sedimentary rocks in saline conditions - Literature review. Nuclear Waste Management Organization Report NWMO TR-2011-12. Toronto, Canada.
- Vilks, P. and N.H. Miller. 2014. Sorption studies with sedimentary rock under saline conditions. Nuclear Waste Management Organization Report NWMO TR-2013-22. Toronto, Canada.
- Vilks, P. and N.H. Miller. 2018. Sorption experiments with sedimentary rocks under saline conditions. Nuclear Waste Management Organization Report NWMO-TR-2018-16. Toronto, Canada.
- Vilks, P. and T. Yang. 2018. Sorption of selected radionuclides on sedimentary rocks in saline conditions – Updated sorption values. Nuclear Waste Management Organization Report NWMO-TR-2018-03. Toronto, Canada.
- Vilks, P., N.H. Miller and K. Felushko. 2011. Sorption experiments in brine solutions with sedimentary rock and bentonite. Nuclear Waste Management Organization Report NWMO TR-2011-11. Toronto, Canada.
- Walker, A., J. Racette, J. Goguen and S. Nagasaki. 2018. Ionic strength and pH dependence of sorption of Se(-II) onto illite, bentonite and shale. Proceedings 38th Annual Conference of the Canadian Nuclear Society, Saskatoon, Canada.
- Walton, G. and M.S. Diederichs. 2015. Dilation and post-peak behaviour inputs for practical engineering analysis. *Geotechnical and Geological Engineering*, 33(1): 15-34.
- Wu, L., N. Liu, Z. Qin and D.W. Shoesmith. 2014a. Modelling the Radiolytic Corrosion of Fractured Nuclear Fuel under Permanent Disposal Conditions. *J Electrochemical Society*, 161: E3259 – E3266.
- Wu, L., Z. Qin and D.W. Shoesmith. 2014b. An improved model for the corrosion of used nuclear fuel inside a failed waste container under permanent disposal conditions. *Corrosion Science*, 84: 85-95.

- Xie, M., P. Rasouli, K.U. Mayer and K.T.B. MacQuarrie. 2014. Reactive transport modelling of in-situ diffusion experiments for the Mont Terri Project: MIN3P-THCm code enhancements and numerical simulations. Nuclear Waste Management Organization Report NWMO TR-2014-25. Toronto, Canada.
- Xie, M., P. Rasouli, K.U. Mayer and K.T.B. MacQuarrie. 2015. MIN3P-THCm code enhancements for reactive transport modelling in low permeability media. Nuclear Waste Management Organization Report NWMO-TR-2015-12. Toronto, Canada.
- Xie, M., D. Su, K.U. Mayer and K.T.B. MacQuarrie. 2018. Reactive transport modeling investigation of elevated dissolved sulfide concentrations in sedimentary basin rocks. Nuclear Waste Management Organization Report NWMO-TR-2018-07. Toronto, Canada.

**APPENDIX A: NWMO TECHNICAL REPORTS, REFEREED JOURNAL ARTICLES AND TECHNICAL CONFERENCE PRESENTATIONS**

## A.1 NWMO TECHNICAL REPORTS

- Briggs, S. and M. Krol. 2018. Diffusive Transport Modelling of Corrosion Agents through the Engineered Barrier System in a Deep Geological Repository for Used Nuclear Fuel. Nuclear Waste Management Organization Technical Report NWMO-TR-2018-06, Toronto, Canada.
- Chen, J., M. Behazin, J. Binns, K. Birch, C. Boyle, J. Freire-Canosa, G. Cheema, R. Crowe, D. Doyle, F. Garisto, J. Giallonardo, M. Gobien, R. Guo, M. Hobbs, N. Hunt, M. Ion, M. Jensen, P. Keech, E. Kremer, T. Lam, C. Lawrence, H. Leung, T. Liyanage, J. McKelvie, C. Medri, M. Mielcarek, L. Kennell-Morrison, A. Murchison, A. Parmenter, U. Stahmer, Y. Sui, E. Sykes, T. Yang, X. Zhang. 2018. Technical Program for Long-Term Management of Canada's Used Nuclear Fuel – Annual Report 2017. Nuclear Waste Management Organization Technical Report NWMO-TR-2018-01, Toronto, Canada.
- Diamond, D. and L. Richter. 2018. Fluid Inclusion Study of Calcite and Celestine in DGR-1 and DGR-3 Drill Core Samples from the Bruce Nuclear Site, Southern Ontario. Nuclear Waste Management Organization Technical Report NWMO-TR-2018-13, Toronto, Canada.
- Dixon, D., A. Man, S. Rimal, J. Stone and G. Siemens. 2018. Bentonite Seal Properties in Saline Water. Nuclear Waste Management Organization Technical Report NWMO-TR-2018-20, Toronto, Canada.
- Engel, K., S. Coyotzi, G. Slater and J. D. Neufeld. 2018. Development of Protocols for Sampling and Assessment of Bentonite and Environmental Samples Associated with in Situ Proof Tests of Engineered Barrier Systems. Nuclear Waste Management Organization Technical Report NWMO-TR-2018-04, Toronto, Canada.
- Garisto, F. 2018. Seventh Case Study: Features, Events and Processes. Nuclear Waste Management Organization Technical Report NWMO-TR-2018-15, Toronto, Canada.
- Gobien, M., F. Garisto, E. Kremer, and C. Medri. 2018. Seventh Case Study: Reference Data and Codes. Nuclear Waste Management Organization Technical Report NWMO-TR-2018-10, Toronto, Canada.
- Guo, R. 2018. Thermal Response of a Conceptual Deep Geological Repository in Sedimentary Rock. Nuclear Waste Management Organization Technical Report NWMO-TR-2018-09, Toronto, Canada.
- Ion, M. 2018. Nuclear Fuel Waste Projections in Canada – 2018 Update. Nuclear Waste Management Organization Technical Report NWMO-TR-2018-18, Toronto, Canada.
- Nagasaki, S. 2018. Sorption Properties of Np on Shale, Illite and Bentonite under Saline, Oxidizing and Reducing Conditions. Nuclear Waste Management Organization Technical Report NWMO-TR-2018-02, Toronto, Canada.
- NWMO. 2018. Postclosure Safety Assessment of a Used Fuel Repository in Sedimentary Rock. Nuclear Waste Management Organization Technical Report NWMO-TR-2018-08, Toronto, Canada.

- Rufer, D. and M. Mazurek. 2018. Pore-water Extraction and Characterization: Benchmarking of the Squeezing and Adapted Isotope Diffusive Exchange Methods. Nuclear Waste Management Organization Technical Report NWMO-TR-2018-14, Toronto, Canada.
- Slater, G., J. Neufeld and B. S. Lollar. 2018. Development of Microbial Characterization Techniques for Crystalline Rock. Nuclear Waste Management Organization Technical Report NWMO-TR-2018-05, Toronto, Canada.
- Vilks, P. and T. Yang. 2018. Sorption of Selected Radionuclides on Sedimentary Rocks in Saline Conditions – Updated Sorption Values. Nuclear Waste Management Organization Technical Report NWMO-TR-2018-03, Toronto, Canada.
- Xie, M., D. Su, U. Mayer and K. MacQuarrie. 2018. Reactive Transport Modelling Investigation of Elevated Dissolved Sulphide Concentrations in Sedimentary Basin Rocks. Nuclear Waste Management Organization Technical Report NWMO-TR-2018-07, Toronto, Canada.

## A.2 REFEREED JOURNAL ARTICLES

- Al-Aasm, I.S. and R. Crowe. 2018. Fluid compartmentalization and dolomitization in the Cambrian and Ordovician successions of the Huron Domain, Michigan Basin. *Marine and Petroleum Geology*, 92: 160-178.
- Bea, S.A., D. Su, K.U. Mayer and K.T.B. MacQuarrie. 2018. Evaluation of the potential for dissolved oxygen ingress into deep sedimentary basins during a glaciation event, *Geofluids*, Article ID 9475741.
- Celejewski, M., D. Barton and T. Al. 2018. Measurement of Cl:Br ratios in the porewater of clay-rich rocks – A comparison of the crush-and-leach and the paper-absorption methods. *Geofluids*, Article ID 9682042. doi:10.1155/2018/9682042.2018.
- Chen, J., Z. Qin, T. Martino, M. Guo and D.W. Shoesmith. 2018. Copper transport and sulphide sequestration during copper corrosion in anaerobic aqueous sulphide solutions. *Corrosion Science*, 131: 245-251.
- Davy, P., C. Darcel, R. Le Goc and D. Mas Ivars. 2018. Elastic properties of fractured rock masses with frictional properties and power-law fracture size distributions. *J Geophysical Research: Solid Earth*, 123. doi.org/10.1029/2017JB015329.
- Farahmand, K., I. Vazaios, M.S. Diederichs and N. Vlachopoulos. 2018. Investigating the scale-dependency of the geometrical and mechanical properties of a moderately jointed rock using a synthetic rock mass (SRM) approach. *Computers and Geotechnics*, 95: 162-179.
- Ghazvinian, E. and M. Diederichs. 2018. Progress of brittle microfracturing in crystalline rocks under cyclic loading conditions. *J South African Institute of Mining and Metallurgy*. 118(3): 217-226.
- Giunta, T., E.D. Young, O. Warr, I.E. Kohl, J. Ash, A.M. Martini and B. Sherwood Lollar. 2018. Methane sources and sinks in continental sedimentary systems: New insights from paired clumped isotopes  $^{13}\text{CH}_3\text{D}$  and  $^{12}\text{CH}_2\text{D}_2$ . *Geochimica et Cosmochimica Acta*, 245: 327-351.
- Grigoryan, A.A., D.R. Jalique, P. Medihala, S.S. Gayscoyne, G.M. Wolfaardt, J. McKelvie and D.R. Korber. 2018. Bacterial diversity and production of sulfide in microcosms containing uncompacted bentonites. *Heliyon*, 4(8), Article e00722.
- Hall, D.S., T.E. Standish, M. Behazin and P.G. Keech. 2018. Corrosion of copper-coated used nuclear fuel containers due to oxygen trapped in a Canadian deep geological repository, *Corros. Eng. Sci. Technology*, 53: 309-315.
- Ibrahim, B., D. Zagidulin, M. Behazin, S. Ramamurthy, J.C. Wren and D.W. Shoesmith. 2018. The corrosion of copper in irradiated and unirradiated humid air. *Corrosion Science*, 141: 53-62.

- Jautzy, J., J.M.E. Ahad, M. Jensen and I.D. Clark. 2018. Molecular and isotopic evaluation of the maturation history of the organic matter in an Ordovician aquiclude (Michigan Basin): Evidence for late diagenetic biodegradation. *Organic Geochemistry* 125:129-141.
- Liu, N., Z. Zhu, L. Wu, Z. Qin, J.J. Noël, and D.W. Shoesmith. 2018. Predicting radionuclide release rates from spent nuclear fuel inside a failed waste disposal container using a finite element model. *Corrosion*, 75: 302-308.
- Nunn, J.A., Y. Xiang and T.A. Al. 2018. Investigation of partial water saturation effects on diffusion in shale. *Applied Geochemistry*, 97: 93–101.
- Packulak, T., J. Day and M. Diederichs. 2018. Role of rock direct shear testing in determining geomechanical properties of fractures. *Tunnels and Tunnelling*, 2: 32-36.
- Paraskevopoulou, C. and M. Diederichs. 2018. Analysis of time-dependent deformation in tunnels using the convergence-confinement method. *Tunnelling and Underground Space Technology*, 17: 62-80. doi:10.1016/j.tust.2017.07.001.
- Paraskevopoulou, C., M. Perras, M. Diederichs, Löw, T. Lam and M. Jensen. 2018. Time-dependent behaviour of brittle rocks based on static load laboratory testing. *J Geotechnical and Geological Engineering*, 36(1): 337–376. doi:10.1007/s10706-017-0331-8.
- Selvadurai, A.P.S. and A. Glowacki. 2018. Estimates for the local permeability of the Cobourg limestone. *J Rock Mechanics and Geotechnical Engineering*, 10(6): 1009-1019.
- Stahmer, U. 2018. Using flight-time to contextualize radiological dose. *The Physics Teacher*, 56(8): 508-511. doi.org/10.1119/1.5064556.
- Standish, T., D. Zagidulin, S. Ramamurthy, P.G. Keech, D.W. Shoesmith and J.J. Noel. 2018. Synchrotron-based micro-CT investigation of oxidic corrosion of copper-coated carbon steel for potential use in a deep geological repository for used nuclear fuel. *Geosciences*, 8: 1-14.
- Turnbull, J., R. Szukalo, M. Behazin, D. Hall, D. Zagidulin, S. Ramamurthy, J.C. Wren and D.W. Shoesmith. 2018. The effects of cathodic reagent concentration and small solution volumes on the corrosion of copper in dilute nitric acid solutions. *Corrosion*, 74: 326-336.
- Vazaios, I., K. Farahmand, N. Vlachopoulos and M. Diederichs. 2018. The effects of confinement on the rockmass modulus: A synthetic rockmass modelling (SRM) study. *J Rock Mechanics and Geotechnical Engineering*, 10(3): 436-456.
- Walton, G., M.S. Diederichs, K. Weinhardt, D. Delaloye and M. Lato. 2018. Change detection in drill and blast tunnels from point cloud data. *International J Rock Mechanics and Mining Sciences*, 105: 172-181. doi:10.1016/j.ijrmms.2018.03.004.

Warr, O., B. Sherwood Lollar, J. Fellowes, C. Sutcliffe, J. McDermott, G. Holland, J. Mabry and C.J. Ballentine. 2018. Tracing ancient hydrogeological fracture network age and compartmentalisation using noble gases. *Geochimica et Cosmochimica Acta*, 222: 340-362.

### **A.3 TECHNICAL CONFERENCE PRESENTATIONS (INCLUDING PROCEEDINGS, ORAL AND POSTER PRESENTATIONS)**

- Abdullah, A., S. Briggs and M. Krol. 2018. Factors influencing nano zero valent iron (nZVI) transport: A COMSOL modelling approach. GeoEdmonton Conference, Canadian Geotechnical Society. Edmonton, Canada.
- Aubertin, J. D., S. Hoentzsch, M.S. Diederichs and H. Milton. 2018. Influence of the creep law on pillar response based on numerical simulations of an underground salt mine. 52nd Rock Mechanics and Geomechanics Symposium, Seattle, USA.
- Avis, J.D., E.P. Kremer and J. Chen. 2018. Determining the most consequential well and source locations for postclosure safety assessment of a conceptual deep geological repository in crystalline rock. 2<sup>nd</sup> International Discrete Fracture Network Engineering Conference. Seattle, USA.
- Blyth, A., S. Hirschorn, A. Vorauer, A. Parmenter, M. Sykes, A. DesRoches, M. Sanchez-Rico Castejon and E. Sykes. 2018. Update on the APM site selection process – Canada's plan for the long-term management of used nuclear fuel. 45<sup>th</sup> International Association of Hydrogeologists (IAH) Congress, Daejeon, Republic of Korea.
- Briggs, S., and M. Krol. 2018. Sensitivity of an engineered barrier system to diffusive transport in a deep geological repository for used nuclear fuel. COMSOL Conference, Boston, USA.
- Calder, N., J. Avis and E.P. Kremer. 2018. Concurrent simulation of linked models at multiple scales of repository gas generation and transport. TOUGH Symposium 2018, Berkeley, USA.
- Chen, J., T. Martino, M. Guo, J.J. Noel and D.W. Shoesmith. 2018. The corrosion of copper nuclear waste containers in sulphide-containing groundwaters, Materials Research Society Symposium, Boston, USA.
- Chen, J. 2018. Watershed-scale fully coupled surface-subsurface flow & transport modelling for a conceptual used fuel DGR in fractured crystalline rocks on the Canadian Shield. 45<sup>th</sup> International Association of Hydrogeologists (IAH) Congress, Daejeon, Republic of Korea.
- Crowe, R. and I. Al-Aasm. 2018. Dolomitization in Cambrian and Upper Ordovician sediments of the intracratonic Michigan Basin: Diagenesis and paleofluid migration. American Association of Petroleum Geologists 2018 Annual Convention, Salt Lake City, USA.
- Crowe, R. and I. Al-Aasm. 2018. Early Paleozoic dolomite paleogenesis and hydrothermal fluid migration in the Huron Domain of Southern Ontario. International Sedimentary Congress, Quebec City, Canada.

- Cruden, A., D. Davis, D. Andjelkovic and A. Parmenter. 2018. Timing and tectonic significance of regional fracture systems in Paleozoic platform rocks, east central North America: new insights from U-Pb dating of vein calcite. European Geological Union Conference, Vienna, Austria.
- Dadashzadeh, N. and M. Diederichs. 2018. Effect of rock strength components' evolution rate on the mechanism of failure in brittle rocks. Tunneling and Trenchless Conference (TT2018 – TAC/NASTT-NW), Edmonton, Canada.
- Dadashzadeh, N. and M. Diederichs. 2018. Reliability of prediction for tunnel excavation damage zone depth in brittle rocks. 10<sup>th</sup> Asian Rock Mechanics Symposium, Singapore.
- Dadashzadeh, N. and M. Diederichs. 2018. Prediction of Excavation Damage Zone depth variability in brittle rocks. Geomechanics and Geodynamics of Rock Masses, ISRM-EUROCK 2018, Saint-Petersburg, Russia.
- Daljeet, R. 2018. Exploring anode/cathode sizing, strength, persistence and distribution on corroding copper surfaces. Aqueous Corrosion Gordon Research Conference, New London, USA.
- Darcel, C., P. Davy, R. Le Goc and D. Mas Ivars. 2018. Rock mass effective properties from a DFN approach. Second International Discrete Fracture Network Engineering Conference, Seattle, USA.
- Grandy, L., J.M. Joseph, G. Whitaker, M. Behazin, P.G. Keech and J.C. Wren. 2018. Effects of radiation on the progression of copper corrosion in stagnant pure water. NACE SOSS Symposium, Toronto, Canada.
- Guo, M., J. Chen, T. Martino, J.J. Noël and D.W. Shoesmith. 2018. The nature of sulphide film formed voltammetrically on copper in slightly alkaline (pH 9) aqueous solutions containing sulphide and chloride. Aqueous Corrosion Gordon Research Conference, New London, USA.
- Guo, R. 2018. Task E: Heater Experiment THM Modelling – Step 3: ALC Experiment. Presentation in the 5<sup>th</sup> Workshop of DECOVALEX-2019. Nancy, France.
- Guo, R. 2018. Task E: Heater Experiment THM Modelling: Step 3: ALC Experiment, and Step 4: 2D and 3D Models. Presentation in the 6<sup>th</sup> Workshop of DECOVALEX-2019. Seoul, Republic of Korea.
- Keech, P. 2018. Contemporary issues in the corrosion of nuclear waste systems. Aqueous Corrosion Gordon Research Conference, New London, USA.
- LeRiche, A., K. Kalenchuk and M. Diederichs. 2018. Estimation of in situ stress from borehole breakout at KGHM's Victoria Project, Canada. 52<sup>nd</sup> U.S. Rock Mechanics/Geomechanics Symposium: ARMA 2018, Seattle, USA.

- Liu, N., Z. Zhu and D.W. Shoesmith. 2018. Predicting radionuclide release rates from spent nuclear fuel inside a failed waste disposal container. CORROSION2018, National Association of Nuclear Engineers Topical Research Symposium "Corrosion Lifetime Prediction: In Memory of Roger W. Staehle", USA.
- Liu, N., Z. Zhu and D.W. Shoesmith. 2018. The electrochemistry of uranium dioxide. Materials Research Society Symposium, Phoenix, USA.
- Liu, N., Z. Zhu, J.J. Noel and D.W. Shoesmith. 2018. Corrosion of nuclear fuel inside a failed waste container; Encyclopedia of Interfacial Chemistry, Surface Science and Electrochemistry, edited by K. Wandelt, Elsevier, Oxford, UK, 172-182 (Book Chapter).
- Liu, N., Z. Zhu and D.W. Shoesmith. 2018. Predicting radionuclide Release Rates from Spent Nuclear Fuel Inside a Failed Waste Disposal Container, CORROSION2018, National Association of Nuclear Engineers Topical Research Symposium "Corrosion Lifetime Prediction: In Memory of Roger W. Staehle, Phoenix, USA.
- Martino, T., J. Smith, J. Chen, Z. Qin, J.J. Noël and D.W. Shoesmith. 2018. Electrochemical evaluation of the pitting susceptibility of copper in aqueous sulphide solutions. Aqueous Corrosion Gordon Research Conference, New London, USA.
- Moinuddin, M., S. Briggs, P. Keech, M. Behazin, M. Kolar, F. King and M. Krol. 2018. Mixed-potential modelling of copper nuclear waste containers. EUROCORR, Krakow, Poland.
- Naghizadeh, M., J.M. Joseph, G. Whitaker, M. Behazin, P.G. Keech and J.C. Wren. 2018. Effect of anions on copper corrosion dynamics. NACE SOSS Symposium, Toronto, Canada.
- Normani, S., A. Snowdon and J. Sykes. 2018. Using geochemistry to inform hydraulic properties of fractured crystalline rock settings. AGU Fall Meeting 2018, Washington, USA.
- Packulak, T., J.J. Day and M. Diederichs. 2018. Practical aspects of boundary condition selection on direct shear laboratory tests. Geomechanics and Geodynamics of Rock Masses, ISRM-EUROCK 2018, Saint-Petersburg, Russia.
- Selvadurai, A.P.S. 2018. Estimation of the Biot coefficient for an ultra-low permeability rock. CouFrac Conference, Wuhan, China.
- Shoesmith, D.W., N. Liu, F. King and J.J. Noel. 2018. Electrochemical simulation of the influence of radiolytically-produced hydrogen on the corrosion of uranium dioxide, Materials Research Society Meeting, Boston, USA.
- Standish, T.E., D. Zagidulin, S. Ramamurthy, J.J. Noël and D.W. Shoesmith. 2018. Corrosion of copper-coated carbon steel at a through-coating defect. Aqueous Corrosion Gordon Research Conference, New London, USA.

- Su, D., K.U. Mayer and K.T.B. MacQuarrie. 2018. MIN3P-THCm-USG: a fully unstructured grid code for subsurface flow and reactive transport simulation, Computation Methods in Water Resources, Saint-Malo, France.
- Tortola, M., I.S. Al-Aasm and R. Crowe. 2018. Petrographic and Geochemical Attributes of Silurian and Devonian Dolomitized Formations in the Huron Domain, Michigan Basin. International Sedimentary Congress, Quebec City, Canada.
- Turnbull, J., M. Mohammad, R. Szukalo, M. Behazin, D. Zagidulin, D.W. Shoesmith and J.C. Wren. 2018. Elucidating the mechanism of nitric acid corrosion on copper coated nuclear waste containers. Corrosion 2018, NACE, Phoenix, USA.
- Vazaios, I., N. Vlachopoulos and M. Diederichs. 2018. A multidisciplinary approach in modelling hard rocks with natural discontinuities: From data collection to numerical simulation. ARMA 2018 Conference, Seattle, USA.
- Vazaios, I., N. Vlachopoulos and M. Diederichs. 2018. The effect of jointing in massive highly interlocked rockmasses under high stresses by using a FDEM approach. IAEG 2018 Conference, San Francisco, USA.
- Walker, A., J. Racette, J. Goguen and S. Nagasaki. 2018. Ionic strength and pH dependence of sorption of Se(-II) onto illite, bentonite and shale. f 42<sup>nd</sup> Annual Canadian Nuclear Society Conference, Saskatoon, Canada.
- Yang, T., P. Vilks, S. Nagasaki, P. Bertetti and M. Hobbs. 2018. Sorption properties of radionuclides in saline Solutions. Goldschmidt 2018, Boston, USA.
- Yang, T. and P. Tremaine. 2018. Thermodynamic properties of actinides and metals at high temperature and high ionic strength. 18<sup>th</sup> International Symposium Solubility Phenomena and Related Equilibrium Processes (ISSP18), Tours, France.
- Zhu, Z., L. Wu, J.J. Noel and D.W. Shoesmith. 2018. Electrochemical study of simulated spent nuclear fuel (SIMFUEL) corrosion in groundwater conditions. International Spent Fuel Workshop, Sheffield, UK.